Investigation of Lubrication Strategies in Ti6Al4V Milling Operations

H.J. Joubert

Masters Thesis

This Masters thesis is presented in partial fulfilment of the requirements for the degree of Master of Science in Industrial Engineering at Stellenbosch University.

Study leader: Mr N.F. Treurnicht

December 2008

Declaration

I, the undersigned, hereby declare that the work contained in this Masters thesis is my own original work and that I have not previously in its entirety or in part submitted it at any university for a degree.

…….. ……..
Signature Date

Acknowledgements

Special thanks have to go out to my study leader, Mr Nico Treurnicht, who motivated and kept me on track throughout the course of this study. Thanks for all the interesting talks on different theories surrounding the scope of my study and machining in general.

To Mr Tiaan Oosthuizen who walked along side me throughout the course of this study. Thanks not only for your inputs on machining, but also for your support and friendship throughout the course of our time here at Stellenbosch University.

To Dr Nedret Can for organizing and giving me the opportunity to do an internship at Elements Six (Pty) Ltd. The knowledge I gained during this working period contributed to a great extent to my understanding of tool wear phenomena.

To Dr Guven Akdogan, my project leader during my internship at Element Six (Pty) Ltd, for assisting me throughout the duration of my project there and helping me to gain knowledge on different analyses techniques used throughout the course of this study.

To Mr Neels Pretorius from Element Six (Pty) Ltd for his inputs on titanium machining and his continuous feedback and involvement throughout this project.

To Prof Dimitri Dimitrov for organizing me the opportunity to attend the CPK 2008 conference in Chemnitz, Germany.

To Mr Mike Saxer who helped me with the 5-axes machine for my experimentations and for his inputs surrounding titanium machining.

To Mr Brent Deez for giving me the opportunity to use the 5-axes machine for my experiments and for sharing his experience regarding titanium machining.

To Mr Craig Apsey for designing the custom tool used for my experiments. Thanks also for your inputs and knowledge regarding titanium machining.

To all the staff at Element Six (Pty) Ltd who assisted me during my analyses of my study. Your contribution is greatly appreciated.

To Element Six (Pty) Ltd for providing me with the PCD inserts used for my experiments and allowing me the opportunity to do my analyses on their machines.

To my parents for allowing me the opportunity to study at Stellenbosch University. Thanks for all the love and support throughout the years. I love you both very much.

Lastly, I would like to thank God for giving me the strength and guidance throughout the course of this project.

Opsomming

Daar is tans ‘n groeiende aanvraag vir titaan produkte. Hierdie aanvraag word meestal gedryf deur die lugvaart industrie. Titaan beskik oor aantreklike eienskappe wat sy gebruik regverdig, beide ekonomies en omgewingsgewys. Die rede waarom titaan so ‘n aanloklike materiaal vir die lugvaart industrie is, is as gevolg van sy goeie sterkte-tot-gewig verhouding. Dit beteken dat die gebruik van titaan komponente in die plek van ander metale ‘n groot besparing in strukturele gewig van ‘n vliegtuig teweeg kan bring. Uit ‘n ekonomiese oogpunt impliseer ‘n laer massa minder brandstof verbruik. Uit ‘n omgewingsbewuste oogpunt impliseer laer brandstof verbruik verlaagde skadelike brandstof emissies.

Van al die titaan allooi produkte wat gebruik word vir vliegtuig komponente word die grootste aanvraag ondervind vir Ti6Al4V. Die probleem met die verskaffing van Ti6Al4V onderdele is dat dit geklassifiseer word as moeilik-om-te-masjineer. Dit kan toegeskryf word aan Ti6Al4V se lae hitte geleidings vermoeë en die klein kontak area tussen die beitel en die spaanders wat tot gevolg het dat hoë sny temperature naby aan die snypunt gekonsentreer word. Hoër sny temperature verhoog gevolglik die tempo waarteen beitel se snyvlakke verweer. Die gevolg hiervan is dat relatief lae sny spoede en voer tempo’s gebruik word vir die masjinering van Ti6Al4V in vergelyking met staal. Ti6Al4V is ook ‘n relatief hoë koste materiaal. Die lae sny spoede en voer tempo’s wat gebruik word in die masjinering van Ti6Al4V verhoog die masjineringskoste van onderdele. Dus, deur gebruik te maak van hoër sny spoede en voer tempo’s kan die masjineringstyd van Ti6Al4V verlaag word wat gevolglik die prys van onderdele daaruit vervaardig kan verlaag.

Die uitdaging met ‘n toename in sny spoed en voer tempo is dat dit gevolglik ‘n toename in sny temperatuur tot gevolg sal hê. Dit beklemtoon die belangrikheid daarvan om die temperatuur te beheer tydens Ti6Al4V sjinering om sodoende die beitel leeftyd te verhoog. Die fokus van hierdie werk was om verskillende verkoelings tegnieke te bestudeer vir freeswerk operasies van Ti6Al4V met polikristallynne diamant (PCD) en wolfram karbied beitels om sodoende verbeterde sny parameters te identifiseer.

Die resultate van hierdie studie toon dat vloed verkoeling die beste resultate opgelewer het vir die PCD beitels. Die “sagter” 60 bar hoë druk verkoeling, verskaf deur die “deur-spindel-verkoeling”, het die beste resultate getoon het vir die wolfram karbied beitels. Deur van hierdie verkoeling strategië toe te pas, kon ‘n snyspoed van 100 m/min en ‘n voer per beiteltand van 0.05 mm/omw vir beide die PCD en wolfram karbied beitels toegepas word met aanvaarde beitel slytasie per volume materiaal verwyder.

Synopsis

There is a growing global demand for titanium. The aircraft industry is the driving force behind the demand for titanium. The reason for this is that titanium has attractive properties that justify its use both economically and environmentally. Titanium alloys have superior strength-to-weight ratios. This implies that by substituting components manufactured from other metals in the aircraft with titanium components, a substantial reduction in structural weight can be achieved. From an economical point of view a lower mass implies lower fuel consumption. From an environmental point of view lower fuel consumption implies less harmful greenhouse emissions.

Ti6Al4V components are the most widely used titanium alloy products in aircraft components. Ti6Al4V is known as a difficult-to-machine material. This is due to its low thermal conductivity and small contact area between the tool and the chips causing higher temperatures to be generated closer to the cutting edge of the insert. This will subsequently increase the rate at which the cutting tool wears. For this reason relatively low cutting speeds and feed rates are employed for the machining of Ti6Al4V compared to the machining of steels. Ti6Al4V is an exceptionally high cost material. The low cutting speeds and feed rates used in Ti6Al4V machining raises the machining cost of parts and contributes to an increase in the price of Ti6Al4V parts. By employing higher cutting speeds and feed rates machining times on Ti6Al4V products could be decreased, subsequently lowering the price for Ti6Al4V components.

An increase in cutting speeds and feed rates will subsequently cause an increase in generated cutting temperatures, resulting in an increase in tool wear. This stresses the importance of controlling the cutting temperature during machining of Ti6Al4V in order to prolong tool life. The focus of this work was to investigate different lubrication strategies for polycrystalline diamond (PCD) and tungsten carbide inserts for Ti6Al4V milling operations in the quest to develop improved feasible cutting parameters.

The results of this study showed that flood lubrication should be utilized for PCD inserts, while a “softer” 60 bar high pressure through spindle lubrication worked best for the tungsten carbide inserts. By utilizing these lubrication strategies, cutting speeds of 100

m/min and feeds per tooth of 0.05 mm/rev for both the PCD and tungsten carbide grades could be attained with satisfactory tool life.

Table of Contents

LIST OF FIGURES

LIST OF TABLES

Glossary

Adiabatic	A thermo dynamical process in which no heat is transferred.
Ambient temperature	Room temperature. Normally has a range of between 20 - 28℃.
Amorphous material	Non-crystalline material
Asperity	Describes the unevenness of a surface. Indicates the irregularities or "high-points" on the surface of a "flat" material.
Ceramic	Defines inorganic non-metallic materials that are formed due to the addition of heat.
Chemical leaching	An extraction process where acid is added in order to remove wanted materials from the material matrix.
Creep	Deformation of a part due to long term exposure to stresses below its yield strength.
EDM	Electrical discharge machining
EDS	Electron dispersive spectroscopy
Enthalpy	Denotes the thermodynamic potential of a system. A negative enthalpy indicates an endothermic reaction, while a positive enthalpy indicates an exothermic reaction.
Ferrous material	A compound containing bivalent iron.
Galling chips	A process that causes the asperities between the chips and the tool to weld together due to friction generated heat.
GDP	Gross domestic product
Isomorphous elements	Elements with the same crystal form (molecular arrangement).
Isotropic	A material whose crystal structure is uniform in all directions.
Lamellar chips	Chips constructed of fine layers.
Metastable	A delicate state of equilibrium that is susceptible to move into a lower-energy state when subjected to only a minor interaction.
Recrystallization	A process by which nucleation and growth of new undeformed grains occur in a deformed metal.
Refractometer	Used to determine the concentration of one substance dissolved in another.
Refractory Metals	Metals with extremely high melting temperatures and high wear resistance. These metals have a poor resistance to corrosion and oxidation wear however and include the following metals: Tungsten, Molybdenum, Niobium, Tantalum and Rhenium.
Rehbinder effect	Reduction in the hardness and ductility of the workpiece material by a surface-active molecular film
RPK	Revenue passenger-kilometers
RTK	Revenue tonne-kilometers (Cargo traffic)

SEM	Scanning electron microscope
Shear	Stress induced deformation of a material where parallel internal surfaces slide past one another.
Shear zone	Describes the place where shearing occurs.
Transverse Rupture Strength (TRS)	Indicates the stress required to break a specimen supported at its ends with a load being applied midway between the supports.
Work hardening	The strengthening of materials by plastic deformation.

1. Introduction

Titanium alloys are classified as difficult-to-machine. This is due to its extremely low thermal conductivity (which could be 8 to 10 times lower than that of steel) and its chemical reactivity with other materials at elevated temperatures. Despite these problems associated with the machining of Ti-alloys, the material possesses properties that make it extremely useful for certain applications, especially in the aerospace industry. These properties include a very low density (up to 60% compared to steel) and a high melting point, consequently making titanium highly useful as lightweight aerospace parts that are subjected to conditions of high temperatures and extreme peripheral speeds.

Ti-alloys can have a relatively high elastic modulus (~112 GPa), but is however still low compared to steel (~200 GPa). This implies that titanium alloys will deflect almost twice as much as steel when subjected to the same load. This is however not a problem. The reduced density of titanium implies that a titanium alloy part with the same dimensions as steel will weigh 40% less. The force exerted on a part subjected to centrifugal motion is proportional to the mass of the part. This implies that the deflection of the part will be similar to that of steel when subjected to high peripheral speeds, such as turbine blade applications. This is especially useful for aeroplane engines, because the use of titanium would mean a reduction in the weight, without sacrificing performance. A reduction in mass will subsequently reduce the amount of fuel that is used. Reduced consumption would not only imply a reduction in flight ticket prices, but it also implies a reduction in greenhouse emissions. This is especially useful when considering the growing concern on global warming.

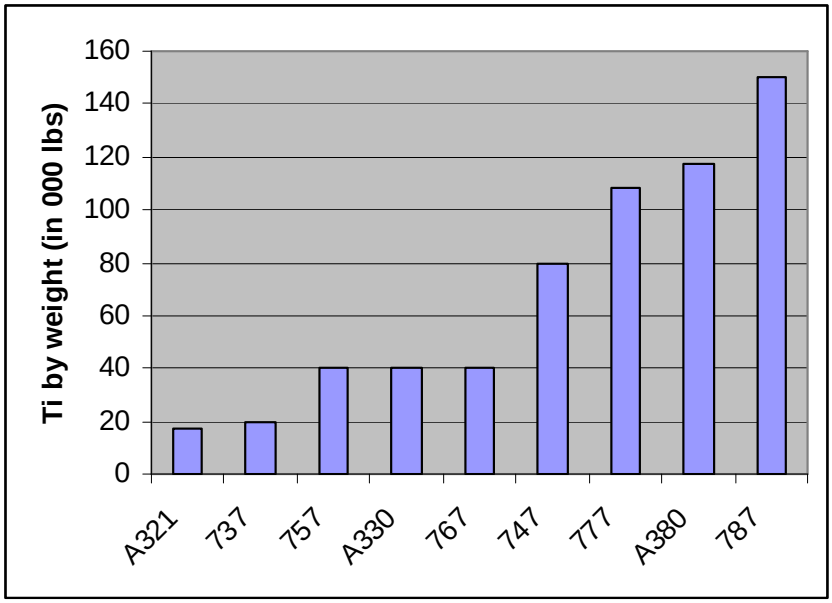

Figure 1: Titanium in current and future aircraft (by weight) [2].

Boeing's latest published market outlook [1] indicated that between 2003 and 2006, due to the increase in fuel prices, fuel expenses grew from 15% to more than 25% of total airline operating costs. The fuel price has increased dramatically since 2006, leading to an even bigger increase in percentage of total airline operating costs. For this reason aircraft manufacturers are moving toward implementing more Ti-alloys and nickel-based superalloys for use in aircraft structural- and engine components. Figure 1 indicates values attained from RMI Titanium Company [2] about the mass of titanium in current and future aircraft.

TIMET is the world's largest supplier of titanium metal products. According to their latest annual report (2007), the demand for titanium has historically been proven to be mainly driven by the demand for aircrafts [3]. After the terrorist attacks of 9/11 on the two Trade Centers in New York in 2001, the demand for commercial aircrafts decreased sharply. This implied a sharp decrease in the demand for titanium as well [4]. This decline was relieved in 2003 when an upswing in the defence aerospace began, and in 2004 the demand for titanium began to soar once again due to an increase in demand for commercial aerospace [4]. This increase in aerospace industry demand is also evident according to Boeing's current market outlook for 2008 [1]. According to the market

outlook, by 2027, only 20% of airplanes used in service will be older than 20 years. More specific figures of this projection are shown in Table 1 [1].

Table 1: Forecast of aeroplanes in service by 2027 [1].

Airplane size	**2007**	**2027**
747 and larger	910	1 340
Twin aisle	3 480	8 290
Single aisle	11 450	23 540
Regional jets	3 160	2 630
Total	**19 000**	**35 800**

At the moment a quarter of the world's international merchandise trade (measured by value) are moved by air. According to Boeing, air cargo has grown by more than 50 times in the last 42 years, and despite competition from other modes of transport, they believe that air cargo will continue to grow at an average of 6.1% per year over the next 20 years [1]. Ignoring air cargo movements within North America and Europe, 42% of the value of goods transported internationally is done by air. When this same figure is taken in terms of weight of cargo moved, it only amounts to about 1% though. For this reason more modified airplane types (such as the 767-300BCF and the 747-400BCF) as well as new designs (such as the 747-8F and the 777F) were introduced in order to restore some of the advantage that air freight have lost over container ships. Figure 2 [1] indicates the prediction of the amount of freighters in service by 2027. This is a massive increase when considering that only 1980 freighters were in service in 2006. Figure 3 indicates the expected market growth rates between 2007 and 2027 [1].

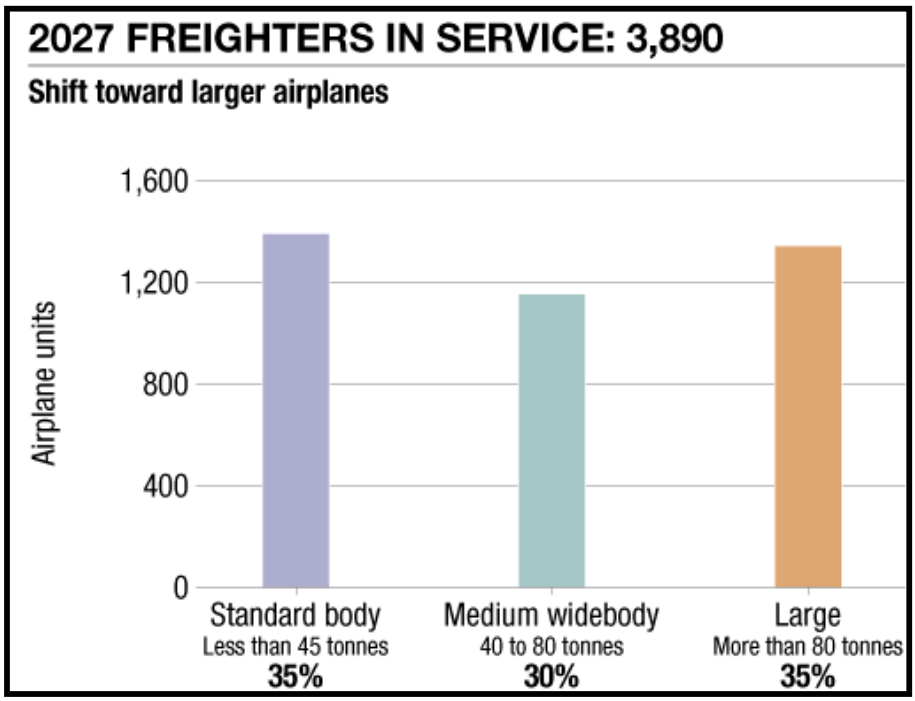

Figure 2: The increase in freighters from 2006 and 2027 [1].

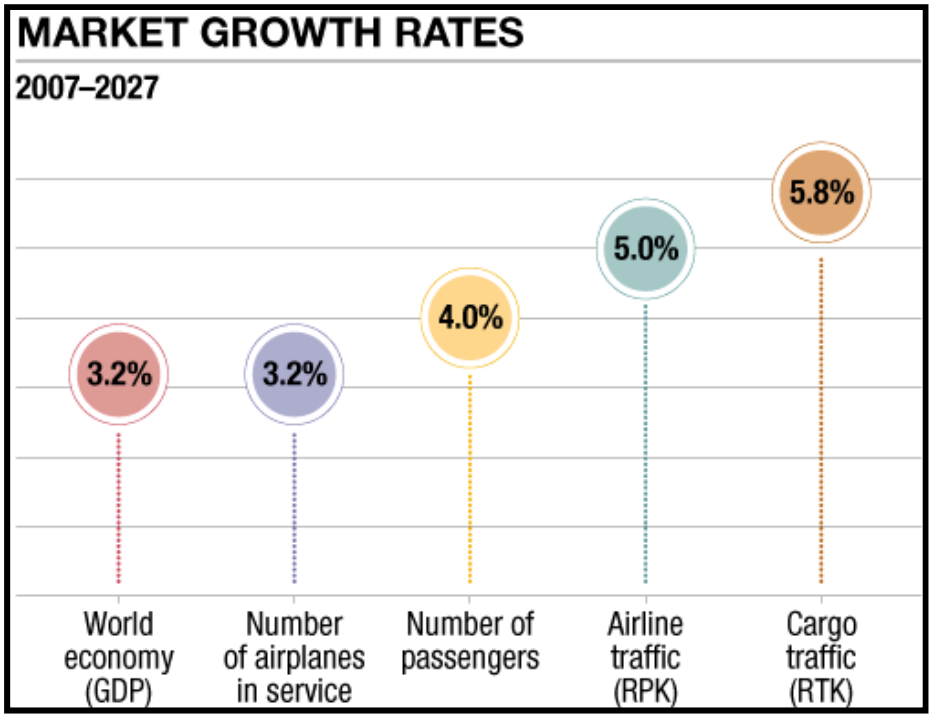

Figure 3: Annual market growth rate [1].

The U.S., Russia and Japan place the biggest demand on titanium, while the demand in China has also risen since 2000 [5]. Figure 4 indicates how this demand has fluctuated between 2000 and 2004. The decrease in demand for titanium in the U.S. in 2002 is probably due to the decrease in demand of commercial aircrafts after the terrorist attack of 9/11. Observation indicates that all the countries show a steady increase in titanium demand for this period.

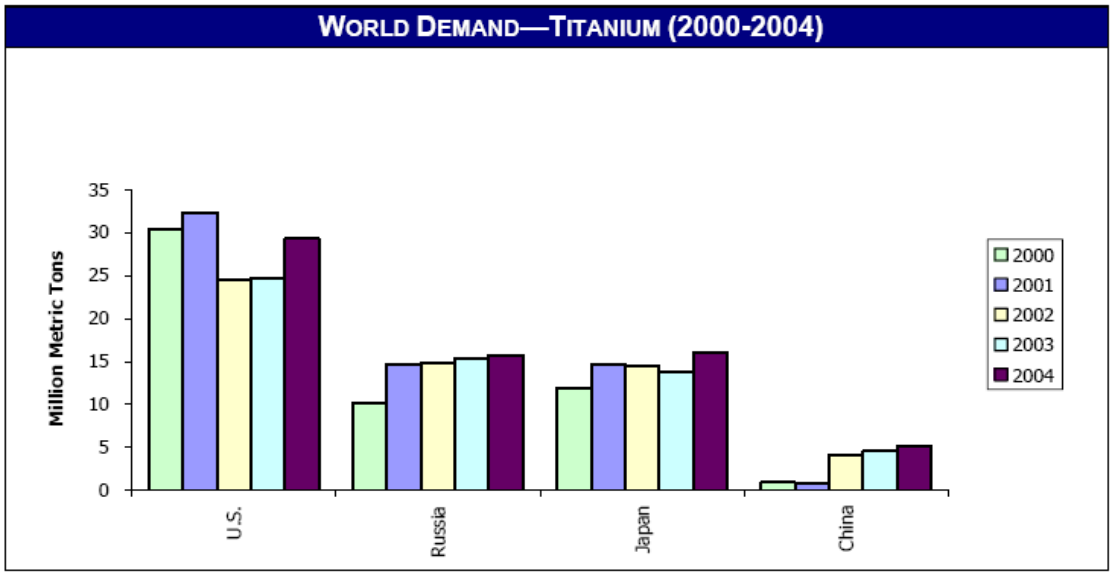

Figure 4: The fluctuation in titanium demand between 2000 and 2004 [5].

From the information presented in this section it becomes clear that the demand for titanium is predicted to keep on rising for at least the next 20 years. This increase in demand suggests an increase in production with titanium, which would tend to place pressure on existing manufacturing capacity to deliver on time. A natural implication would be that lead times on titanium products need to be decreased. Several factors and their suitable combinations play an important role in reducing such lead times. These factors include the machining parameters such as cutting speeds and feed rates, as well as the choice in cutting fluid and the method of applying it onto the cutting area.

Some aeronautical parts also require high precision and surface integrity for the part to be functional in its working conditions. All of these factors have to be taken into account when considering the correct cutting parameters. Rather few studies have been conducted on machining Ti6Al4V with PCD inserts and even less studies have been

conducted on investigating the effect of different lubrication strategies in the machining of Ti6Al4V. Barnett-Ritcey [6] experimented with different directed through spindle tool designs and found that PCD performed better with an increase in through spindle supply pressure from 10 to 40 bar. Heavy chipping of the PCD inserts was also observed at feed per tooth values of higher than 0.051 mm/rev. Nabhani [7] compared tool wear of coated carbide inserts, cubic boron nitride (CBN) and PCD for the machining of titanium alloys and found that both PCD and CBN performed superior compared to the coated carbide inserts. It was also concluded that PCD performed better than the CBN inserts. Kuljanic et al. [8] investigated the milling of titanium compressor blades with a PCD cutter and found that suitable results were attained up to a cutting speed of 110 m/min when using soluble oil lubrication comprising of 7% oil and 93% water. Narutaki et al. [9] compared K10 carbide tools against natural diamond tools for titanium machining and found that the natural diamond tool's high thermal conductivity allowed for suitable cutting up to 200 m/min. Limited work has been done to investigate newer lubrication strategies such as high pressure through spindle lubrication for Ti6Al4V milling.

The focus of this study is thus to determine the effectiveness of through spindle lubrication and flood lubrication at different cutting speeds and feed rates for PCD and tungsten carbide inserts for milling of Ti6Al4V in the quest to develop optimum cutting parameters for Ti6Al4V.

2. Superalloys and Titanium

2.1 Superalloys

Superalloys are alloys that have good combinations of properties. Most superalloys are used in aircraft engine components where they are subjected to conditions of high temperatures and high oxidizing environments for a reasonable period of time. The mechanical integrity of materials under these conditions is critical. In this regard, an important consideration is the density of the material. A reduction in material density will subsequently cause a reduction in the centrifugal stresses exerted on the rotating parts. Superalloys are classified according to the predominant metal in the alloy. These metals may be cobalt, nickel or iron. Other alloying elements include the refractory metals such as Nb, Mo, W, Ta, Cr, and Ti. Apart from turbine applications, these parts are also utilized in petrochemical equipment and nuclear reactors [10].

Machining is used to manufacture superalloy parts. Superalloys are considerably more expensive to machine than conventional steels. Much of the high costs associated with superalloy machining can be accredited to the fact that cutting speeds for superalloys are only 5 to 10% of those used for steel [11].

The surface condition of superalloys, especially after machining, plays an important role in determining the mechanical properties of superalloys under cyclic conditions. For this reason machining processes are not only of concern to cost of material removal, but also to the impact it has on the cyclic behaviour of superalloys [11].

Strengthening of superalloys can be done by any of the following methods [11]:

- Solid-solution hardening – Substituted atoms interfere with deformation.
- Work hardening – Energy is stored by deformation.
- Precipitation hardening – Precipitates interfere with deformation.
- Carbide production – A favourable distribution of secondary phases interferes with deformation.

Factors that affect the mechanical/machining properties of superalloys are [11]:

- Superalloys retain their strength at elevated temperatures, where common steels begin to soften.
- Superalloys have unusually high dynamic shear strength.
- Superalloys contain hard carbide particles in their microstructure, making them very abrasive.
- Work hardening occurs during metal cutting.
- Superalloys possess poor thermal diffusivity, thus increasing the cutting temperature at the tool-chip interface.
- Superalloys form a tough, continuous chip during metal cutting.

2.2 Titanium alloys

Ti-alloys presents an attractive combination of properties for aerospace applications. Titanium in its pure form has a relatively low density (4.5 g/cm^3), a high melting point of 1668 ˚C, and an elastic modulus of 107 GPa. Ti-alloys are also highly ductile [10].

A major limitation of titanium is its chemical reactivity with other materials at higher temperatures. In spite of this chemical reactivity of titanium alloys at elevated temperatures, its corrosion resistance at ambient temperatures is normally high. Titanium alloys are virtually immune to air, marine, and a wide range of industrial environments. Titanium alloys are most widely used in aircraft structures, space vehicles, surgical implants, and in the petroleum and chemical industries. In aircraft engines Ti-alloys are mostly used in rotating components and axial compressors [12].

Table 2 indicates several titanium alloys and their mechanical properties [10].

Table 2: Compositions and Mechanical properties of typical Ti-alloys [10].

Alloy Type	Common Name (UNS Number)	Composition (wt%)	Condition	Tensile Strength [Mpa]	Yield Strength [MPa]	Ductility [%EL in 50mm]
Commercially Pure	Unalloyed (R50500)	99.1 Ti	Annealed	484	414	25
α	Ti-5Al-2.5Sn (R54520)	5Al, 2.5Sn, balance Ti	Annealed	826	784	16
Near α	Ti-8Al-1Mo-1V (R54810)	8Al, 1Mo, 1V, balance Ti	Annealed (duplex)	950	890	15
α-β	Ti-6Al-4V (R56400)	6Al, 4V, balance Ti	Annealed	947	877	14
α-β	Ti-6Al-6V-2Sn (R56620)	6Al, 2Sn, 6V, 0.75Cu, balance Ti	Annealed	1050	985	14
β	Ti-10V-2Fe-3Al	10V, 2Fe, 3Al, balance Ti	Solution + aging	1223	1150	10

Titanium alloys can maintain good strength properties at elevated temperatures above 500 ˚C. Apart from their good anti-corrosion properties Ti-alloys also possess good creep properties [12].

Another application where titanium is commonly used is for low and high pressure compressors of stationary gas turbines. These compressor blades operate at extremely high peripheral speeds. Parts working at these conditions therefore need to have a low density. Materials that have a high Young modulus, E, and a low density, ρ, (thus having a high specific modulus, E/ρ) will be ideal [8]. Titanium has less than 60% of the density of steel and heat treated titanium alloys can have a tensile strength of up to 1390 MPa [12]. This makes titanium alloys an ideal material to use for this application.

The main metallurgic characteristic of titanium is the presence of an allotropic α to β transformation at a temperature of 885 ˚C. The stable phase existing below this temperature has a hexagonal structure and is less ductile than the β phase, especially when hardened through solid solution alloying. By adding different metallic elements

and metalloids (oxygen), the zone of stability for the α and β phases can be broadened. It can also bring forth a zone in which the two phases co-exist (the α-β phase) [12]. The addition of elements like Al, Ga, and Sn will increase the temperature of allotropic transformation, while the addition of elements like V, Nb, and Ta will lower the temperature of allotropic transformation. This means that the properties and microstructure of the titanium alloy can be greatly altered through heat treatment and the addition of different alloying elements [13].

As depicted in Table 2, Ti6Al4V is an α-β Ti-alloy. This means that Ti6Al4V has a mixture of structure α and β. The α structure is hexagonal close packed and is very hard and brittle, with a strong hardening tendency. The β structure is body centred cubic and is more ductile and easily formed with a strong tendency to adhere [8].

Some titanium alloys, although a lot lighter than steels, can have a Brinell hardness value of more than 400. When considering these properties, it might seem that Ti-alloys would be machined quite readily. These alloys have, however, their own cutting characteristics that make them quite difficult to machine [12].

Titanium alloys fall into the following main classes [12]:

- Unalloyed titanium where the α alloys contain α stabilising additions. In the case of "super α" alloys, β eutectoid and/or β isomorphous elements are used as stabilising additions. These alloys show little response to heat treatment, except for high temperature behaviour. It also has good strength properties at elevated temperatures.
- The α-β alloys where the two phases co-exist at ambient temperature. These alloys are responsive to heat treatment processes such as air cooling and ageing.
- The metastable β alloys. These alloys are responsive to heat treatment and can be structurally hardened.

The ductility of titanium is indirectly proportional to its strength. Hence, an increase in strength by alloying or heat treatment will have an inverse effect on the ductility. The modulus of elasticity remains mostly unaffected though. At a value between 100 to 125 GPa, the Young's Modulus, E, of titanium is between 30 to 50% less than the value for

steels. This implies that the titanium is likely to deflect twice as much as steel under a given load when compared to steel with a similar configuration [12].

The machinability of Ti6Al4V depends to a large extent on its low thermal conductivity. Ti6Al4V has a thermal conductivity that is much lower than the thermal conductivity of steel (6.7 W/mK for Ti6Al4V compared to typically 40 W/mK for steel). This low thermal conductivity will lead to extreme thermal stresses on the cutting edge, leading to an extensive increase in tool wear [8].

For this reason, to ensure the biggest improvement in tool life, it is necessary to suppress the generated cutting heat as much as possible. 80% of the heat that is generated in the cutting process is retained in the tool. The other 20% is retained in the chip [14]. Polycrystalline diamond (PCD) has a thermal conductivity of about 500 W/mK, thus making it probably the best suited tool material for the machining of titanium alloys [9].

Another problem associated with the machining of titanium alloys is the unusually small contact area that exists between the face of the tool and the titanium chip at the tool-chip interface. This is caused due to the formation of segregated chips during the machining of Ti6Al4V. This area can be as small as a third of the contact area of a plain carbon steel chip that is produced at the same feed rate. The small contact area in conjunction with the low thermal conductivity of titanium alloys result in the generation of extremely high temperatures at the tool face. The small contact area implies that maximum wear occurs closer to the tool cutting edge when compared to most other materials [12].

As already mentioned, during the machining of titanium alloys high temperatures are generated. This is especially a problem when considering that titanium becomes chemically active at temperatures in the region of 500 ˚C. In this state titanium easily combines with gases and other metallic materials. The affinity that titanium has for most materials when heated leads to galling and seizing of chips on the cutting tool. Once this happens, the build up of titanium on the cutting tool is rapid, since titanium welds itself quite easily [12]. The controlling of heat is thus essential to the successful machining of titanium alloys at high cutting speeds [15]. In most milling operations less heat is generated than in continuous turning operations. The tool face temperatures in turning

can be seen as an upper bound of temperatures expected in milling. An increase in cutting speed will bring forth an increase in temperature until the melting point of Ti6Al4V (1604-1660 ºC) is reached [16].

Titanium is a strong carbide-forming element [17]. According to Pettifor [6], the affinity of a metal to carbide is determined by its enthalpy. The more negative the enthalpy, the greater the affinity of the metal to carbon. A negative enthalpy implies that energy was given off in the chemical reaction (thus exothermic). The more negative the enthalpy, the more reactive the elements thus are. As can be seen in Table 3, the reaction of titanium and carbon has a very low enthalpy and therefore a high affinity to each other [8].

Table 3: The enthalpy of the formation of certain metal-carbides.

Metal	Carbide	ΛH kj/mol
Ti	TiC	-92
Nb	NbC	-71
V	VC	-51
Mo	MoC	-5

In the experiments conducted by Barnett-Ritcey [16] it was found that the machinability of Ti6Al4V for finish edge milling depended to a large extent on different cutting conditions such as cutting speed, radial immersion, maximum chip thickness and the coolant application conditions.

3. Polycrystalline Diamond

Polycrystalline Diamond (PCD) is a material that is almost as strong and as hard as a single crystal diamond and has two considerable advantages. Although single crystal diamonds are extremely strong, it fractures relatively easily along certain cleavage planes. In the case of PCD however, the crystals are oriented in different directions. When a crack occurs along the cleavage plane of one of the crystals, the propagation tends to be held up when passing from one crystal to the other. PCD is therefore a much tougher material than single crystal diamonds. Another advantage of PCD is that it can be produced in relatively large blocks. This is because the sintering process avoids problems involved in the growing of large single crystals [18].

Substitutes for natural diamonds can be obtained through the sintering of fine diamond particles to form a polycrystalline mass. The blanks that are manufactured in this way can be used directly or after mechanical-, wire EDM-, or laser cutting, to produce cutting tools, mining bits or wear resistant part blanks [19]. The sintering process for PCD relies on the same principles as other sintering processes, where intense heat and pressure is applied until particles fuse together. In the case of sintering for most metals, it is found that the sintering proceeds quite rapidly at temperatures that are about 70% of the material's melting temperature. The melting point of diamond is about 3300 K. This implies that the crystallites should be raised to a temperature of 2300 K and a pressure of 70 kbar to maintain stability of the diamond [18].

When the diamond powder is compressed the maximum pressure is experienced at the points of contact between the grains and not in the voids between the grains. The pressure in this region will be much lower. As a result of the high temperatures, the diamond adjacent to the voids will transform to graphite. This is why the standard method of sintering with heat and pressure cannot be used successfully with diamonds [18].

To avoid the formation of graphite, the arrangement, illustrated in Figure 5, is used in the reaction chamber prior to the sintering. Under these conditions the cobalt will melt because of the high temperature and pressure. The melted cobalt will infiltrate into the voids and thus maintain the pressure on the diamond surfaces, preventing the formation of graphite [18].

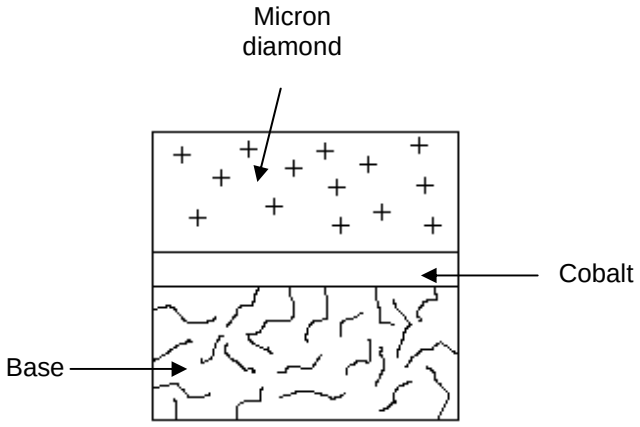

Figure 5: The arrangement in the reaction chamber prior to sintering.

The strength of the PCD does not depend primarily on the cobalt acting as a binder, as would be the case in many other composite materials. The strength of PCD rather relies on the strength and extent to which the diamond-diamond bonds, produced by the crystallites, are grown together at their points of contact [18].

PCD is normally used in high temperature environments. For this reason the application fields of PCD can differ according to the thermal expansion coefficients of the binders used in the production of PCD. When ferrous metals are used as binders, it contributes to the formation of carbides and the graphitization when the PCD blank is heated. This also implies that there exists a large difference in relative thermal expansion coefficients between the binder and the diamond. This will increase the risk of blank fracture at temperatures above 1000 K. The thermal resistance of synthetic PCD can be improved by eliminating the cobalt binder. This can be done through chemical leaching and will cause the blank to have a porous structure [19].

Figure 6 depicts thermal expansion coefficients of different materials.

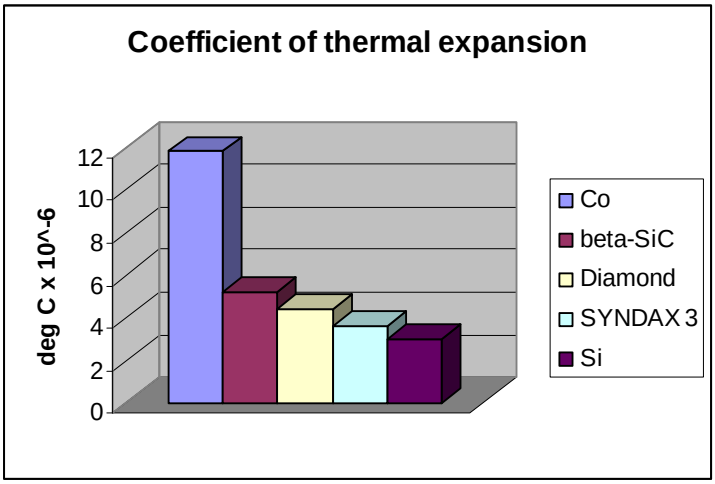

Figure 6: The coefficient of thermal expansion for different materials [19].

When sintering at very high pressure, it may occur that the diamonds react with the binder and form intermediate layers at the diamond-binder interfaces. The phase boundaries between the diamond and the binder material are made less abrupt due to the mechanical and thermal properties of these intermediate layers. The advantage of these intermediate layers is that abrupt phase boundaries normally lead to the generation of different kinds of thermo-mechanical stresses brought on by the difference in thermal expansion and mechanical properties of the different constituents in materials. These intermediate layers therefore make the material more thermo-mechanically stable [19].

The isotropic physical and chemical properties of synthetic PCD differentiate it from other synthetic diamond crystals. Tough and cohesive PCD materials can only be produced under production circumstances of high pressure and temperature. Plastic strain in diamonds is observed at a temperature of 1570 K, the region of its thermodynamic stability. Particle recrystallization can also occur under these circumstances and happens due to the intergrowth of fine particles to form more coarse particles [19].

The typical uses of PCD include face milling of Al-alloys and other non-ferrous materials. Another application is for machining of medium-high Si-Al alloys where the tools need to display high abrasion resistance. PCD inserts are also widely used in the automotive industry where parts like cylinder heads, transfer cases, intake manifolds and oil pump bodies are machined to specification [20]. It is not advisable to use PCD for the machining of ferrous alloys, because these alloys chemically attack the diamond, leading to an increased tool wear [21].

PCD is available in different grades that are differently suited for the machining of non-metals and nonferrous metals. The addition of other substances that act as a type of binder that facilitates the intergrowth of diamond crystals, will have an effect on the properties of the final product. This binder phase can be either a metal or carbide, although boride and nitride are also occasionally used. The binder can be added as a powder or as a coating on the diamonds [19]. The goal of these elements is to support the production process or to improve certain properties. For example, the addition of boron oxide to the cutting material matrix increases the diamond grains' ability to resist oxidation. The property profile of PCD is thus determined by the cutting material components and their specific properties. These components are diamond grains of different sizes and an intermediate phase made of metal or ceramic. Other elements are also present in small amounts in the cutting material matrix [22].

Fowler [21] identified how characteristics of the different PCD grades influence their machining properties:

- Smaller grain size requires more binder material to sinter ➔ Lower maximum working temperature.
- Reduction in grain size increases transverse rupture strength, but reduces toughness of the cutting edge ➔ Increased resistance to crack formation, but lower resistance to crack propagation.
- There is an increase in thermal conductivity with an increase in E, relative to the amount of cross-linking between diamond grains ➔ Reduced thermal gradients within the insert during machining.

Some important tool material properties have been set out as possible requirements for machining titanium [23]:

- Strong interfacial bonding between the tool and the chip in order to create seizure conditions at the tool-chip interface.
- A low chemical solubility in titanium in order to decrease the amount of diffusion and subsequently lowering the flow of tool constituents into the chip.
- Sufficient mechanical strength and hardness to maintain physical integrity.

PCD possesses all of these properties. The formation of TiC has a large negative enthalpy value (refer Table 3). This TiC film will form due to the reaction of PCD with Ti and act as a barrier, limiting the amount of diffusion between the tool and the workpiece. The toughness of PCD is also relatively high (it is higher than a single crystal diamond) [8].

Conventional tools that are used to machine Ti – alloys include high speed steels and carbide tools. Due to the low thermal conductivity of Ti-alloys these tools can only be used at relatively low cutting speeds. When machining at higher cutting speeds these tools have a relatively short lifetime and it has become accepted that frequent cutter regrinding is necessary. In previous studies conducted by Nabhani [7], it was found that new cutting tool materials (such as PCD) had an increased tool life and produce a better surface finish when compared to the traditionally used tungsten carbide tools. PCD therefore shows promise as an alternative to the traditional tungsten carbide grades for Ti-alloy machining. In order to attain higher cutting speeds when machining titanium alloys such as Ti6Al4V, the tool that is used should be able to suppress the heat generated in the cutting process as much as possible, while dissipating it quickly. The higher thermal conductivity of PCD could therefore perhaps allow for higher cutting speeds to be achieved [9]. Another problem that could occur when employing lower cutting speeds for Ti-alloy machining is case gouging caused by the springback effect of the material. The corner of the case on the cutter exit side can often become gouged due to the springback of material. The increase in cutting speed means that the cutter shears the material with less force and subsequently reduces the amount of springback and resulting surface gouging [21].

In most PCD cutting tool applications, the PCD is only a thin layer (which is typically 0.7 mm thick) that is produced integrally on a thicker tungsten carbide base (which could be up to three to four times thicker). The PCD provides the cutting edge, while the less costly tungsten carbide will supply the tool with the necessary strength and toughness [18]. This configuration for the insert is similar to the inserts used for experimentation in this thesis.

From the information provided in this section it becomes clear that PCD shows promise for the machining of titanium. The hardness of the tool in conjunction with a thermal conductivity second only to natural diamond could provide a solution for machining at higher cutting speeds while still maintaining sufficient tool life.

4. Chip Formation, Cutting Forces, and Cutting Temperature

4.1 Chip Formation

The chips that are formed during machining operations are an important output. The analysis of the chips can reveal what happened during the machining operation. Chips could give information regarding both forces and temperatures experienced at the cutting zone.

Different theories exist about the mechanics surrounding chip formation. Chip formation is influenced by cutting speed as well as feed rate. An increase in cutting speed could bring forth a transition in chip formation from continuous to segmented chips [24]. Figure 7 [25] illustrates the difference between the two different chip formations. The mechanics of segmentation is illustrated in Figure 8 [26].

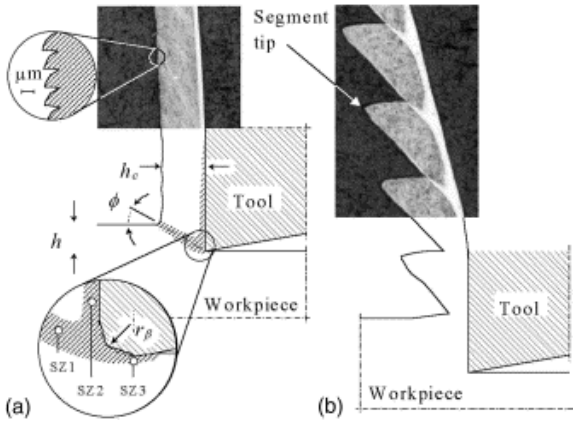

Figure 7: a) Continuous chip and b) Segmented chip [25].

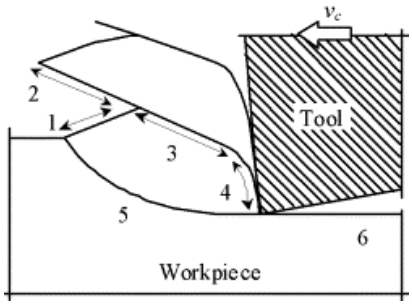

Figure 8: Segmented chip formation for the machining of Ti-alloys [26].

According to Komanduri et al. [27] and Bing Hou et al. [28], the transition from continuous to segmented chip formation is a discontinuous process brought forth as a result of thermoplastic instability in the shear zone (refer to line 5 in Figure 8). The transformation of high amounts of energy due to deformation, in combination with short term processes, causes adiabatic conditions to exist in the shear plane. This phenomenon is known as catastrophic shear [29, 30, 31, 32, 33]. An assumption that is made by these authors is that plastic deformation leads to an increase in strength. At the same time an increase in temperatures are brought forth due to deformation. This temperature increase leads to thermal softening of the workpiece material in the shear zone. Due to the large amount of heat generated in the small shear zone, it can be assumed that the thermal properties are adiabatic and lead to high temperatures. If plastic deformation causes a balance between the thermal softening and the increase in strength, a sudden shearing of the chip segment will be caused [24].

Shaw and Vayas [34, 35] believe that the reduction of shear strength is caused by other effects. They believe that chip segmentation is caused by microcracking. These microcracks are formed due to the brittle nature of many materials when subjected to high deformation rates. This implies that chip formation at high cutting speeds is due to brittle fracture sensitivity in the workpiece material. The shear rate rises with an increase in cutting speed, decreasing the contact area of two consecutive chip segments. The further increase in the cutting speed will eventually lead to a total separation of two consecutive chip segmentations. Another difference when comparing continuous chip formation processes to a cutting process with segmented chip is that less deformation of the workpiece is required for segmented chip formation processes [24].

Barry et al. [25] studied chip formation for Ti6Al4V at cutting speeds that ranged between 15 – 180 m/min and feeds between 0.02 – 0.1 mm. They found that chip formation for titanium was segmented across the range of all the experiments that were done. At lower feed or cutting speeds the segmentation of the chips were aperiodic. An increase in either feed or cutting speed would eventually lead to a transition from aperiodic segmented chips to periodic segmented chips.

Kuljanic et al. [8] investigated finish milling of titanium compressor blades with a PCD cutter and found that the chip morphology was lamellar. The formation of lamellar chips influences the periodical change in the cutting force and thermal stress. Even more so, because of the mechanism of milling, there is a sudden increase in cutting force and temperature as the insert enters the material, and a sudden decrease as the inserts exits the material.

With regard to what is mentioned in this section, the importance of doing analysis of chips is stressed. The output of this could help to determine what happened at the tool-chip interface. For this reason chips were gathered and analysed during the experimentation stages of this thesis.

4.2 Cutting Forces

The analysis of cutting forces could help to determine the effect of altering certain cutting parameters such as cutting speed, feed rate and depth of cut. It could also help to determine mechanical property requirements for cutting tool materials for different cutting processes. The accurate prediction of cutting forces can also contribute in the controlling of tool deflection and machining accuracy.

An important consideration to take into account when milling at higher cutting speeds and forces is to ensure that the inserts as well as the component parts of the milling cutter remain securely in place. The cutters that are designed for high speed milling applications have a tapered thickness which, when tightened into the pocket with wedges, will lock securely against the cutter body. The insert will tend to push back into the pocket under the influence of the centrifugal forces. It is also important to ensure that the cutter body is well balanced at high cutting speeds, because a slightly off-balance cutter would transmit vibration back into the workpiece, causing a reduction in tool life and a poor surface finish [21].

In milling operations cutting forces are mainly determined by the maximum chip thickness, the cutting speed, and the average flank wear. An increase in chip thickness will lead to an increase in cutting forces. The opposite is true when increasing cutting

speed. This means that if the cutting speed is decreased enough it could reach the TRS (transverse rupture strength) of the tool material and subsequently cause chipping of the cutting edge [16].

The diamond crystals of PCD used for milling inserts are larger than the crystals used in turning inserts. This makes the milling inserts more impact resistant. The increased resistance to fracture by impact is the main cause for increased tool life in interrupted cutting applications, such as milling [21].

In the experiments that were conducted by Narutaki and Murakoshi [9], cutting forces were measured for the machining of titanium alloy Ti6Al4V and a carbon steel (0.45% C). Both these materials were cut with a tungsten carbide tool under similar cutting conditions. The reason for these experiments was to find a comparison between the cutting forces for titanium alloy and carbon steel machining. It was found that cutting forces during titanium machining were almost half of the cutting forces measured during carbon steel machining. This brought forth the conclusion that machinability of titanium alloys are quite reasonable when considering cutting forces and that the main cause for tool wear during titanium alloy machining is probably the generation of high cutting temperatures.

4.3 Cutting Temperature

Cutting temperature has a significant influence on both the tool life and the cutting forces. Figure 9 indicates typical cutting temperatures that can be expected for titanium machining at different cutting speeds [94].

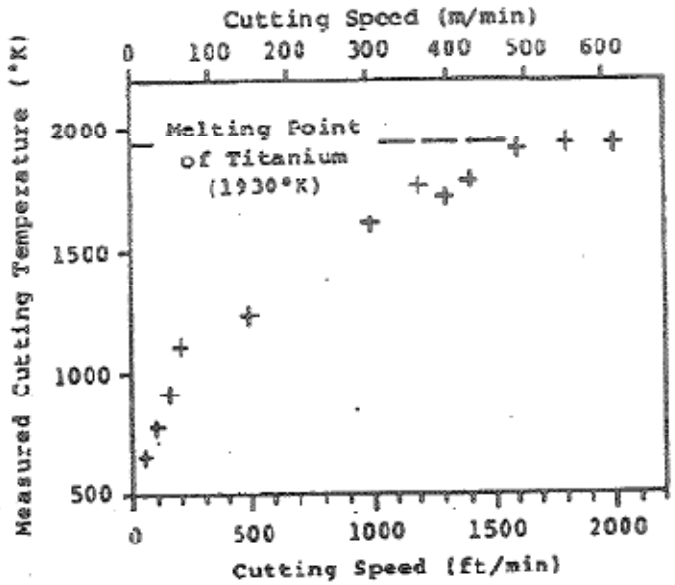

Figure 9: Cutting temperatures for titanium at different cutting speeds [94].

The thermal conditions in intermitted machining operations like milling differ significantly from the heat conditions in continuous cutting operations such as turning. In milling operations the tool is submitted to cyclic heating and cooling when the tool enters and exits the workpiece material. This will lead to a phenomenon known as thermal fatigue [36]. Thermal fatigue (or shock) plays a significant role in shortening tool life for tungsten-carbide tools, but has a much less significant effect on PCD inserts, due to the higher thermal conductivity of PCD leading to a reduction in thermal shock experienced by the insert.

The cutter teeth are heated intermittently at the corners through the contact with the workpiece during milling. The temperature of the cutting tooth material varies through the insert. This variation of cutter teeth temperature involves two processes. The first process happens when the tooth enters the workpiece. Heat is now generated in the

contact area between the chips and the rake face. The generated heat raises the temperature to a high level and it is conducted into both the tooth and the chip. The result of this is a steep temperature gradient. The second process happens as the tool exits the workpiece. The temperatures on the former contact area between the tool and the chip will now suddenly decrease due to the absence of a heat source and forced convection conditions at the rake face. This causes the temperature in the tool to redistribute. The temperature rise and drop occurs cyclically [36]. This sudden decrease in temperature is the result of the cold air stream (or coolant stream) and causes tensile stresses on the tool surface. This causes cracks to develop in the tool and ultimately leads to thermal fracturing of the tool [36].

Figure 10 indicates temperatures measured by Kitagawa et al [96] during milling operations of Ti6Al6V2Sn at a cutting speed of 100 m/min and a feed rate of 0.1 mm/rev with K10 carbide inserts. In the case of dry machining temperatures fluctuated between about 820 ℃ for tool entry, and 200 ℃ for tool ex it. The dashed line indicates the temperature fluctuation when using flood lubrication (50 times diluted soluble oil supplied at 6 ℓ/min). For these experiments temperatures fluctuated between about 820 ℃ for tool entry, and 100 ℃ for tool exit. This illustr ates that thermal shock could be amplified by the addition of coolant to a milling process.

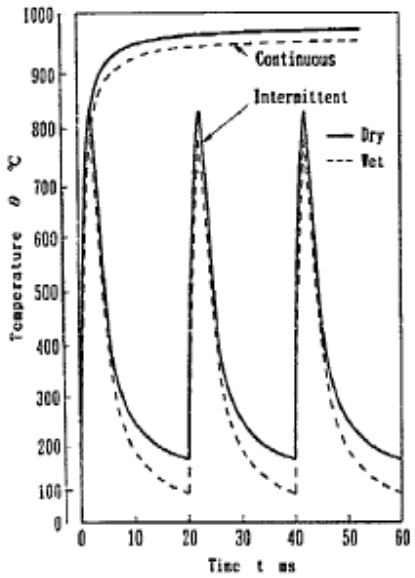

Figure 10: Temperature fluctuation in milling operations of titanium [96].

The formation of thermal cracks is a familiar sight in intermittent cutting applications such as milling. Su et al. [37] conducted experiments investigating the effects of cooling methods on the tool wear of WC-inserts in high-speed end milling of Ti6Al4V, and found that the alternation of stress and the periodic thermal shock resulted in the initiation of thermal cracks which propagated as cutting progressed. According to Viera et al. [38] and Lui et al. [39], the application of a lubricant could amplify the temperature differential between the tool's in-cut and tool exit, and subsequently accelerate the formation and propagation of thermal cracks for tungsten carbide inserts. Thermal cracks that are formed at high cutting speeds weaken the cohesive bonding strength of the tool substrate. This can cause pieces of the cutting tool material between these cracks to be pulled out of the cutting edge. In some studies it was found that the impact of thermal cracks on tool life were minute, and it was concluded that they only caused chipping and fracturing of the cutting tool once they have formed and propagated to a severe extent [40, 41, 42].

According to Barnett-Ritcey et al. [6] a material's thermal shock resistance is a function of its toughness and thermal conductivity. The thermal conductivity of PCD is typically 500 W/mK, which is about 5 times higher than most carbide tools. Carbide tools have a higher fracture toughness than PCD however. PCD is thus more susceptible to mechanical shock, but more resistant to thermal shock. This implies that PCD is more suited to higher cutting speeds where more heat is generated and lower cutting forces occur.

This stresses the importance of applying the correct lubrication strategy for the correct cutting tool and process. An abundance of coolant could increase the thermal shock influenced by the insert, while a lack of lubricant could cause an increase in thermo-chemical attack and also lead to a decrease in tool life.

4.4 Influence of Cutting Parameters

Alternating different cutting parameters (cutting speed, feed rate, depth of cut and radial immersion) will have an effect on the chip morphology, generated cutting temperature and the load exerted on the insert.

In previous studies that were conducted on machining performance, the effects of alternating different cutting parameters were examined. Mori et al. [43] concluded that for a given cutting speed, by alternating the cutting conditions the heat input into the system can be reduced. Komanduri et al. [44] proved the same by alternating the tool geometry (radial rake, clearance, and edge preparation). Koening [45] also reduced the heat to the system by increasing the thermal diffusivity of the tool, while Fritzsimmons et al. [46] and Lui et al. [47], removed heat through the application of an external coolant supply.

The experiments conducted by Barnett-Ritcey et al. [6] yielded good values for tool geometry during the milling of Ti6Al4V. It was found that better results were attained for inserts that had a sharp edge opposed to a hone of 20 μm and that inserts with higher clearance angles also performed better. It was found that inserts with a 10˚ clearance angle were less susceptible to flank wear than those with a 6˚ clearance angle. According to Komanduri et al. [44] the reason for this is the fact that an enlarged clearance angle results in a shorter contact length between the cutting edge and the previously machined surface. Larger nose angles also outperformed smaller ones.

Barnett-Ritcey et al. [6] compared two carbide inserts against each other at similar cutting speeds for peripheral finish milling of Ti6Al4V. It was found that a certain tool (tool A) performed better than the other tool (tool B) at a cutting speed of 152.4 m/min, while tool B outperformed tool A at cutting speeds of 229 and 305 m/min. This phenomenon was credited to the tool geometry. The included edge angle of tool B (64˚) was smaller than that of tool A. This made tool B more susceptible to mechanical stress. As the cutting speed is increased, the cutting forces are lowered (as discussed previously) and the required tolerance to mechanical stress is reduced. As the cutting speed is increased, more heat is generated. This is where the tool rake angle will play

an important role. Less heat was generated for tool B at higher cutting speeds because of its larger rake angle (20˚) opposed to the smaller rake angle (6˚) of tool A. The reduction in heat generation subsequently led to an increase in tool life for tool B at higher cutting speeds. It is also important to remember that by increasing the rake angle, the insert becomes more susceptible to mechanical shock. In the experiments it was found that flank wear was the dominant wear mechanism for the small (6˚) rake angle inserts, while rake face chipping occurred for larger rake angles (20˚).

The influence of different feed rates and axial depth of cut were also investigated by Barnett-Ritcey et al. [6]. It was found that for all the experiments, high feed rate values resulted in excessive chipping of the whole cutting edge, causing a shortened tool life due to mechanical stresses. Adequate feed values were determined to fall in the range 0.025 – 0.038 mm. It was also found that axial depth had little influence on the tool life, other than determining the position where the flank wear will occur.

Barnett-Ritcey et al. [6] also concluded that larger nose radii performed better under all cutting conditions. In the case where an insert have both a positive effective rake- and clearance angle, the initial contact between the tool and the workpiece will occur at the tip, which is most susceptible to mechanical shock. By increasing the nose radius, the edge tip is better supported against mechanical shock and enabling it to resist chipping better than a small radius.

An increase in the clearance angle will reduce the contact zone between the tool and the workpiece. This will reduce the heat that is generated due to friction between the workpiece and the cutting edge and subsequently reduce the heat generated by the cutting process. An increase in clearance angle will lead to a smaller included angle and subsequently weaken the cutting tool. A clearance angle of 10˚ will work best for roughing applications with flood cooling, while a 5˚ clearance angle should be used for milling operations employing through spindle lubrication [6].

According to the conclusions made by Barnett-Ritcey et al. [6], the following cutting configurations will increase the milling performance of Ti6Al4V with PCD inserts:

- The feed should be relatively low (between 0.025 – 0.038 mm) in order to reduce chipping.
- A sharp edge should be employed with a 6 – 10˚ clearance angle.
- A 6˚ rake angle works well in most milling applications, but a 20˚ rake angle works better for high speed finishing.
- Use a large nose radius if possible.

The information presented above shows that a small change in certain parameters can have a vast influence on the final performance of the machining process. The sensitivity of parameters to a reduction in tool life differs though. Figure 11 was taken from Sandvik's titanium machining application guide [48] and is a good indication of the sensitivity of some parameters (z – amount of inserts, ap – depth of cut, f_z – feed per tooth, a_e – radial immersion, v_c – cutting speed) to a reduction in tool life for tungsten carbide inserts. It was decided that the two parameters that were to be altered for final experimentation would be the cutting speed and feed per tooth. It can be seen that these parameters are very sensitive to a reduction in tool life for tungsten carbide inserts. The effect of these parameters will therefore also be tested for PCD inserts.

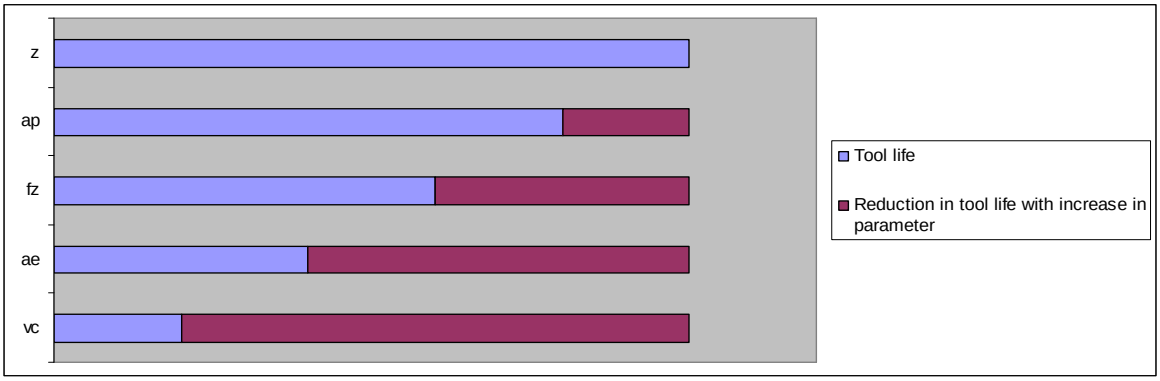

Figure 11: Sensitivity of cutting parameters to a reduction in tool life for titanium machining with tungsten carbide inserts [48].

5. Tool Wear Characteristics

All machining operations will have detrimental effects on the tool. As will be discussed, the severity of the tool wear depends to a great extent on the combination of all the machining parameters. Tool wear has an influence on not only the machining productivity, but it also on the manufacturing efficiency (for instance energy consumption). One of the most important objectives of cutting research is therefore to assess tool wear in order to predict tool life [49].

The ability to predict tool life plays an important role in the design of cutting tools, and the determination of cutting conditions and tool change strategies. Tool life depends on a number of different variables which can include the machine tool, tool material and geometry, work material and cutting conditions [50]. In order to accurately predict the tool life at different cutting speeds, F.W. Taylor formulated an equation that could determine tool life as a function of cutting speed. This is widely known as the Taylor tool life equation:

$$vT^n = C \qquad (1)$$

with v = cutting speed (m/min); T = tool life (min); and n and C are constants that are determined through experimental procedures. This means that if you measure your tool life at two different cutting speeds, the values of n and C can be determined by solving the simultaneous equations. Once this has been done, all the unknown values have been solved for the tool-workpiece Taylor equation. The tool life can now be accurately determined for any cutting speed [51].

A cutting tool's useful life can be defined in terms of the progressive wear that occur on a tool's rake face (crater wear) and on the clearance face (flank wear). It makes more sense to define tool life in terms of the flank wear land width. The reason for this is that once a certain level is reached, the flank wear land width will have a significantly negative influence on the dimensional accuracy and surface finish of the workpiece as well as the stability of the whole machining process [50]. This is also an extremely important consideration for the machining of thin components, such as titanium

compressor blades, where worn tools would cause self-induced vibrations [8]. According to the wear growth curve, tool wear can be divided into three regions (see Figure 12 [51]):

- Break-in period: The sharp cutting edge wears rapidly at the beginning of its use.
- Steady state wear region: Follows the break-in period. The wear occurs at a fairly uniform rate.
- Failure region: Follows the steady state wear region. The wear reaches a level at which the wear rate starts to accelerate once more. At this stage the cutting temperature is higher and the general efficiency of the cutting process is reduced. If the cutting operation is allowed to continue, the tool will finally fail due to temperature related failure.

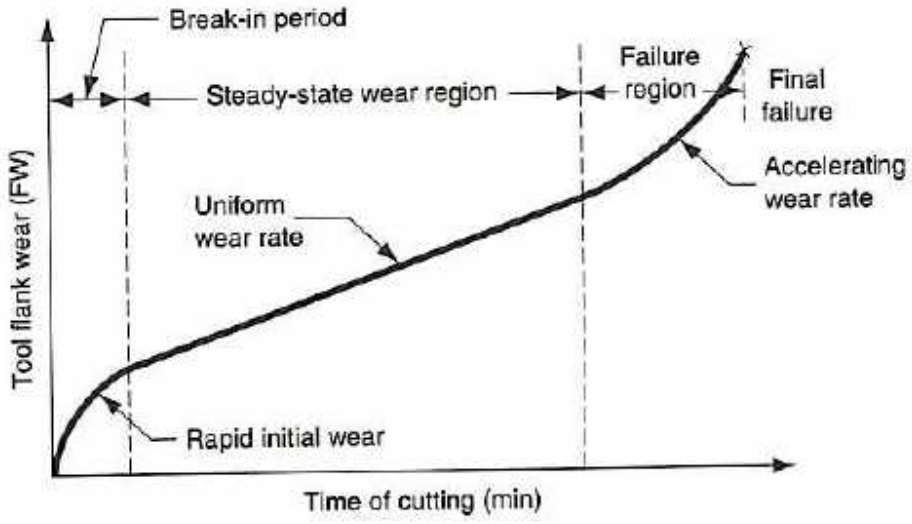

Figure 12: Tool wear as a function of cutting time [51].

The main reason that titanium alloys are viewed as difficult-to-machine materials is predominantly due to the increased tool wear associated with titanium alloy machining. The machining of titanium alloys are characterized by an extremely high cutting temperature and a strong adhesion between the tool and the workpiece material. These phenomena are due to the low thermal conductivity and chemical reactivity of titanium alloys [9].

In the experiments conducted by Hung et al. [52], where the tool wear of PCD was considered when machining hard-to-machine materials, it was found that PCD tools with larger grains (e.g. 50 µm) performed better than PCD grades with smaller grains (e.g. 5 µm). According to Arsecularatne et al. [50], the wear of PCD tools is not yet fully understood. The reason for this is that different scientists have different theories about the major wear mechanisms of PCD tool in machining operations of hard-to-machine materials.

Experiments conducted by Hung et al. [52] also concluded that the main causes for PCD tool wear were abrasion by dislodged diamond grains and/or fatigue and micro-cracking. Lin et al. [53], Antonio et al. [54], El-Gallab et al. [55] and Andrews et al. [56] investigated PCD tool wear in the machining of an aluminium alloy reinforced with 20% SiC particles. Lin et al. [53], Antonio et al. [54] and El-Gallab et al. [55] concluded that the main cause for the grooved wear patterns observed on the flank faces on the PCD inserts was abrasion. The grooves were assumed to be the product of abrasion between the cutting tool and the hard SiC particles. Andrews et al. [56] on the other hand attributed the wear to abrasion and adhesion. It was concluded that, since the hardness of PCD is higher than that of SiC, abrasion should rather be associated with micro-mechanical damage than micro-cutting.

Chipping of the rake face occurs due to mechanical overloading or thermal shock. To avoid chipping due to mechanical overload it is important for the transverse rupture strength (TRS) of the tool not to be exceeded by the mechanically applied load. In order to avoid chipping due to thermal shock it is important to maximize certain parameters. For Ti6Al4V milling it is important to use a tool with both a high TRS and thermal conductivity, coupled with a low E and thermal expansion value. During the milling operation the highest mechanical load will be experienced when the insert enters the workpiece material and the highest thermal shock will occur when the insert leaves the workpiece and enters the coolant stream [16].

Barnett-Ritcey et al. [15] concluded that the mode of wear is determined by the heat transfer coefficient (*h*) of the coolant application. For low values of *h* it was found that the mode of tool wear was flank wear (mode I), while chipping of the rake face is the wear mode for high values of *h* (mode II). An increase in *h* for mode I will cause a

reduction in the amount of flank wear and increase the tool life. An increase in *h* for mode II will lead to an increase in the thermal stress and subsequently cause rake face chipping to occur earlier. For *h* values that lies between mode I and mode II, both micro-chipping and flank wear is observed (mode I & II).

Mode I & II begin as soon as the stress caused by thermal shock exceeds the TRS of the tool material. For *h* values below a certain threshold, the probability of chipping on the rake face is 0% (mode I). For values of *h* above a certain threshold the probability of chipping on the rake face is 100% (mode II). Between these thresholds, there exist a *h* value, corresponding to the TRS of the tool material, where the tool life for mode I & II will decrease from mode I to mode II [15].

In the experiments conducted by Davim et al. [57], it was found that the main wear mechanism for PCD tools were an abrasive form of flank wear in both turning and drilling applications. Although genuine PCD particles are harder than most of the particles found in the workpiece material, PCD employed in cutting tools usually contain cobalt as a cementing agent and tungsten carbide. These particles have a lower hardness than some particle found in the workpiece materials, in which case bond between the cobalt and the tungsten carbide can be damaged by the harder particles, leading to the degrading of the tool [57]. According to Lane [58], this mechanical wear experienced during machining operations is credited to the transfer of kinetic energy from the reinforcement particles to the cutting edge and is mainly dependent on the particle dimensions and cutting speed.

Nabhani [7] conducted experiments where the performances of PCD and PcBN tools were measured against tungsten carbide tools when machining titanium alloys under similar conditions. It was found that the PCD yielded the best results and had the longest tool life (about 3 times that of PcBN and tungsten carbide). According to the author it is possible that diffusion across the tool-chip interface resulted in the formation of an interfacial layer of titanium carbide. This layer would then act as a barrier for further diffusion, reducing the loss of tool material in the chip flow.

5.1 Causes of Different Tool Wear Mechanisms

In order to analyse the wear scar of the PCD and tungsten carbide grades tested during experimentation, it is necessary to look into more detail at the mechanisms behind the formation of the different modes of tool wear. This will assist in developing more accurate interpretation of results. The next section will go into more detail regarding the different tool wear mechanisms.

5.1.1 Diffusion

Diffusion can be considered to be the predominant cause of tool wear at elevated cutting speeds. During the phenomenon of diffusion, atoms from the tool's atomic structure are diffused to the chip at the contact area (refer Figure 13 [59]). These atoms are then carried away in the chip flow of material. The flow of atoms from the tool to the chip will eventually lead to the formation of an adhesion layer and buildup edge [60]. The formation of a crater on the tool rake face is also a common phenomenon when machining at extreme cutting conditions. These wear phenomena are discussed in more detail later.

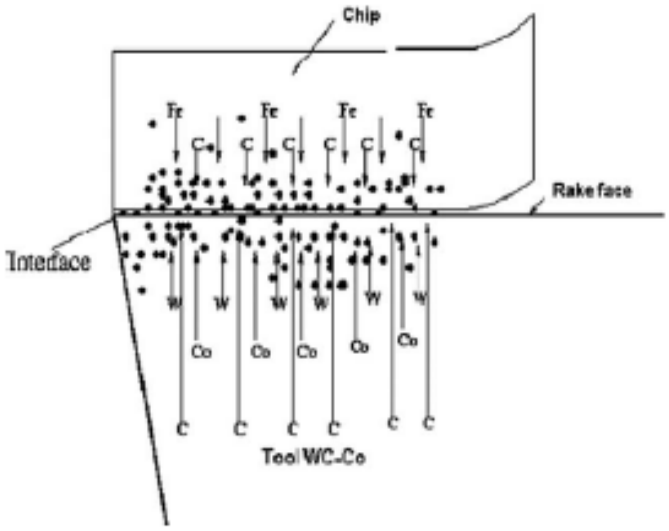

Figure 13: A schematic representation of the diffusion process between a WC-Co cemented carbide tool and steel [59].

Diffusion causes the formation of a crater on the rake face of the tool. Crater wear happens due to the interaction between the underside of the chip and the tool face. This contact happens under conditions of high stresses, high temperature and interface thermo-chemical reactions. All of these conditions will facilitate the wear by diffusion process. It can therefore be assumed that wear at high cutting speeds is a product of a diffusion effect [61].

5.1.2 Abrasive Wear

Abrasive wear occurs when hard particles slide on a softer surface and subsequently damage the interface by either plastic deformation or fracture [62]. The phenomenon of abrasive wear in cutting applications of metal occurs due to hard inclusions of the workpiece material or the separated particles of the tool material that is taken into the tool-chip interface. These inclusions will cause scratch marks that are mostly found on the flank face of the tool. Abrasion wear accelerates the tool wear while the tool is weakened due to crater formation on the rake surface caused by diffusion [63]. In most cases where abrasive wear is present, these scratch marks are clearly visible and are orientated in the direction in which sliding has occurred [62].

Abrasion wear is the predominant wear mechanism when machining at lower cutting speeds. Temperatures on the tool rake face are relatively low at these machining conditions. An increase in cutting speed will subsequently bring forth a rise in the generated rake face temperature. When using lubrication methods such as high pressure through spindle air lubrication or even dry machining instead of flood cooling, the tool rake face temperature will increase even more. This increase in temperature is caused due to the deformation that can be associated with large shear strains in the primary shear zone and the effects of friction caused along the tool-chip interface [64]. This causes the phenomenon known as diffusion. The mechanisms behind abrasive wear by plastic deformation and fracture will now be discussed in more detail.

A - Abrasive Wear by Plastic Deformation

During abrasive wear by plastic deformation material removal can occur due to the following deformation modes (refer Figure 14) [62]:

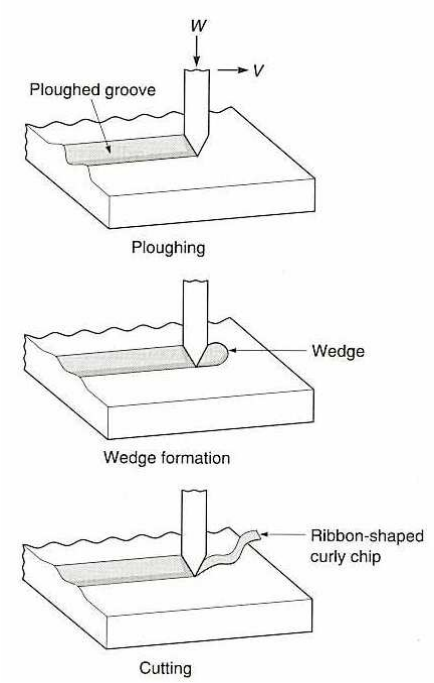

Figure 14: Mechanisms for abrasive wear due to plastic deformation [62].

- Ploughing – A series of grooves formed as a result of plastic flow of the softer material. In the case of ploughing, the material is displaced from a groove to the side without removing any material. If the surface is ploughed repeatedly however, the removal of material will occur due to a low-cycle fatigue mechanism.
- Wedge formation – During this abrasive wear an abrasive tip ploughs a groove and develops a wedge on its front. This phenomenon will normally occur when the shear strength of the interface relative to the shear strength of the bulk material is high (in the region of 0.5 – 1). During wedge formation only part of the material is displaced to the side of the groove. The rest of the material shows up as a wedge.

- Cutting – In cutting abrasive wear the abrasive tip, with large attack angle, ploughs a groove in the material and removes the material in the form of discontinuous or ribbon-shaped debris particles. This process results in significant removal of material with a small displacement of material to the side of the groove.

B - Abrasive Wear by Fracture

At conditions of low loads, a sharp contact will cause only plastic deformation and abrasive wear will subsequently be due to plastic deformation. At loads above a certain threshold brittle fracture occurs through lateral cracking at a sharply increased rate [62].

Fracture wear mechanisms mostly happen in amorphous materials. In these cases lateral cracks are formed due to residual stresses associated with the deformed material [65]. As the sharp contact slides over the surface, these lateral cracks will grow in an upwards direction to the free surface from the base of the region in which subsurface deformation occurs (refer Figure 15 [62]). Material is thus removed in the form of platelets from the region bounded by the lateral cracks and the free surface [62].

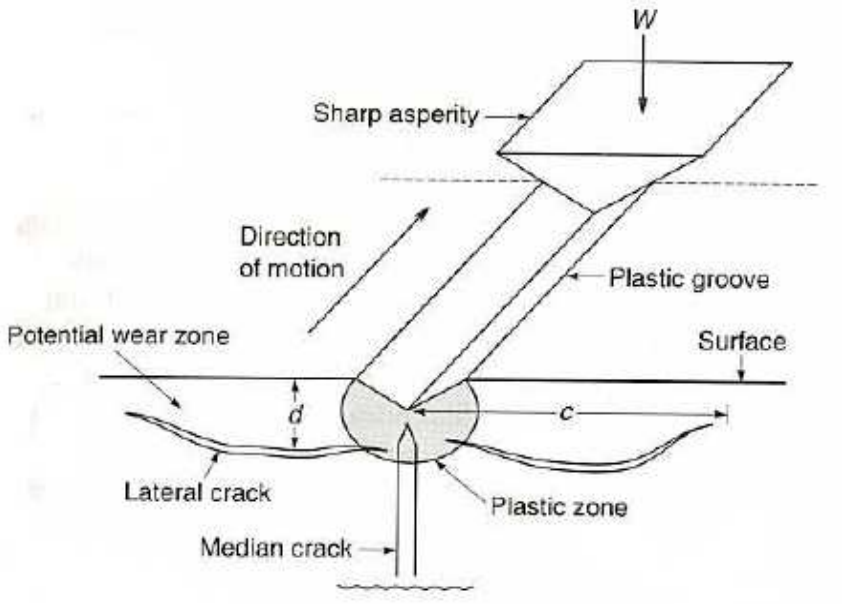

Figure 15: Abrasive wear due to fracture [62].

5.1.3 Oxidation Wear

Chemical or corrosive wear happens due to sliding between two bodies in a corrosive environment. In air, oxygen is the most dominant corrosive medium and therefore chemical wear in air is mostly known as oxidation wear. If there were no sliding taking place, the chemical products of the corrosion (e.g. oxides) would form a thin film layer on the material surface that would act as a barrier and slow the corrosion down. When sliding occurs, the sliding action will wear this thin layer away and causes the chemical attack to continue. Oxidation wear therefore requires both a chemical reaction (corrosion) and rubbing [62].

One of the most important physical properties of sintered PCDs is its resistance to oxidation. In cutting conditions where the tool is subjected to very high cutting temperatures and relatively low pressure, sintered PCD undergoes irreversible changes. These irreversible changes include oxidation, grain boundary weakening, decrease in density and worsening mechanical properties [66].

The reason for this is that at high temperature and normal pressure the oxygen in the air diffuses into the PCD along the grain boundary. Also under these conditions diamond would be changed into graphite. When considering the carbon phase diagram (refer Figure 16), under normal pressure and high temperature, diamond exists in the stable graphite region. This would lead to the grain boundary weakening, a decrease in density and worsened mechanical properties. Also, the oxygen reacts with the graphite and escapes in the form of CO and CO_2 along the weakened grain boundary, causing the PCD to lose weight [66].

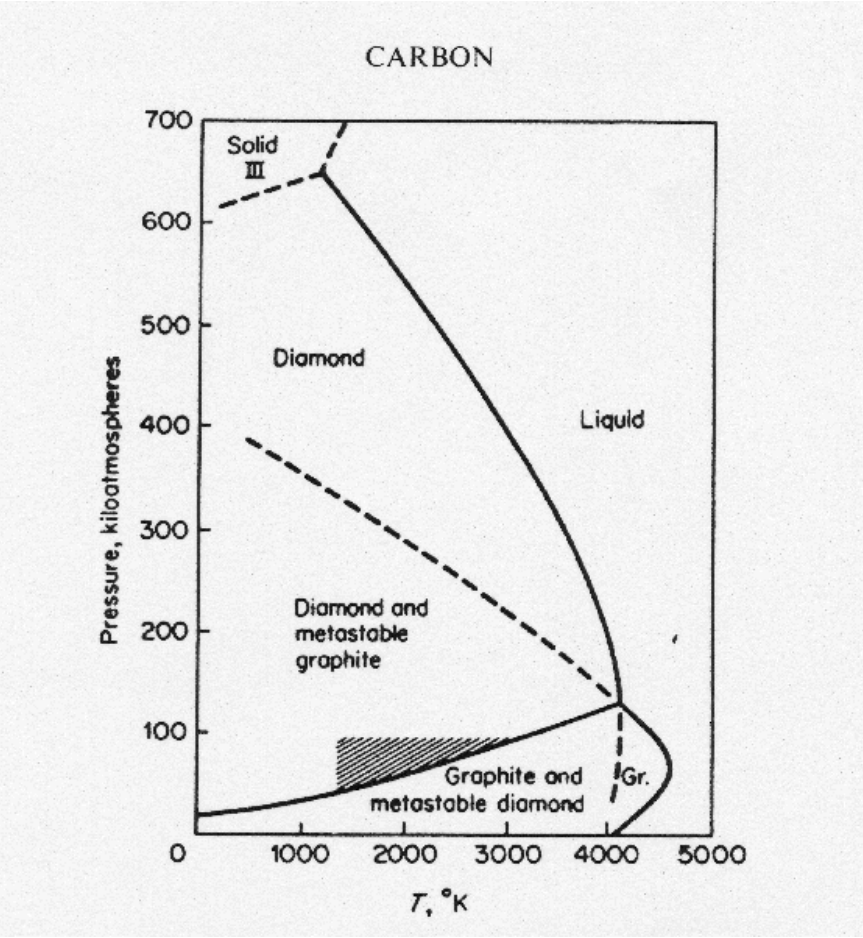

Figure 16: The carbon phase diagram [67].

5.1.4 Adhesion Wear

Adhesive wear occurs when two nominally flat bodies are in sliding contact. Adhesion will occur at the asperity contacts at the interface between these two bodies. Shearing of these contacts occur due to the sliding effect and could result in the detachment of a fragment from the one surface and attachment to the other. These transferred fragments can become detached from the new surface and be transferred back to the original surface, or it can form loose wear particles. Some of the loose fragments become fractured due to a fatigue loading and unloading action and eventually form loose particles [62].

Adhesion wear to a tool operates in a wide range of cutting temperatures [68]. Direct adhesion is adhesion wear that is caused due to the flow of atoms from the tool to the chip. In addition to this type of adhesion wear, adhesion wear can also be caused due to the integration of fragments from the workpiece material to the tool. This type of adhesion wear is known as indirect adhesion wear [69].

Indirect adhesion can occur in two zones of a cutting tool [69]. These zones are the cutting edge of the tool and the tool's rake face. At the tool's cutting edge the formation of buildup edge (BUE) occurs. Adhesion causes the formation of buildup layer (BUL) on the tool's rake face. BUL are observed on the wear scars of tools and are formed as a result of chemical reactions between elements/compounds in the tool/workpiece and the atmosphere. The reactionary products seem to have a melting point that is lower than those of the tool/workpiece materials [70].

During machining operations a tool's nose radius it is subjected to severe conditions of heat and stress. The flank face, which is located near the nose radius of the tool, will therefore also be subjected to severe heat conditions. This will eventually lead to the weakening of the tool. High temperatures will assist in thermal softening, oxidation and chemical attack. As the intergranular bond between the grains of the cutting tool weakens, the grains tear apart under the action of the machining shear stress and are dislodged and pulled out of the workpiece's matrix [63]. As mentioned before, titanium has a high affinity for carbon becomes chemically reactive at temperatures above 500 ˚C. During the machining of titanium high temperatures are generated. Taken that PCD is comprised mostly out of carbon atoms, the formation of TiC is inevitable. The titanium's high affinity for carbon will therefore form a thin layer of TiC which will act as a barrier to diffusion and therefore lessen the pull out of carbon atoms from the PCD tool.

During the machining of strongly adherent workpieces (such as titanium alloys), the workpiece maintains an intimate and sustained contact with the tool rake face through an interfacial layer. The shear that takes place to form the base of the chip exists in the flow zone, situated at or within the interfacial layer. It would be ideal for the material to separate on the chip side of the interfacial layer. In this case the layer would provide protection to the cutting tool [7].

As is expected, the cutting process is not completely ideal. When this interfacial layer is detached on the tool side, the high adhesion forces will result in the pulling out of hard particles from the tool material. This will cause the tool surface to become grooved and the crater depth to increase. During this part of the cutting process, the tool material's resistance to plastic deformation at elevated temperatures is an important property. The higher the resistance to plastic deformation at elevated temperatures, the more resistance the tool will have to this type of wear [7].

The flank face of the tool will also wear in a similar manner under the influence of adhesion forces and grooving. The wear on the flank face will eventually lead to deterioration in the surface finish of the machined workpiece. The combination of the flank wear and crater formation will have a significant impact on the integrity of the cutting edge and will eventually lead to the chipping of the tool. It is during this stage of the process that the facture toughness of the tool material is of importance. A higher fracture toughness will result in a higher resistance to chipping [7].

5.1.5 Ledge Formation

In some cases the formation of a ledge occurs on the edge of a crater. Although this ledge will resist the widening of the crater, the movement of chips will exert a fatigue mode of failure at the inner side of the ledge. This will lead to the deepening of the crater in this zone [63].

5.2 Conclusions from Different Tool Wear Mechanisms

From the information given in these sections it becomes clear that there exists a wide range of wear mechanisms in every cutting process. It is therefore important to determine the main mode of tool wear at different cutting conditions. This will help to better understand which mechanical and thermal properties of tool materials are needed for different cutting conditions and workpiece materials. It can also help to identify which cutting conditions and tool materials cannot be used for certain workpiece materials.

6. Lubrication

Cutting fluids should be considered in an integrated manner in the relevant cutting context. When considering the correct application method and type of lubricant to use, other machining parameters, such as tool geometry, cutting speeds and workpiece material have to be taken into account. The sufficient use of cutting fluids thus depends to a great extent on the machining conditions [71].

The selection of the correct cutting fluid can have a significant impact on the performance of a tool. A situation that is frequently encountered is that considerable effort is put into the selection of the correct tool parameters and machining configuration while the selection of the correct cutting fluid, which could play a significant role in prolonging of the tool life and improving overall machining performance, is sometimes neglected [72].

When deciding on the correct lubricant to use it is important to consider some factors that have nothing to do with the metal cutting process it is used for. Factors such as cleaning, the cost of recycling, the cost of disposal and environmental and health related impact are considerations that need to be taken into account [73]. For example, if the use of a lubricant plays a prominent role in prolonging the tool life and thus increases productivity, but the cost of disposing the lubricant is more than the benefit, the company will be better off without using lubrication.

The first lubricant that was used more than 100 years ago was water. Water has some attractive lubrication properties, such as a very high thermal capacity. Water would therefore assist significantly in reducing the heat generated at the tool-chip interface, but lacked sufficient lubrication abilities. Using water as lubricant led to problems such as corrosion on tools and water was therefore considered a poor lubricant for most machining operations [74].

When the limitations of water as a lubricant became evident, the industry moved towards finding an improved substance to use as a coolant. The obvious choice was oil. Oil offered better lubrication properties than water and although it lacked the thermal

capacity of water, it was still an overall improvement as a lubricant. A consideration that needs to be taken into account is the cost of lubrication oil which is much higher than the cost of water [74].

Soluble oils are a solution that consist of a combination of water and lubrication oil. The idea behind soluble oils is that this lubricant will provide both good lubrication and cooling properties to the machining operation. Different substances are also added to soluble oils in order to prevent foaming, and the formation of bacteria and fungi. Most of the problems associated with using either water or oil individually as a lubricant, were resolved by using soluble oils [74]. Soluble oils will be discussed in more detail below.

According to van der Bijl [72], coolants can be divided into four groups:

- Neat/Straight oils
- Soluble oils
- Synthetic fluids
- Semi-synthetic fluids

Neat oils: These types of oils are derived from either a petroleum (mineral oils), animal or vegetable origin and is used without dilution into water. They prevent rusting and provide good lubrication. Bacteria cannot survive in these oils and cause it to degrade. This is because neat oils do not contain any water for the bacteria to live in. Neat oils can be a blend of one or more base oils and can also contain boundary and/or extreme-pressure additives such as sulphur, phosphorous or chlorine compounds [75].

Neat oils reduce the cutting forces to subsequently produce a smooth surface finish on the workpiece. Neat oils also guard against microscopic welding. A disadvantage of these oils is that they are not flame retardant and can therefore give off smoke that creates an unfriendly machining environment for operators. Oils containing additives are more expensive than the oils without additives, but they are essential in processes where tool life and surface finish are critical [75].

Soluble oils: These oils are mostly suitable for light to heavy-duty machining operations that can include either ferrous or nonferrous applications. Wetting agents and extreme-pressure additives can also be used to expand the application range to include heavy-duty processes normally handled with neat oils [75].

Soluble oils can be divided into semi-synthetic and true soluble oils. These two types differ according to the amount of oil used in the concentrate. Soluble oils normally contain 40% or more oil in the concentrates that are mixed with water to create the final lubricant [75].

The addition of water provides sufficient cooling, while the combination of water and oil contribute to the lubrication capabilities of the liquid. Although soluble oils promote long tool life, they do not provide the same level of lubrication associated with neat oils. As mentioned previously, the addition of water also causes more maintenance to be required, because water makes soluble oils more prone to bacterial growth. Table 4 indicates the functions of different soluble oil constituents [75].

Table 4: Functions of soluble oil constituents [75].

Constituent	**Function**
Mineral oil	Lubrication, rust protection
Fatty oils, esters	Increased lubrication
Extreme-pressure additives (sulphur, phosphorus, chlorine)	Increases tool life
Emulsifiers	Allow mixing with water
pH boosters	Improved rust protection, biostability
Biocides	Controls bacteria and fungi
Defoamers	Controls foam
Antioxidants	Prevents oxidation, varnishing
Dyes, Fragrances	Customer preference

Synthetic fluids: These coolants do not contain petroleum-based oils. Synthetics are also included in concentrates that are mixed with water to formulate the coolant. The addition of water provides the coolants with high cooling power allowing for high-heat and high-velocity metalworking such as surface grinding [75].

Additives can increase the lubrication capabilities of synthetics. When added to some synthetics, additives can improve the lubricating characteristics to be better than some neat oils without additives [75].

Synthetic coolants can be divided into different classes based on their composition [75]:

- **Simple fluids** – Used for light-duty grinding applications.
- **Complex fluids** – Used for moderate to heavy-duty machining at high speeds.
- **Emulsifiable fluids** – Contains chemicals to create specific lubricant characteristics.

Disadvantages of synthetic coolants are that they are more expensive than their oil counterparts. Because they contain no oils, they tend to be more aggressive toward human skin [75].

Semi-synthetic fluids: These coolants are formulated with up to 40% petroleum-oil in a water-soluble concentrate. Constituents that could be added include emulsifiers, wetting agents, corrosion inhibitors, extreme-pressure components and biocides (refer Table 4 for functions) [75].

These coolants can be used for a wide range of tooling applications and provide a good lubrication for moderate to heavy-duty operations. Semi-synthetic coolants allow operators to cut at

higher speeds and feed rates, because they have better cooling and wetting properties than soluble oils [75].

These coolants possess better settling and cleaning properties than neat and soluble oils due to the fact that they contain less oil. Less smoke is also generated due to the decrease in oil. The disadvantages associated with semi-synthetic oils are similar to those of soluble oils (for instance foaming) [75].

Table 5 indicates characteristics of basic coolant types regarding lubrication and cooling (note: in descending order; does not include the effects of additives) [75].

Table 5: Characteristics of basic coolant types [75].

Lubrication	**Cooling**
Neat oils	Synthetic fluids
Soluble oils	Semi-synthetic fluids
Semi-synthetic fluids	Soluble oils
Synthetic fluids	Neat oils

Although the use of lubrication may seem attractive, it has to be taken into account that it may be possible for some operations to be performed without the presence of cutting fluids. Operations such as these are known as dry machining operations. Most machining operations of grey cast iron, pure aluminium and magnesium alloys can be performed as dry machining operations [74].

The application and operation of lubricants are different for low and high cutting speeds [76]:

- At low cutting speeds: The cutting surface is lubricated by the application of cutting fluid. At lower cutting speeds the lubricant can penetrate the interfaces by either hydrodynamic lubrication or by boundary lubrication. The aspect of cooling is not that important, because less heat is generated at lower cutting speeds.

- At high cutting speeds: More heat is generated, resulting in higher temperatures. The added heat makes it more difficult to apply cutting fluid to the interfaces. The cutting fluid is applied to the cutting tool, the work piece and the chip in order to reduce or contain the temperature rise. The tool life is extended through the cooling process. The use of lubrication allows for higher cutting speeds and for an increased production rate.

Although cutting speeds for titanium machining are relatively low compared to the other metals, a much higher temperature is generated. This requires that the cooling power of the lubricant should be high for sufficient machining of titanium alloys, even though lower cutting speeds are employed.

Advantages that can be attributed to the use of cutting fluids are [71]:

- Increased tool life
- Improved surface finish
- Improved tolerances
- Reduction in cutting forces
- Reduction in vibration

Another important advantage of lubrication is that the lubricant also assists in the removal process of chips from the cutting zone. The lubricant also facilitates in the breaking of the chips and can play an important role in the prevention and reduction of corrosion [76].

There are different application techniques of lubricants [77]:

- Hand application
- Flood cooling
- Through spindle flood cooling
- Minimal Quantity Lubrication

Hand application:

This technique is used mostly in small batch production. The reason for this is that it is not practical to have a continuous supply of cutting fluid to the workpiece when the process can be done with much less lubricant. Hand application is mostly used in the machining of parts that are machined at lower cutting speeds where cooling is not that important. The operator will then be able to control the supply of lubricant to the machining operation when needed. Hand application guarantees a low level of lubrication, cooling and chip removal.

Flood cooling:

This application technique is the most widely used in the machining industry. It provides the machining operation with a good level of lubrication, cooling and chip removal. This technique makes it possible to orientate the nozzle for the clearance of the tool surface to reduce the flank wear at low cutting speeds.

Through spindle flood cooling:

Similar to flood cooling this application method also supplies an abundance of lubricant to the cutting area. The lubricant is supplied at high pressure through an internal channel (running through the cutting tool). This allows the lubricant to reach the tool-chip interface where lubrication is most needed. This technique supplies sufficient lubrication and cooling to the cutting process.

Minimal Quantity Lubrication:

Similar to through spindle flood cooling, this technique also supply lubrication at high pressure through an internal channel in the cutting tool. The only difference is that with this technique a very

small amount of lubricant is used. The lubricant is also sprayed directly on the cutting area. This technique guarantees a good level of lubrication, but the cooling capabilities are limited and chip removal is obtained by the air flow used to transport the coolant.

Other methods, such as the supply of liquid nitrogen through the inner channel of the tool shank and the construction of a special tool shank with a built – in large copper plate to act as a heat sink, have been utilised in machining applications instead of using cutting fluids [9].

Some alternative methods have also been reported to control the high cutting temperatures associated with titanium alloy machining. Hong et al. [78] proposed a new economical cryogenic approach that uses focused liquid nitrogen supplied to both the tool-chip interface at the point of the highest temperature and the flank face at the cutting edge through the use of specially designed micro-nozzles in order to improve tool life. Wang et al. [79] used liquid nitrogen cooling in turning applications of Ti6Al4V and found that tool life was subsequently increased by three times. Kovacevic et al. [80] improved tool life and surface finish by using high-pressure waterjet cooling in the milling of titanium alloy. Man [81] compared the effects of using nitrogen-oil-mist and air-oil-mist in high-speed end milling of Ti6Al4V and found that use of nitrogen-oil-mist led to lower tool wear. Yamakazi et al. [82] studied the effect of cooling air in turning applications of Ti6Al4V and found that the tool wear using cooling air was equivalent to that with minimal quantity lubrication. Su et al. [37] investigated the effect of different cooling/lubrication methods on tool wear of coated cemented carbide inserts in high-speed end milling of Ti6Al4V and concluded that flood lubrication is not suitable for high-speed end milling of Ti6Al4V and that compressed cold nitrogen gas and oil mist is the optimal cooling/lubrication condition to improve tool life.

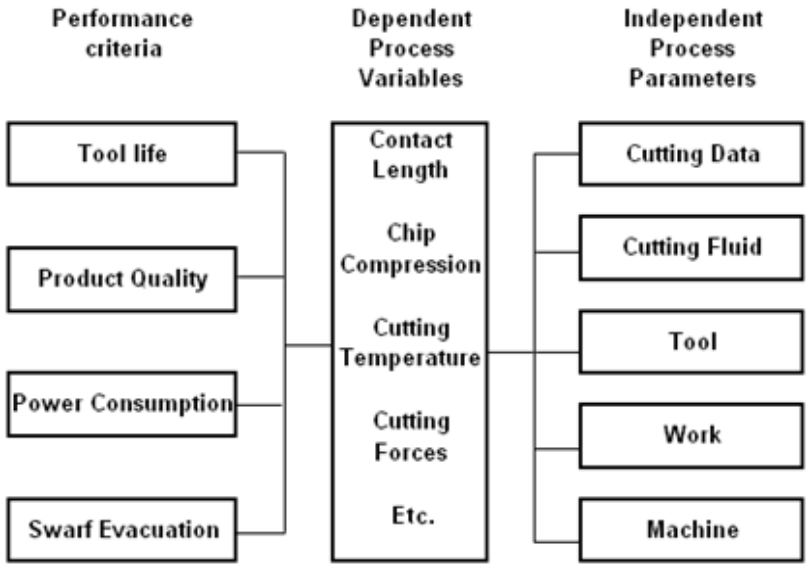

Figure 17: Schematic view of process variables in metal cutting [71].

Figure 17 gives a good representation of the different process variables for cutting processes. It also indicates the interrelationship between cutting fluid and other independent process parameters [71].

It is important to remember that a cutting fluid that gives large improvements in one machining operation for a given performance criterion, may not give the same improvements for other machining operations or performance criteria [71].

The cutting fluid works in two places. It partially improves the cutting process at the cutting point (where the tool is engaged into the workpiece) and partially outside the cutting point. The mechanisms of the working of lubricants can be captured in the following steps [71]:

- Cooling
- Lubrication
- Other physio-chemical effects
- Mechanical swarf removal

Although physio-chemical effects and mechanical swarf removal play an important role in the protection of the newly formed work surface from wear phenomena such as

oxidation, cooling and lubrication have the most pronounced effects on wear reduction [71].

6.1 Cooling

The cutting fluids used during machining operations acts as coolants on the workpiece, tool and swarf. An increase in cutting temperature will have a significant effect on wear mechanisms, such as diffusion and oxidation. For this reason, the sufficient cooling of a machine tool could play an important role in increasing the tool life. Cutting fluids reduces the amount of thermal expansion experienced by the tool during machining operations by reducing the amount of heat generated. The cooling effect of cutting fluids thus plays an important part in keeping tolerances within suitable limits [71].

Cooling also plays a significant role in acquiring a good surface finish, by controlling the formation of buildup edge. The lowering of cutting temperatures produces a shift of the BUE range towards higher cutting speeds. Lubrication (discussed in the next section) also has a significant effect on BUE formation. The cooling of swarf, tool, machine and workpiece also improves the environmental conditions [71].

6.2 Lubrication

Lubrication in cutting processes occurs partially at the cutting point as rake face lubrication and partially as general lubrication outside the cutting point along the flutes of the drill/flanks of a cutting insert. During rake face lubrication less chip compression occurs, while BUE formation, workpiece surface roughness, cutting forces and power consumption, is reduced. During rake face lubrication, a soft film of lubricant is formed at the tool-chip interface that reduces the coefficient of friction [83].

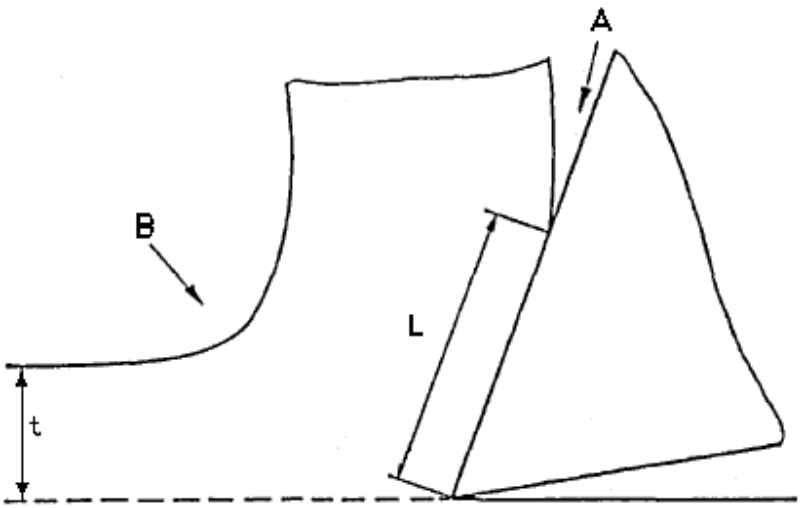

Figure 18: The tool-chip contact length reduction theory [83].

De Chiffre [83, 84] developed a quantitative model for cutting which explains lubrication in terms of contact length between the chip and the tool at the tool-chip interface. The reduction of the contact length between the tool and the chip occurs due to the following mechanisms (refer Figure 18) [83]:

- The presence of lubricant on the tool rake face at A reduces the adhesion of the fresh chip surface onto the tool in the region away from the cutting tool.
- Chip curl is promoted at B due to a Rehbinder effect at low speeds and high cooling rates. These surface mechanisms are expected to work synergistically with the rake face contamination at A.
- The overall reduction of cutting temperature through the cooling effect, lowering the adhesion tendency of the chips to the tool and thus restricting the contact area. The restriction of the contact area implies that there is a reduction in the frictional drag on the tool rake face. This will in turn contribute to a reduction in cutting forces, power consumption and cutting temperature.

According to De Chiffre [84], the reduction in contact length implies:

- The formation of thinner chips due to a reduction of the chip compression factor.
- A reduction in the degree of deformation of the chip.
- A reduction in the chip contact time with the tool.

- The reduction of cutting forces, e.g. the main cutting force that is approximately proportional to the chip compression.
- The decrease in cutting forces leads to a reduction in vibration.
- The formation of BUE is reduced proportionally to the contact length.
- The amount of power required for the cutting process is decreased.
- The heat generated during machining operations is reduced.

6.2.1 Influence of Machining Parameters on the Mechanism of Lubrication

Another important performance indication would be to investigate the influence of machining parameters on the mechanism of lubrication which can be done by considering how the tool-chip contact length is influenced by the different independent process parameters [71]:

- As already discussed, the addition of cutting fluid to a cutting process will reduce the contact length.
- The ductility- and adhesion properties of the workpiece material are of great importance to the magnitude of the contact length.
- The thermal conductivity of the tool along with the affinity between the tool and the workpiece are also important factors. According to Friedman et al. [85], the contact length can be reduced by using different coatings on the tool to reduce the amount of adhesion between the tool and the workpiece material.
- By improving the surface quality of the tool, the contact length can be reduced.
- The tool rake angle influences the contact length. Small rake angles will produce longer contact lengths and vice versa.
- An increase in cutting speed will result in a reduced contact length up to a point (except in the BUE speed range).
- By increasing the feed ratio, a reduction in the contact length factor ($\eta = L/t$ – refer Figure 18) could be attained.
- RC tools (Restricted contact tools) and tools with chip formation geometries will produce a shorter contact length.

It is important to identify cutting configurations where the addition of lubricants will, and will not, have a significant impact. Lubricants will have the most significant impact for cutting conditions where the tool-chip contact length is large, the cutting speed is low or if the workpiece material is extremely adherent. The addition of rake face lubrication will be less required in situations with more favourable cutting conditions, such as high cutting speeds and less adhesive cutting materials [71].

6.3 Lubrication Strategies for Titanium Machining

An important consideration when deciding on the correct coolant to be used is that machining operations of titanium alloys that are done at relatively high cutting speeds could generate enough heat to ignite the titanium chips. In cases such as these, non-flammable coolants should be used [12].

Experiments conducted by Barnett-Ritcey et al. [6] explored the influence of different through spindle lubrication methods regarding the direction and position of the coolant exit (refer Figure 19). The pressure was also altered. The reason for the position of the different exit channels is because of excessive flank wear at the tip for low axial depths and near the depth of cut for large axial depths. The pressures that were used for the experiments were between 150 psi (1031.55 kPa ~ 10 bar) and 600 psi (4126.2 kPa ~ 40bar).

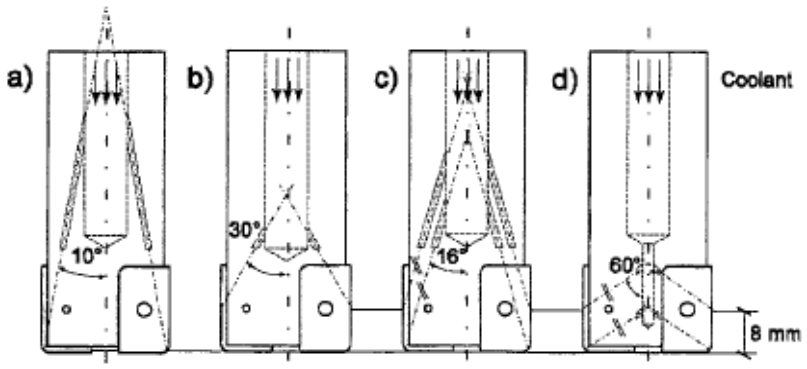

Figure 19: The different through spindle experimental designs [6].

The configuration seen in Figure 19 a) is a typical through spindle design that aims one stream at the nose of the insert at a low angle (10 - 15˚). In the experiments, this configuration increased tool life by 3.3 times compared to flood cooling. When the depth of cut was increased, this configuration helped to reduce flank wear at the nose, but did little for the flank wear in the region near the depth of cut [6].

In the configuration seen in Figure 19 b), the coolant stream is aimed at an angle of 30˚ at the region near the depth of cut. This method extended tool life by 40% compared to the configuration discussed previously and by a factor of 4.6 compared to flood cooling. Where the first method did not suppress flank wear in the region of near the depth of cut, this method did not suppress flank wear at the nose [6].

The configurations seen in Figure 19 c) and d) were designed with the purpose to reduce flank wear in both critical regions. The only difference between these designs is the angle at which the coolant exits the tool. The flank wear for the configuration in figure 19 c) the tool life was similar to that of configuration b). This is probably due to the reduction in the diameter (2.4mm) of the coolant holes, lowering the mass flow of coolant to the critical regions. Another reason that could have an influence is the angle of the exit channels (16˚) which was closer to configuration a) (10˚) than b) (30˚). The angle that the stream exits influences the wear. A larger exit angle results in a more aggressive angle for the coolant to penetrate the area between the rake face and the chip at the cutting edge. The exit channels configuration d) had a diameter of 1.2mm (halve the diameter of configuration c)). This had a significant impact on tool life. The tool life for this configuration was 62% of the configuration in c). This can be attributed to the reduction in cooling power brought on by the reduction in cooling stream diameter. The tool life improvement brought on by the better attacking angle was thus over shadowed by the reduction in cooling power [6].

When considering the effect of different pressures in through spindle lubrication some conclusions were made through the experiments conducted by [6]. When considering carbide tools, an increase in pressure from 150 – 300 psi (10 – 21 bar) improved the ability of the coolant stream to remove heat from the cutting zone and extend tool life. A further increase in pressure caused thermal shock on the tool. At low pressures the

mode of tool wear was flank wear near the depth of cut, while at high pressures rake face chipping was the main mode of wear [6].

According to Barnett-Ritcey [16], increasing the supply of air pressure will increase the tool life over dry milling while avoiding thermal shock to the insert. The heat transfer coefficient of air can reach a value of 2000 W/m^{2}K while water can reach a value of up to 25000 W/m^{2}K. The heat transfer coefficient determines the thermal stress gradient in the insert that leads to thermal shock. The higher the coefficient, the more shock is experienced. Barnett-Ritcey et al. [15] also concluded that it is better to use a "soft-cool" with pressurised air instead of a "hard-cool" with water in high-speed milling of Ti6Al4V when using tungsten carbide inserts.

6.3.1 Recommendations for Through Spindle Lubrication

From the experiments conducted by Barnett-Ritcey et al. [6] the following recommendations regarding through spindle coolant milling of Ti6Al4V were made:

- For small axial depth it is necessary to aim the coolant stream at the nose of the insert. For larger axial depth it would be ideal to supply coolant streams to both the nose and to the region situated at 0.66-0.8 times the axial depth of cut.
- The coolant should reach the crucial region at an angle of 30° in order to increase its penetrating power.
- The coolant stream should have a diameter as large as possible to maximize cooling power.
- High pressure (when assisted by an increase in lubricant mass flow) will assist in dissipating heat from the cutting zone, but could cause an unwanted amount of thermal shock if applied in excess.

6.4 The Minimisation of Coolants Used in the Cutting Process:

In order for a machining process to be stable a balance must exist between the heat that is generated and the heat that is removed during the process. Too much heat during machining operations can cause [49]:

- An increase in tool wear.
- Changes the microstructure of the workpiece.
- Residual stresses on the surface layers of the workpiece.
- Reduction of the accuracy of the operation due to thermal expansion.

When considering a reduction in the amount of coolant to use for a given cutting process, the following requirements should still be met [49]:

- The process must be capable of sufficient heat removal.
- The process must ensure the avoidance of heat buildup above a critical temperature.
- The process should be capable of sufficient chip removal from the cutting zone.
- The process should guarantee acceptable surface finish.
- The process should produce a stable tool wear rate.

There are a few steps that can be taken to meet these requirements. The first step would be to test for alternative forms of lubrication. If dry machining cannot be made feasible, other alternatives should be considered to reduce the amount of lubricant, such as using coolants that are chemically more stable as well as using improved methods of applying the coolants [49].

The tools used during the machining applications can also contribute to the reduction in cutting fluids used. The cutting process can be made more stable by using tools with a high hot hardness and tools that are covered with low-adhesion coatings [49].

Another alternative is to use metallurgical treatments. For example, by adding a small amount of calcium to the tool, the generated cutting temperature can also be reduced, that is, if the workpiece still meets the strength requirements of the component [86]. This

phenomenon is due to the formation of a thin layer on the face of the cutting edge that contributes to the reduction in friction and consequently a decrease in tool wear.

Although considered ideal, not all cutting operations can be done without the use of coolants. Figure 20 [49] illustrates the alternative cutting fluid strategies for cutting processes. A reduction in the amount of coolants used can be done by oil spraying or misting of the coolant, instead of flooding the contact zone with lubricant. Although the amount of lubrication added may be too small to carry sufficient heat away from the contact zone, it could be enough to provide the required lubrication needed to prevent heat generation in the first place [49].

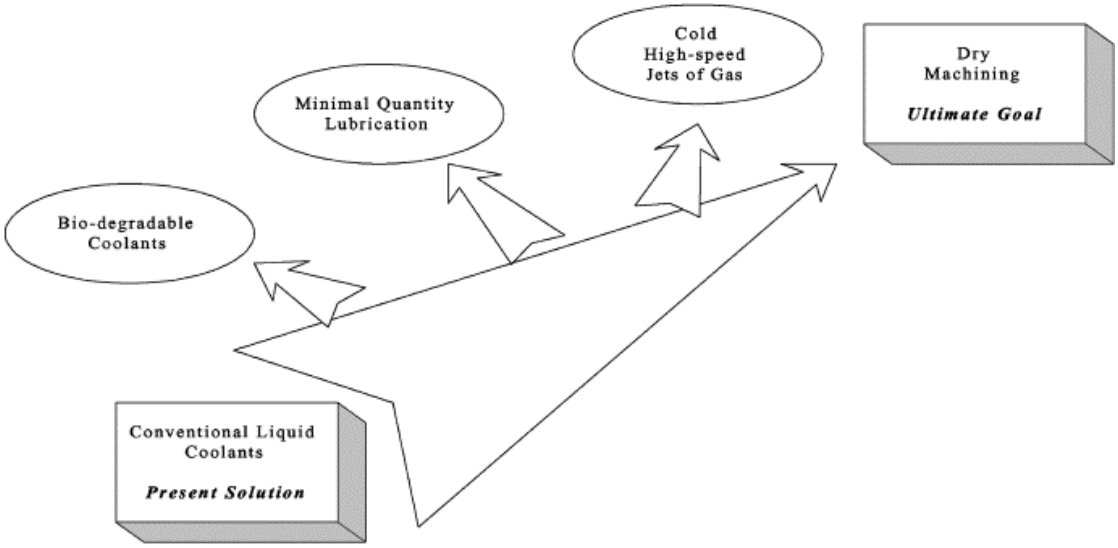

Figure 20: Alternative cutting fluid strategies for cutting processes [49].

7. Pilot Testing

Before experimentation could be conducted, it was decided to do pilot testing on the Ti6Al4V sample with tungsten-carbide inserts in order to determine feasible cutting parameters and strategies for the final experimentation. The different lubrication strategies that were used included flood lubrication, high pressure air lubrication and dry machining. The same type of insert was used for all the experiments in the pilot testing. These inserts were SECO's 218.19-125T-T3-M07 F40M. Wear scar analysis was conducted using an optical microscope.

Figure 21 indicates the tool life in terms of flank wear that was attained in the experiments of Elmagrabi et al [90]. They tested milling operations of Ti6Al4V with coated tungsten carbide inserts at a cutting speed of 77.5 m/min, a feed of 0.1 mm/rev per tooth and a depth of cut of 1 mm.

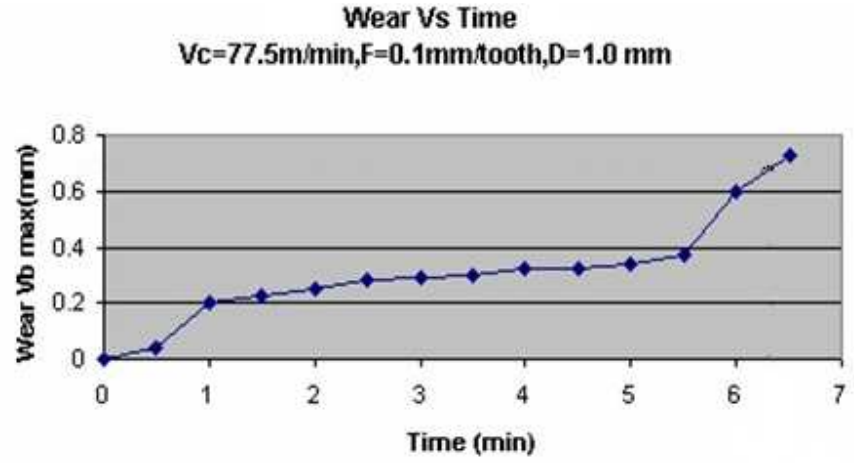

Figure 21: Tool life during the experiments of Elmagrabi et al [90].

Using a failure criteria of a maximum flank wear V_B = 300 µm ([6] and [87]), it could be seen from figure 21 that the insert should last at least 4 min in order to draw useful conclusions from these experiments. Each insert was inspected after 2 min and after 4 min in order to see the wear progression during machining. For the initial experiments it was decided to do a roughing cut at a cutting speed of 120 m/min with a feed per tooth of 0.6 mm/rev and a depth of cut of 0.8 mm. These cutting conditions are extreme for

tungsten carbide considering that a maximum cutting speed of 55 m/min is advised when machining at a feed per tooth of 0.2 mm/rev [93]. Figure 22 a) illustrates the cutting strategy that was also employed during these initial pilot tests. Only one insert was tested at these conditions for both flood cooling and dry machining.

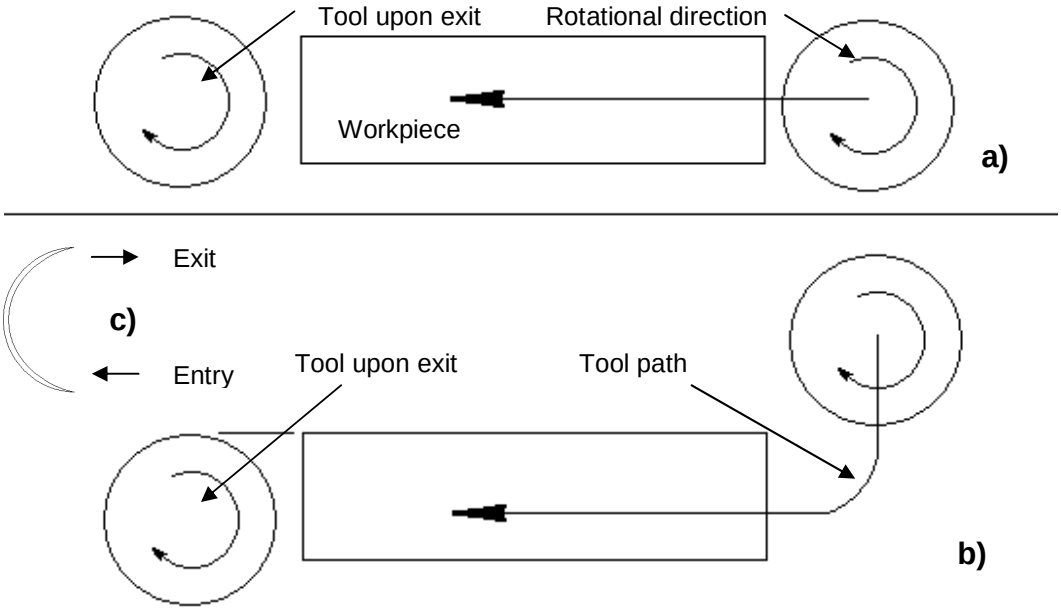

Figure 22: Different cutting strategies used during pilot testing.

The tool only lasted 1.45 min under flood cooling conditions and 35 sec under dry conditions before tool failure. Considering the short tool life, it was decided to alter the cutting strategy and parameters. The cutting speed was reduced to 90 m/min and the depth of cut to 0.5 mm. The feed per tooth was held constant at 0.6 mm. This is more than 3 times the material removal rate of the experiments conducted by Elmagrabi et al [90]. Figure 22 b) shows the new cutting strategy that was employed for these experiments. This strategy is based on different theories that support better cutting practice. The tool is moved off-centre over the workpiece as opposed to centred (refer a)). The strategy also employs a “roll-into-cut” tool path. This strategy promotes tool life by reducing the effective chip thickness as the tool exits the workpiece after each cut. Figure 22 c) shows the effective chip thickness as the tool moves through the workpiece.

The maximum chip thickness (which is equivalent to the feed per tooth) is in the middle of the cut, while the thinnest chips are formed as the tool enters and exits the workpiece. This strategy will lower the cutting and impact forces experienced by the tool during the workpiece entry and exit phases of each cut and subsequently increase the tool life [48].

By employing these strategies, optical microscope images indicated that the rate of tool wear was significantly reduced. Hence, useful conclusions could be made to determine feasible cutting parameters for the final experiments. During these pilot tests the type of insert, as well as the cutting parameters were held constant with only the lubrication strategy (flood, air, and dry) being changed. The finding of these pilot tests are discussed in the next section in more detail.

7.1 Results for Pilot Testing

Figure 23 shows the flank face prior to machining of the SECO 218.19-125T-T3-M07 F40M insert. It was used as reference when comparing the wear progression for the different lubrication strategies used during the pilot tests.

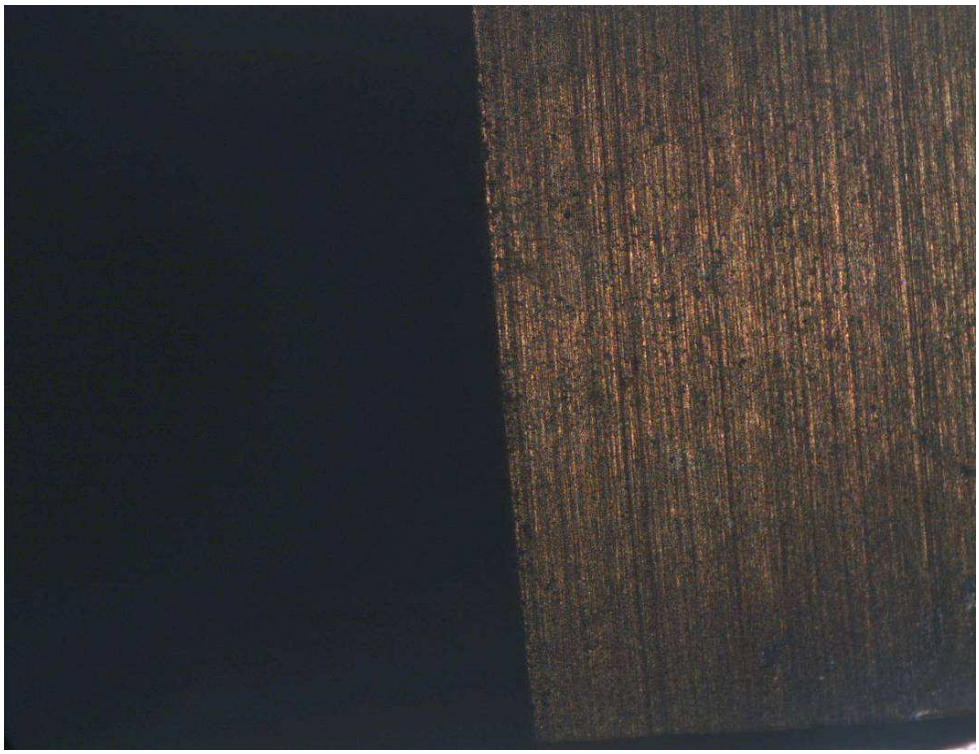

Figure 23: Flank face of an unused insert used during pilot testing (x50).

7.1.1 Dry Machining

This lubrication strategy was used as a benchmark to determine what the effect of adding different lubricants to the cutting process will have on the tool life.

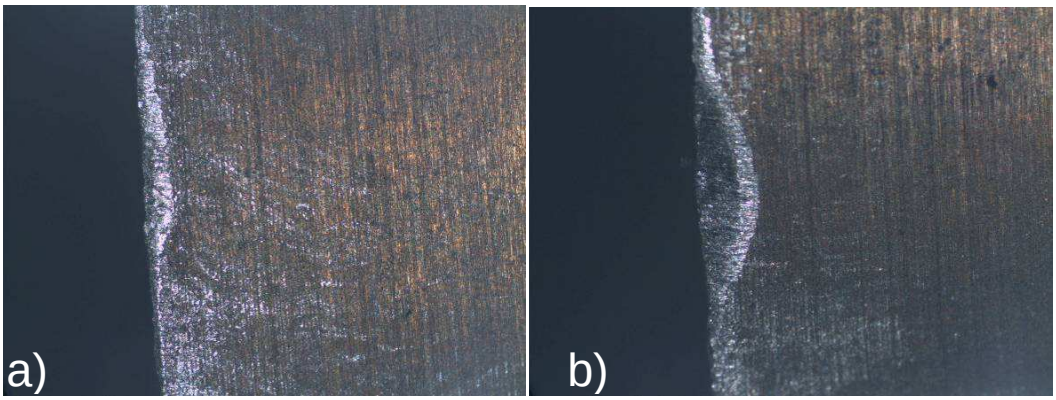

Figure 24: Flank wear after 2min of dry machining (x50).

Figures 24 a) and b) show the flank wear that was recorded after 2 min of machining. Even after this short amount of time substantial flank wear is already visible. This extensive flank wear can be attributed to the expected high temperatures generated during the machining operations at these extreme cutting conditions [9] and [94].

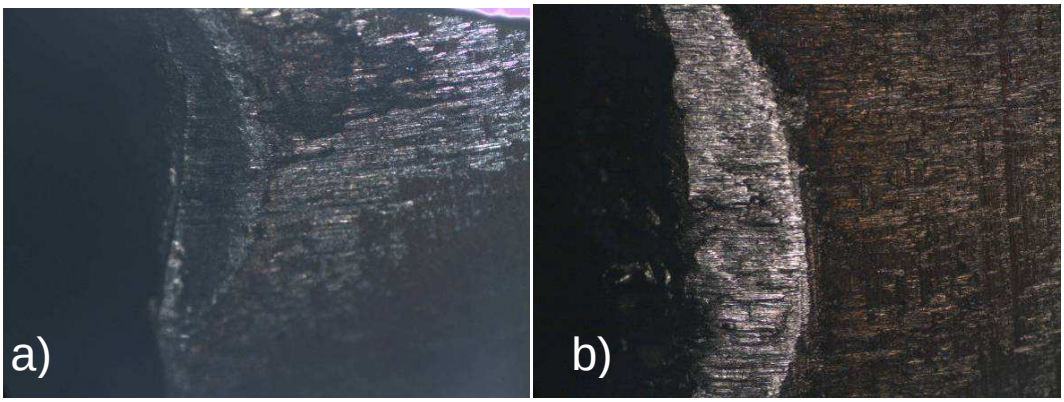

Figure 25: Flank wear failure for dry machining (x50).

Figures 25 a) and b) show the flank wear after further machining at the same cutting conditions. In both cases the tool failed catastrophically due to extensive flank wear as

detected by audible means. The insert in Figure 25 a) failed after 3min of machining. Figure 25 b) indicates the flank wear for an insert after 4 min of machining. After 3.5 min the wear on the insert caused excessive tool vibration and it was decided to lower the feed rate to 50%. It can once again be seen that the tool is not suited for machining operations under these extreme conditions. A flank wear as extensive as witnessed here would have a substantial impact on the integrity of surface finish of the machined Ti6Al4V. This was also witnessed in these experiments where the highly worn insert left a very rough surface finish. These experiments show that dry machining is not suited for the high speed machining of Ti6Al4V with tungsten-carbide inserts. For this reason it was decided not to test dry cutting operations for tungsten-carbide grades during the final experimentation.

7.1.2 Air Lubrication

The same experiments were repeated to assess the effect of using air lubrication. Air was supplied at a pressure of 8 bar to the cutting zone through an external nozzle. The reasoning behind this method is that the supplied air will reduce the cutting temperatures as well as assist in the removal of chips from the cutting zone. Figures 26 a) and b) show the flank wear after 2min of machining. At this stage no real flank wear was visible. The only aspect causing concern was the presence of material transferred to the insert. The chemical composition of this material was not determined. This could either be Ti6Al4V that has been transferred to the insert (start of a buildup edge), or an oxide layer that has formed.

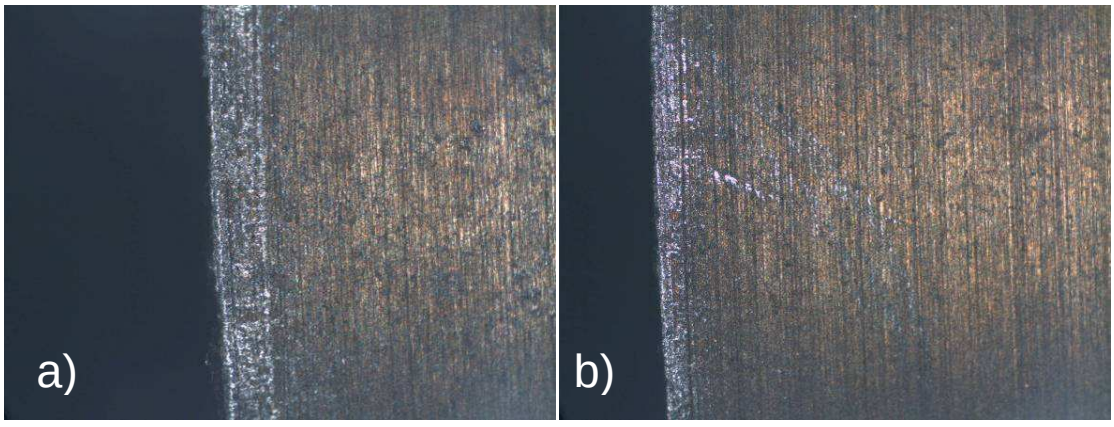

Figure 26: Flank wear after 2min of machining with air lubrication (x50).

The cutting time for this lubrication strategy was then extended to 4 min. The tool did not fail after this time extension and a smooth surface finish, similar to that witnessed after 2 min of machining, was still achieved. Figures 27 a) and b) show the appearance of the inserts after 4 min of machining. Once again a small amount of flank wear was observed. The amount of material transferred to the insert however increased drastically. This could be explained by insufficient cooling and lubrication, causing the workpiece material to stick to the surface of the insert. No crater wear was also observed on the tool's rake face. Therefore the air lubrication assisted sufficiently in the removal of chips. This could perhaps identify a feasible lubrication opportunity by suspending a small amount of lubricant oil or water in the air mixture to assist in lowering the amount of material transferred to the insert. Caution has to be taken when machining at extreme conditions where higher cutting speeds and feed rates are employed, giving rise to higher cutting temperatures. Air lubrication (without suspending any oil in the air flow) could increase the likelihood of causing a fire hazard due to the increased amount of oxygen supplied to the cutting area.

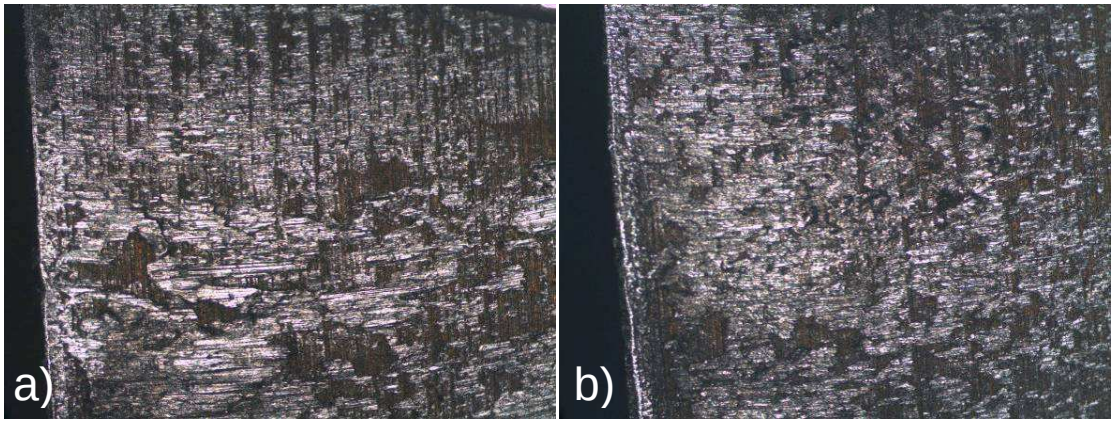

Figure 27: Flank wear for air lubrication after 4 min machining time (x50).

7.1.3 Flood Lubrication

From the first experiments with air lubrication and dry machining it became evident that this lubrication method should theoretically outperform the previous methods, because it solves the cooling and lubrication problems associated with the other methods.

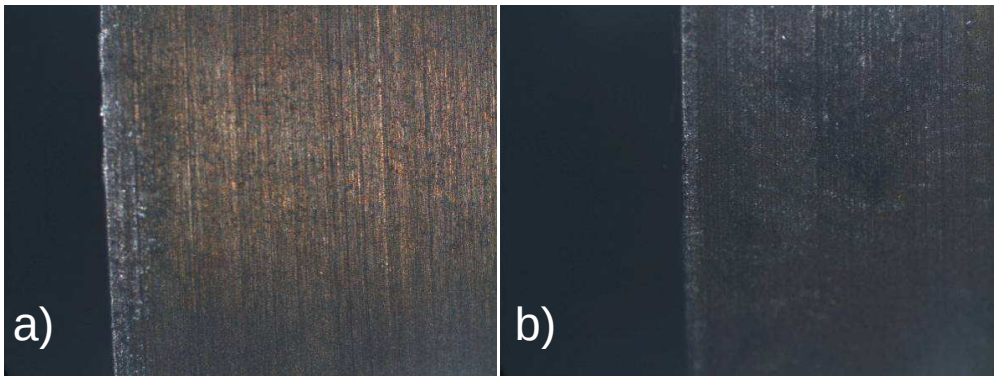

Figure 28: Flank wear after 2min of machining with flood lubrication (x50).

Figures 28 a) and b) shows the flank wear of the inserts after 2 min of machining. There is almost no sign of wear up to this point (compare to Figure 23). It is clear that the sufficient cooling and lubrication properties provided by flood lubrication decreased the amount of flank wear and material transferred to the insert compared to the previous experiments. As in the previous experiments, flood lubrication was tested for 4 min of machining at the same cutting conditions. Figures 29 a) and b) show the flank wear for flood lubrication after 4 min of machining.

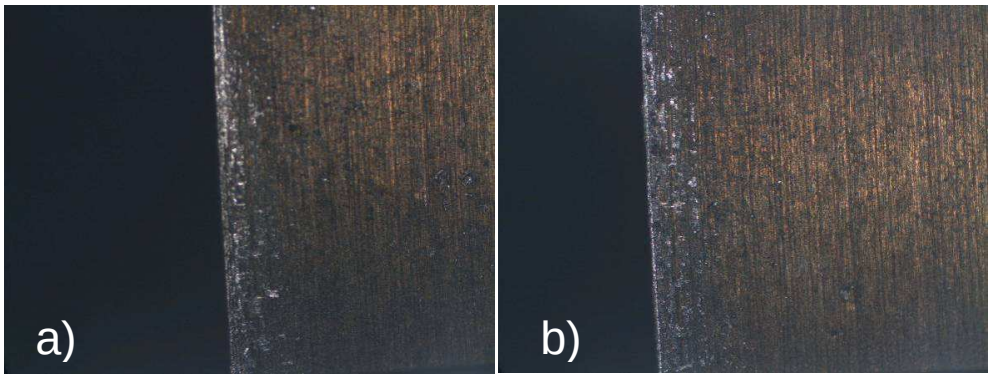

Figure 29: Flank wear for flood lubrication after 4 min machining time (x50).

It is interesting to note the similarity of the wear after 4 min to the wear after 2 min. This shows that wear progression is very slow for flood lubrication, even at these extreme cutting conditions. The purpose of these pilot tests was to determine feasible cutting conditions for the final experimentation. For this reason the tool life of the insert was not determined, because it already proved a sufficient method for lubrication that will be fully tested in the final experimentation. It could however be concluded thus far that flood lubrication performed better than air lubrication and dry machining under similar cutting conditions.

7.2 Conclusions from Pilot Tests

From the pilot tests it became evident that dry machining would be an insufficient lubrication method for high speed machining of Ti6Al4V with tungsten-carbide inserts. The tool lasted less than 4 min. For this reason it was deemed unnecessary to do further testing on dry machining in the final experimentation.

Air lubrication proved to be an improvement over dry machining by providing more cooling and chip removal assistance to the cutting process. This method shows promise as an alternative to flood lubrication when machining at lower cutting speeds and feed rates where lower temperatures are generated. Higher cutting speeds and feed rates could perhaps be achieved by suspending water or oil in the air. This could perhaps assist in an increase in the tool life.

Flood lubrication performed the best of the lubrication methods. This strategy provided the best lubrication and cooling for the cutting process and reduced the amount of material transferred to the insert significantly. No real flank wear was also witnessed, even after 4 min of machining time.

High pressure through spindle lubrication is also a relatively new concept for the milling of Ti6Al4V. It would therefore also be interesting to compare how this application method will perform when compared to flood lubrication.

8. Experimental Setup and Design

The experimental setup and design was constructed in accordance with the project objectives. A secondary objective of the experimental setup was to make economical use of extreme high cost workpiece material (the TI6Al4V test sample, dimensions 560x35x30 mm, cost ± R25 000). A specific aim of the experimental design was to yield conclusive experimental results for interpretation of the effectiveness and suitability of different lubrication strategies.

8.1 Experimental Setup

All of the experiments were performed on a Hermle C40 5-axis high speed milling machine. The specifications of the machine are listed in Appendix A. Figure 30 shows the experimental setup that was used. The titanium sample was held in position using a standard machine tool workholding vice. The initial sample lengths were 560 mm. In order to minimize vibration experienced during the machining process, each sample was cut in halve, yielding two lengths of 280 mm each. This meant that only 40 mm of workpiece material was not clamped at each side. For each experiment the tool passed twice over the length of the Ti6Al4V sample. Each insert was thus used for a cutting distance of 560 mm. After the experiment the insert was removed from the tool and the wear scar was analysed using an optical microscope and a scanning electron microscope (SEM).

Figure 30: The experimental setup

Figure 31 shows a close up of the tool clamped in the machine's toolholder. The arrow indicates the nozzles from which the flood lubrication was supplied.

Figure 31: The external nozzles that direct coolant at the cutting zone for the flood lubrication experiments.

8.1.1 Cutting Tools and Workpiece Material

For the purpose of the experiments two different PCD grades and a tungsten carbide grade were tested. The two PCD grades were CMX850 and CTM302. The tungsten carbide grade was Mitsubishi's VP15TF.

Table 6: Thermal and Mechanical Properties of CTM302 [16] and [87].

Thermal Conductivity (W/mK)	650*
Average Grainsize (µm)	Between 2 – 30
E (GPa)	1049
TRS (MPa)	1152

*Estimated value

Table 6 summarizes the mechanical and thermal properties for CTM302. The thermal conductivity and TRS values for CMX850 are proprietary information that are not

available yet. The CMX850 has a very small grainsize in the order of 1 micron (refer Figure 32 a)). CTM302 has a coarse grain size (in the order of 30 µm, refer Figure 32 b)) compared to CMX850. Using the grain size as the indicative parameter, CMX850 can be expected to have a lower thermal conductivity than CTM302. Similarly, CMX850 is expected to have a higher TRS value than for the CTM302. These values relative to TRS and thermal conductivity values of CTM302 were confirmed by Element 6 researchers [87].

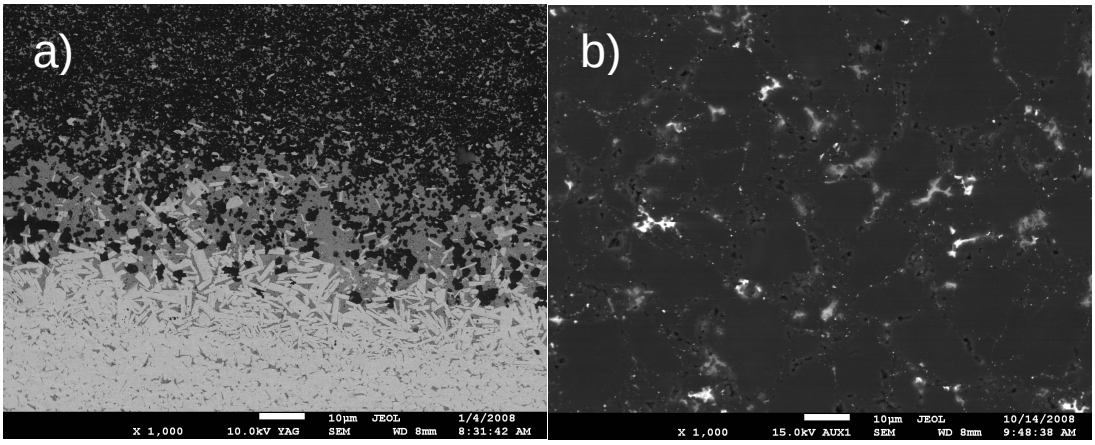

Figure 32: Microstructure of a) CMX850 (x1000) and b) CTM302 (x1000)

The tool maker was concerned that normal insert clamping could lead to a brittle fracture of the PCD. The concern was that the small clamping area of a normal clamp could result in a stress concentration causing the TRS of the PCD to be exceeded. In order to reduce this risk, a customized toolholder which would allow for an increased clamping area was designed for both PCD grades.

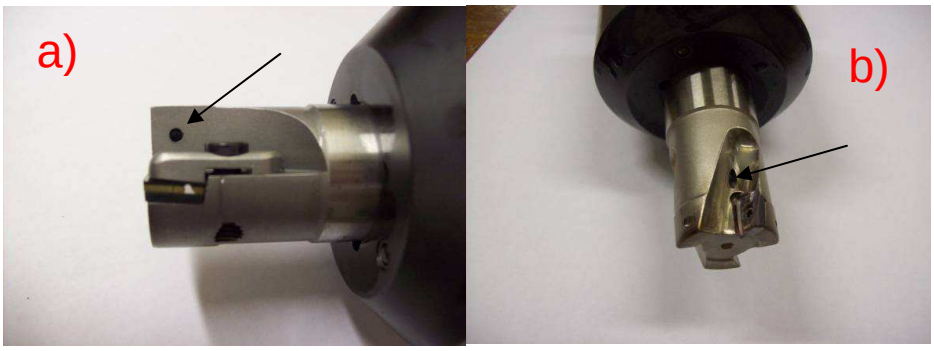

Figure 33: a) The customized toolholder for the PCD grades; b) The toolholder for the VP15TF

Figures 33 a) and b) show how the inserts were secured into their toolholders. The arrows indicate the through spindle lubrication exit holes for both the toolholders for the PCD grades and the VP15TF. All the holes had a 2 mm diameter. The tool for the PCD inserts had 2 exit holes, while the tool for the VP15TF had 3 exit holes. An important consideration that has to be taken into account is the angle at which the cutting fluid exits the spindle. Due to the increased clamping needed in the customized toolholder, a higher exit angle had to be used in order for the cutting fluid to reach the tool-chip interface. The angle that fluid is supplied for the tungsten carbide tool is 10°, while the custom tool has a very high angle in the range of 60°. According to Barnett-Ritcey [16], a larger attack angle could assist coolant penetration between the chip and the insert. Taking this into account, it can be expected that the customized tool holder, with larger coolant supply angle, will provide less sufficient tool-chip penetrating ability which could lead to a reduction in the tool life for the similar through spindle experiments of the PCD inserts compared to the tungsten carbide inserts. The results in this case are therefore considered a conservative indication of the performance of PCD for through spindle lubrication.

The design of the PCD inserts made it difficult for the tool designer to mount it at any angle other than 90º in the toolholder. It was therefore decided to keep the insert at a 90º approach angle and to do shoulder milling operations for the experiments. The roll-into-cut method (discussed in the pilot testing section) was employed in these experiments. The PCD inserts fit into the toolholder in such a way that a 4º rake angle and 3º clearance angle are presented to the workpiece for each cut.

Two samples of Ti6Al4V were used for the experiments. Each of these samples were initially 560 mm in length but reduced to 4 samples of 280 mm each. The samples that were used were grade 5 solution heat treated and aged. It had a tensile strength of 1080 MPa and a Vickers hardness of 360. Table 7 indicates the chemical composition of grade 5 Ti6Al4V, while Figure 34 illustrates the microstructure of Ti6Al4V.

Table 7: Chemical composition of grade 5 Ti6Al4V [91].

	C	Fe	N_2	O_2	Al	V	H_2 (Bar)	Ti
Composition wt%	<0.08	<0.25	<0.05	<0.2	5.5-6.76	3.5-4.5	<0.0125	Balance

Figure 34: Microstructure of grade 5 Ti6Al4V [92].

8.1.2 Cutting Strategy

Due to differences in mechanical and thermal properties between the PCD grades and the VP15TF, different cutting strategies were employed. The CNC program used for the PCD inserts in the experiments are detailed in Appendix B, while Appendix C contains the program used for the tungsten carbide experiments. All the S (Spindle speed in rpm) and F (Feed rate in mm/min) codes in *italic* can be altered to suite the experiment.

PCD has a very high thermal conductivity which makes it less susceptible to thermal shock compared to the tungsten carbide inserts [6]. The toughness of the VP15TF inserts is higher than the PCD though, making the VP15TF less susceptible to

mechanical impact. Considering the chip thickness theory discussed in the pilot testing section 7, it was decided to employ conventional milling for the PCD inserts and to use climb milling for the VP15TF experiments. Figure 35 [88] shows the difference between conventional and climb milling.

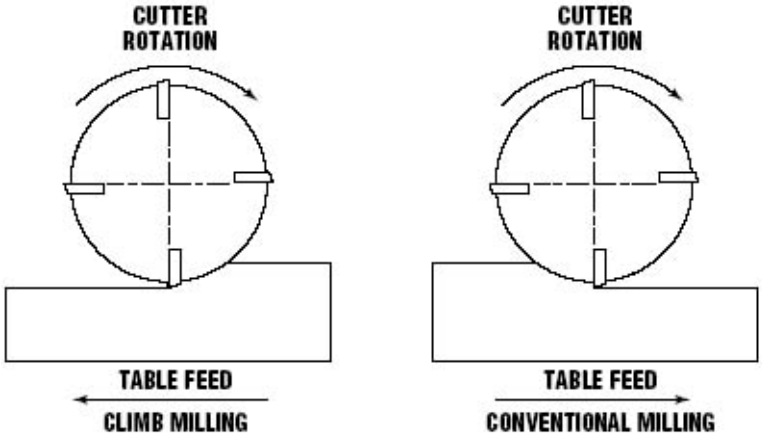

Figure 35: Different milling strategies [88].

The rationale is that by employing conventional milling for the PCD inserts, the tool enters the cut at a small chip thickness, lowering the mechanical impact experienced by the insert. The sudden exit from the cut while cutting with a large chip thickness, results in a rapid transition from a high thermal load (cutting with a large chip thickness) to an extreme low negative thermal load (no cutting, full coolant stream exposure). Because of PCD's high thermal conductivity these thermal shock conditions do not present failure risks.

In the case of the tungsten carbide, the reasoning is the opposite. The increased toughness of tungsten carbide compared to PCD allows it to be more resistant to mechanical impact, while its lower thermal conductivity makes it less resistant to thermal fracturing. Therefore, by employing climb milling for the VP15TF inserts, the result is that the tool enters the workpiece with a larger chip thickness (higher mechanical impact) and exits the workpiece with a small chip thickness (lower thermal load differential). Although this increases the mechanical impact experienced by the insert, this technique minimizes the thermal shock exerted on the insert.

8.1.3 Cutting Fluid

The cutting fluid that was used during the experiments was ROCOL® ULTRACUT 260. This cutting fluid is an emulsion designed specifically for superior performance in severe cutting conditions of ferrous and non-ferrous materials, including difficult-to-machine alloys such as titanium. The oil has a density of 1.00 g/cm^3 at 20ºC and a pH value of 9.4 when diluted 25:1. Table 7 shows different refractometer readings for different water-to-oil mixing ratios. A ratio of 30:1 was used for all the experiments (flood lubrication and high pressure through spindle lubrication). This means that the percentage water is high (about 96%). Taking into account the high cutting temperatures that are expected for titanium machining, the high percentage water (which has a high thermal capacity) will help to sufficiently remove heat. Narutaki et al [9] found that cutting temperatures for Ti6Al4V with K10 tungsten carbide inserts ranged between 1000 – 1400 K for cutting speeds ranging between 60 – 180 m/min. It is however not the highest water : oil mixing ratio (refer Table 8). The choice of the medium dilution ratio in the range recommended by the manufacturer of the cutting fluid was intended to be a precaution against extreme heat conduction capacity which is associated with thermal shock in titanium machining.

Table 8: Refractometer Calibration for the ULTRACUT 260

Dilution Ratio	10:1	20:1	30:1	40:1	50:1
Refractometer Reading	9.2	5.1	3.6	2.8	2.3

Figure 36 shows the supply of lubricant through the external nozzles during the flood lubrication experiments. The cooling lubricant unit has a pump capacity which can supply coolant at 50 l/min at an approximate pressure of 3 bar.

Figure 36: Flood lubrication supplied through the external nozzles.

Figure 37 a) shows how the through spindle lubricant was supplied for the PCD experiments at pressures of 40 bar and 80 bar (TSL40 and TSL80). Figure 37 b) shows how the through spindle lubricant was supplied for the tungsten carbide experiments. Due to the additional exit hole of the VP15TF tool, a maximum supply pressure of only 60 bar could be sustained by the machine (TSL60). From these photographs the difference in angle of the exit coolant streams are shown. The pump capacity of the machine differs according to the pump pressure. The pump capacity is 31 l/min at a pressure of 40 bar, approximately 25 l/min at 60 bar and 20 l/min at a pressure of 80 bar. Table 9 summarizes the amount of coolant supplied to the cutting edge per experiment.

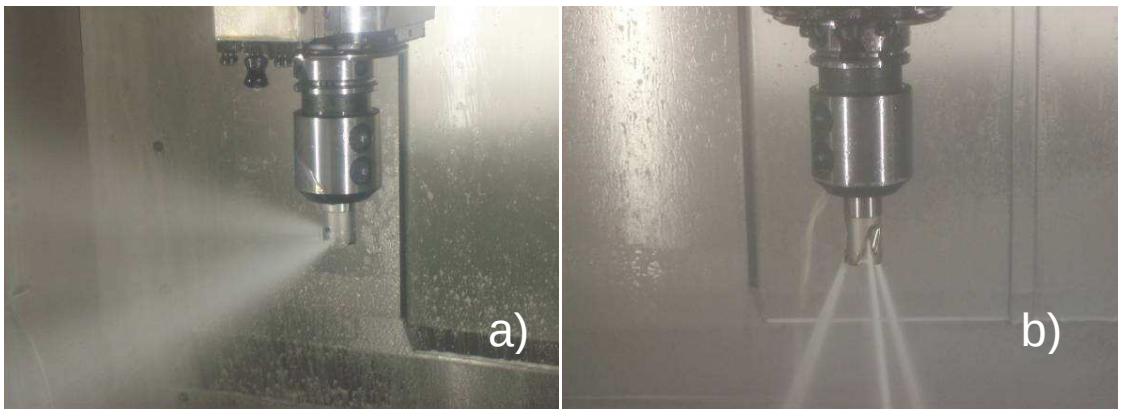

Figure 37: Through spindle lubrication for a) the two PCD grades and b) the tungsten carbide grade.

Table 9: Amount of Coolant Supplied per Through Spindle Experiment

Pump Pressure (bar)	40	60	80
Amount of coolant supplied (l/min)	31	25	20
Amount of exit holes: • PCD grades • Tungsten carbide grade	 2 3		
Amount of coolant supplied to each insert (l/min): • PCD grades • Tungsten carbide grade	 15.5 10.33	 - 8.33	 10 -

8.2 Experimental Design

As discussed, the aim of the experimental design was to yield conclusive experimental results for interpretation of the effectiveness and suitability of different lubrication strategies.

Table 10 indicates the experimental design that was chosen for the experiments. The design allows for comparison between different lubrication strategies (flood cooling (Flood), high pressure through spindle lubrication at 40 bar (TSL40), high pressure through spindle lubrication at 60 bar (TSL60) and high pressure through spindle lubrication at 80 bar (TSL80)). Two different cutting speeds (100 and 200 m/min) and two different feed per tooth (0.025 and 0.05 mm/rev per tooth) were employed. These values were taken from previous studies conducted by Barnett-Ritcey [16], Kuljanic et al. [8], Narutaki et al. [9] and Nurul Amin et al. [89]. The reasoning behind using different values for the feed and cutting speed is to determine whether certain lubrication strategies work better at certain cutting configurations and to determine the sensitivity of certain cutting parameters (cutting speeds and feeds) when using specific lubrication strategies. Only one insert was used at a time. This implies that the feed per tooth is equal to the feed per spindle revolution ($f = z.f_z$, $z = 1$). Other cutting parameters such as depth of cut ($a_p = 2$ mm) and axial immersion ($a_e = 0.5$ mm) were held constant.

Table 10: Experimental Design

#Experiments	Grade	Lube Type	Cut Speed [m/min]	Feed [mm/rev]
1	CMX850	Flood	100	0.05
2	CMX850	Flood	200	0.05
3	CMX850	Flood	100	0.025
4	CMX850	Flood	200	0.025
5	CMX850	TSL40	100	0.05
6	CMX850	TSL40	200	0.05
7	CMX850	TSL40	100	0.025
8	CMX850	TSL40	200	0.025
9	CMX850	TSL80	100	0.05
10	CMX850	TSL80	200	0.05
11	CMX850	TSL80	100	0.025
12	CMX850	TSL80	200	0.025
13	CTM302	Flood	100	0.05
14	CTM302	Flood	200	0.05
15	CTM302	Flood	100	0.025
16	CTM302	Flood	200	0.025
17	CTM302	TSL40	100	0.05
18	CTM302	TSL40	200	0.05
19	CTM302	TSL40	100	0.025
20	CTM302	TSL40	200	0.025
21	CTM302	TSL80	100	0.05
22	CTM302	TSL80	200	0.05
23	CTM302	TSL80	100	0.025
24	CTM302	TSL80	200	0.025
25	VP15TF	Flood	100	0.05
26	VP15TF	Flood	200	0.05
27	VP15TF	Flood	100	0.025
28	VP15TF	Flood	200	0.025
29	VP15TF	TSL40	100	0.05
30	VP15TF	TSL40	200	0.05
31	VP15TF	TSL40	100	0.025
32	VP15TF	TSL40	200	0.025
33	VP15TF	TSL60	100	0.05
34	VP15TF	TSL60	200	0.05
35	VP15TF	TSL60	100	0.025
36	VP15TF	TSL60	200	0.025

9. Results and Discussions

After all the experiments were completed, the inserts were analyzed using an optical microscope, SEM analysis and EDS analysis. The outputs that were analyzed included the flank wear of each insert, the chip formation and the surface roughness.

9.1 Tool Wear Mechanisms

Tool wear on the flank face was used as the primary output for the experiments. The maximum flank wear (V_B) was measured and used as performance indicator. This is a similar performance indicator to the experiments conducted by Barnett-Ritcey et al. [6]. The flow diagram below (refer Figure 38) shows the methodology followed in order to correctly quantify V_B. A detailed discussion of the flow diagram will follow.

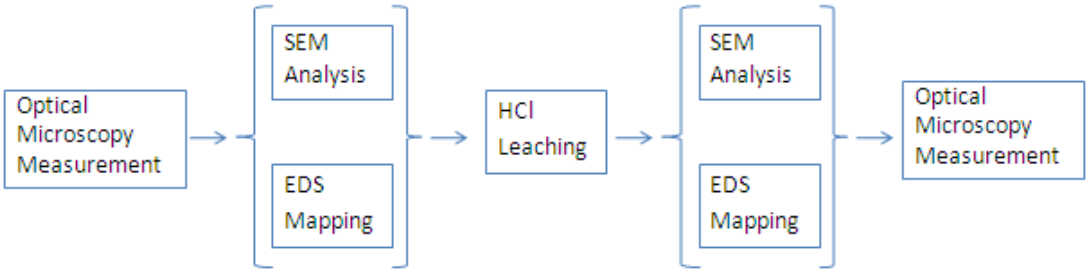

Figure 38: Flow diagram of wear scar analysis methodology.

When the inserts were initially inspected with the optical microscope it was difficult to quantify the size of the wear scar. Figure 39 shows a typical indication of a flank wear scar analyzed with an optical microscope. It could not be determined whether the wear scar was a type of chipping, abrasion or a buildup edge. It was therefore decided to use SEM and EDS analysis to examine the wear scar more closely in order to determine the exact causes of tool wear for the PCD inserts.

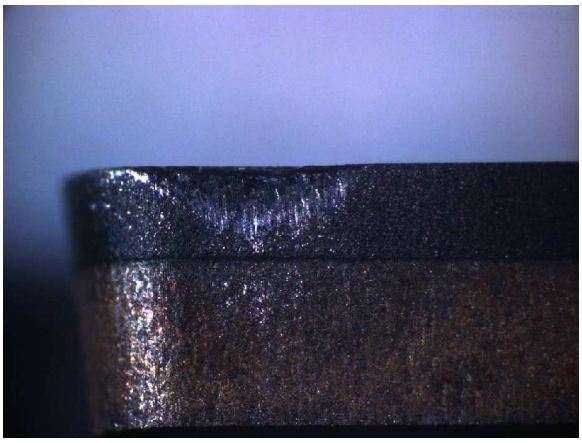

Figure 39: A typical wear scar using optical microscopy (x50).

Figure 40 illustrates the same sample analyzed using a scanning electron microscope. Chip movement is into and at the top of the image. It can be seen in this image that there is some buildup of material on the flank face of the insert. Although this buildup was thought to be Ti6Al4V, it was still deemed necessary to do EDS mapping of the image to determine the elements present.

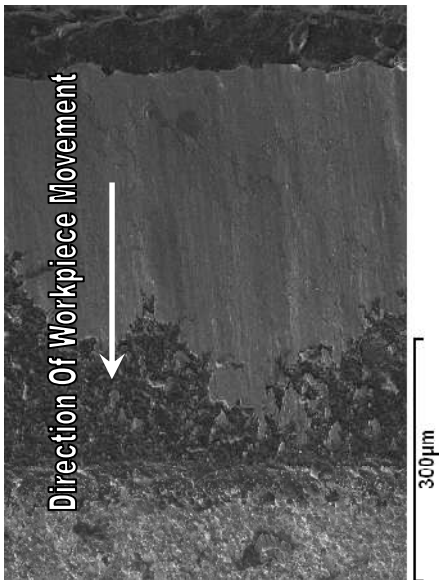

Figure 40: SEM photo of flank wear scar.

The EDS mapping of this image is presented in Figure 41. This mapping of the elements present confirmed the original theory that the material buildup was indeed Ti6Al4V. A problem that this posed was that the wear scar could not be quantified, because there was no indication of whether this was just material adhering to the undamaged surface of the insert, or whether this was workpiece material filling up the void of the insert's wear scar. If it could be proven that the buildup of material is caused due to the presence of a previously formed wear scar, the assumption could be made that the size of the buildup edge is indeed equivalent to the size of the wear scar underneath the buildup edge. This value could then be used to quantify the wear experienced by the insert during the experiment.

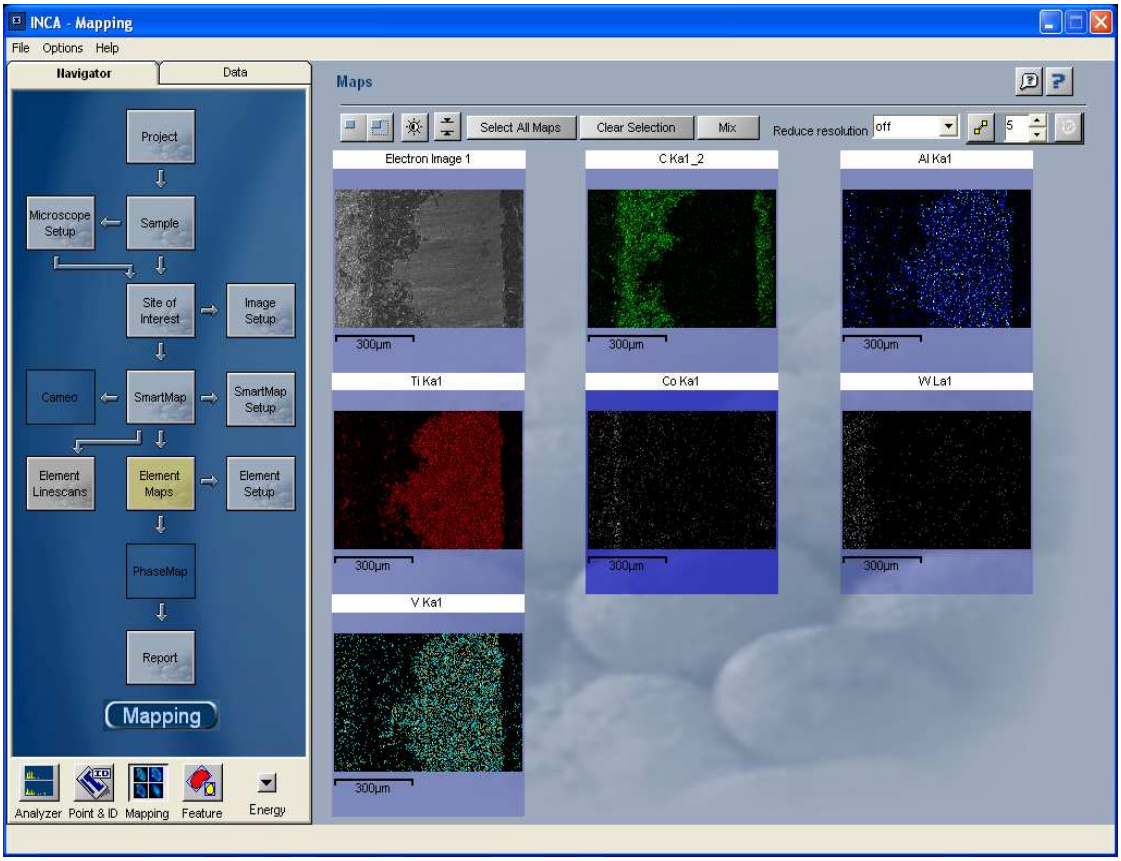

Figure 41: EDS mapping of the wear scar proving the presence of Ti6Al4V.

HCl is reactive with most constituents of Ti6Al4V. In order to analyse the wear scar underneath the buildup of Ti6Al4V it was decided to boil the insert in HCl. The PCD inserts were placed in HCl was held at a constant temperature above 100 ºC for 1 hour, and then left to cool down for a further 8 hours to ensure that most of the Ti6Al4V would have been removed. The reactions that the HCl will have with the different constituents of the Ti6Al4V (Ti, Al, and V) are shown in the reaction Table 11. Vanadium is the only constituent that will not react with the HCl, leaving a residue of Vanadium as a finish product in the HCl. The HCl will thus remove all of the buildup from the wear scar, resulting in a clean wear scar for further analysis.

Table 11: Reaction between HCl and Ti6Al4V constituents.

Constituent	Reaction
HCl reaction with Ti	Ti (s) + 6 HCl (l) ➔ $[TiCl_6]^{3-}$ (purple solution) + 3 H_2 (g)
HCl reaction with Al	Al (s) + 3 HCl (l) ➔ $AlCl_3$ (colourless solution) + 1.5 H_2 (g)
HCl reaction with V	Vanadium is not soluble in HCl.

After the leaching of the Ti6Al4V from the insert, it was once more inspected using SEM and EDS analyses. This SEM photograph is shown in Figure 42. From this it can be seen that all of the Ti6Al4V have been removed from the flank face. This result shows that there is flank face chipping present underneath the buildup of Ti6Al4V.

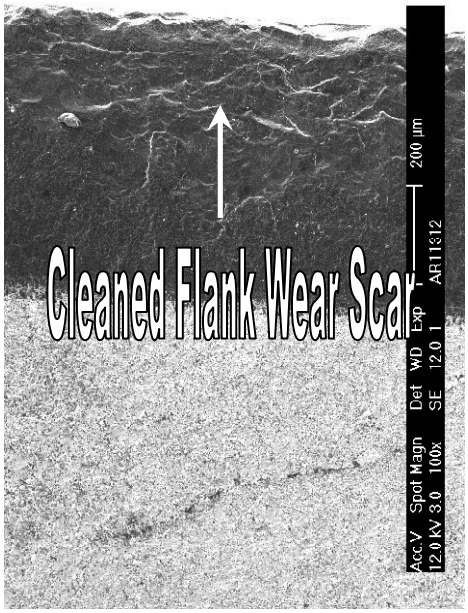

Figure 42: The HCl cleaned flank face (x100).

Zooming in further at the wear scar the mechanism behind tool wear can be examined. Figures 43 a) and b) show close up images of the wear scar. From these photographs the initiation and propagation of lateral cracks can clearly be seen. This was also confirmed by researchers at Element Six (Pty) Ltd. [87].

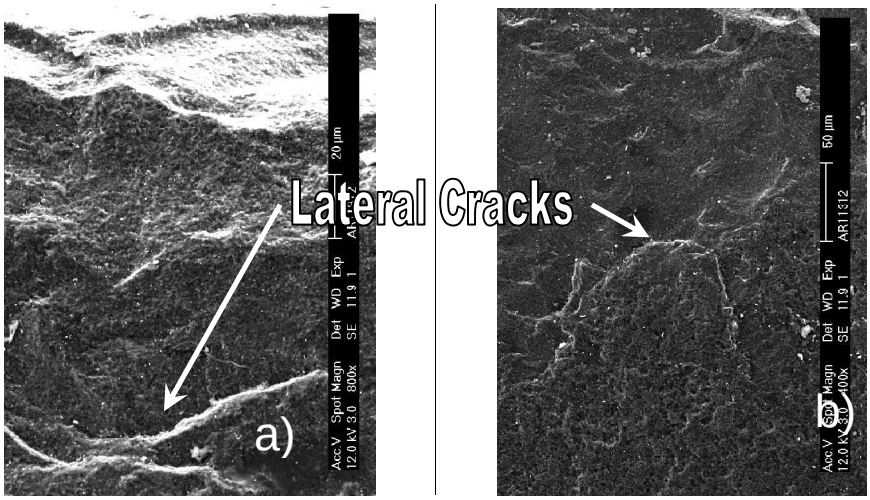

Figure 43: SEM analysis of wear scar after HCl leaching a) (x800) and b) (x400).

To better understand how the wear progresses, a similar sample was analyzed using the SEM. The only difference is that this sample was not HCl leached. This sample was instead EDM wire cut through the wear scar and the side surface polished. A side view of the wear scar could therefore be examined. Figure 44 illustrates this view captured on the SEM.

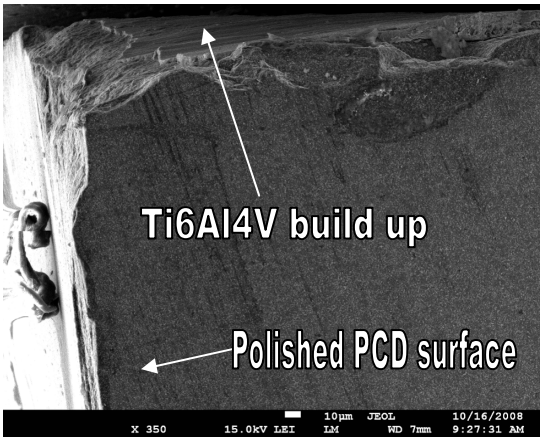

Figure 44: SEM side view of the wear scar (x350).

A buildup of Ti6Al4V on the wear scar of the insert can be observed. The direction of workpiece movement is from left to right as seen on the pictures. During milling, the highest load is exerted on the edge of the insert. This is also the place where the most chipping occurs. Chipping of the flank face progresses from here downward (to the right in the figure). The wear mechanism can be associated with abrasion caused by brittle fracturing of the insert (refer to Figure 15). This type of wear for PCD was also observed by Hung et al. [52]. The repeated flow of workpiece material over the flank face of the insert will cause subsurface lateral cracks to develop. These cracks will propagate to the free surface of the flank face, causing insert material to be removed in layers. This is known as delamination. Ti6Al4V is a very adherent material [7]. According to Nabhani [7], when junctions between the PCD and the Ti6Al4V are broken, there are three possible routes that crack propagation can follow. These routes are either through the workpiece, the interface, or the bulk of the ultra-hard material. It was also observed that in all the experiments crack propagation occurred through the bulk of the PCD [7]. The same can be said for the crack propagation observed in Figure 43.

After the wear scar mechanisms were determined, the inserts were again inspected using optical microscopy. It was decided to investigate the similarity between wear scar measurements taken before HCl leaching and measurements taken after HCl leaching. Figure 45 indicates a measurement taken before HCl leaching, while Figure 46 indicates a measurement taken after HCl leaching.

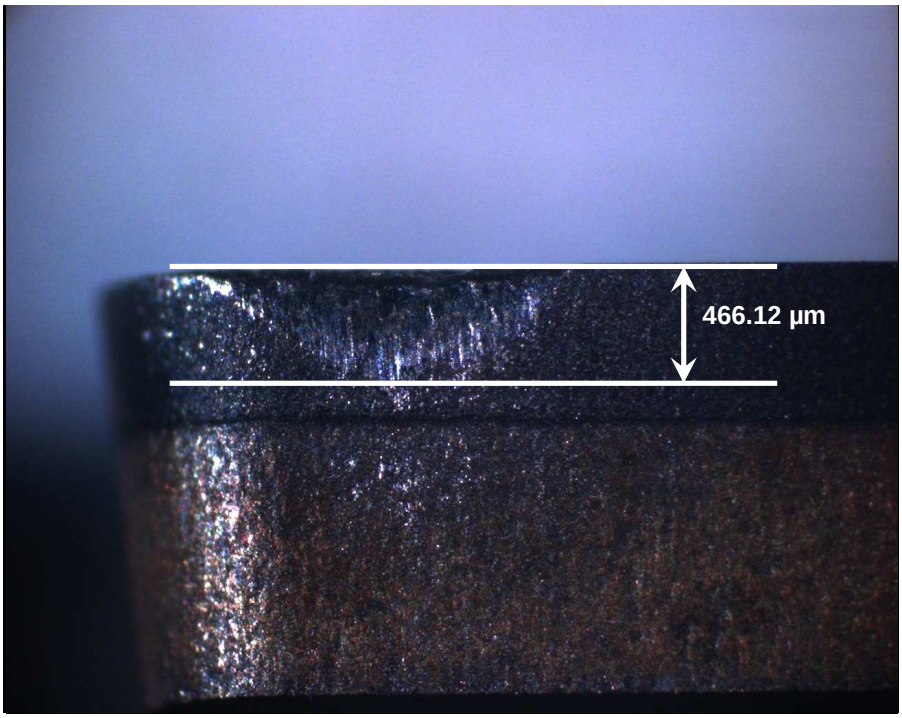

Figure 45: The wear scar measurement before HCl leaching.

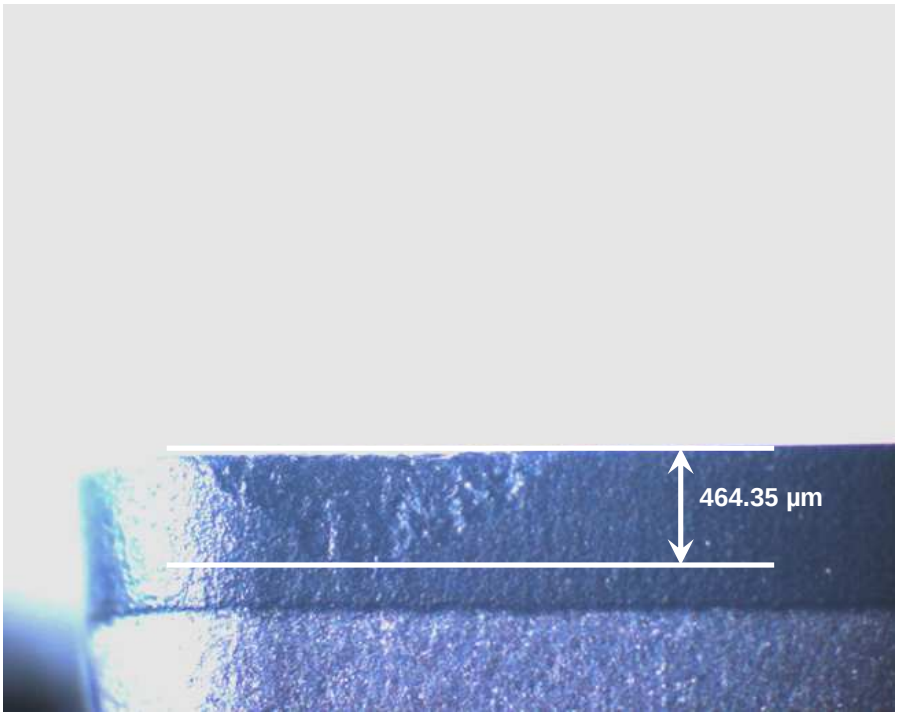

Figure 46: The wear scar measurement after HCl leaching.

Several other samples were also HCl cleaned and measurements were also taken before and after leaching. Table 12 summarizes the comparison between these measurements taken before and after HCl leaching. These results implied that the measurements taken before HCl leaching are quite similar to the measurements after HCl leaching. Acid cleaning of all the samples potentially could yield more information regarding wear mechanisms. It was decided that the focus of this part of the research was on determining wear scar size. Therefore the correlation evident from the 8 samples that were acid cleaned was considered sufficient indication that it was not necessary to acid clean all the samples.

Table 12: Comparison between wear scar measurements before and after HCl leaching.

Insert and cutting condition	Measurement before HCl leaching (V_B in micron)	Measurement after HCl leaching (V_B in micron)
CMX850, Flood, Vc = 200, fz = 0.025	211.15	221.86
CMX850, Flood, Vc = 200, fz = 0.05	79.75	71.42
CMX850, TSL40, Vc = 200, fz = 0.05	466.12	464.35
CTM302, TSL80, Vc = 100, fz = 0.025	91.21	94.41
CTM302, TSL80, Vc = 100, fz = 0.05	106.61	101.84
CTM302, TSL80, Vc = 200, fz = 0.025	265.93	259.83
CTM302, TSL80, Vc = 200, fz = 0.05	260.21	252.59

The tests were repeated 3 times in order to achieve average flank wear values for each cutting condition. The average flank wear values that were measured are summarized in Table 13. The results captured for the PCD grades were then analysed using a 2^3 full factorial design of experiments. Because the tungsten carbide inserts differed severely from the PCD inserts regarding geometry and through spindle capabilities, it was decided to analyse them separately. Due to the lack of factors for a factorial design, it was decided to analyse the results for the VP15TF graphically and compare its performance to the best performer of the PCD grades.

Table 13: Average flank wear for each experiment.

#Experiments	Grade	Lube Type	Cut Speed [m/min]	Feed [mm/rev]	Avgerage Flank Wear (µm)
1	CMX850	Flood	100	0.025	60.52
2	CMX850	Flood	100	0.05	53.51
3	CMX850	Flood	200	0.025	174.7
4	CMX850	Flood	200	0.05	93.5
5	CMX850	TSL40	100	0.025	62.47
6	CMX850	TSL40	100	0.05	101.21
7	CMX850	TSL40	200	0.025	191.44
8	CMX850	TSL40	200	0.05	356.8
9	CMX850	TSL80	100	0.025	113.48
10	CMX850	TSL80	100	0.05	74.56
11	CMX850	TSL80	200	0.025	62.57
12	CMX850	TSL80	200	0.05	432.52
13	CTM302	Flood	100	0.025	127.36
14	CTM302	Flood	100	0.05	105.99
15	CTM302	Flood	200	0.025	173.2
16	CTM302	Flood	200	0.05	152.08
17	CTM302	TSL40	100	0.025	117.83
18	CTM302	TSL40	100	0.05	132.905
19	CTM302	TSL40	200	0.025	350.485
20	CTM302	TSL40	200	0.05	405.205
21	CTM302	TSL80	100	0.025	96.565
22	CTM302	TSL80	100	0.05	122.695
23	CTM302	TSL80	200	0.025	307.54
24	CTM302	TSL80	200	0.05	312.83
25	VP15TF	Flood	100	0.025	184.87
26	VP15TF	Flood	100	0.05	193.945
27	VP15TF	Flood	200	0.025	187.47
28	VP15TF	Flood	200	0.05	170.815
29	VP15TF	TSL40	100	0.025	158.235
30	VP15TF	TSL40	100	0.05	201.08
31	VP15TF	TSL40	200	0.025	164.925
32	VP15TF	TSL40	200	0.05	172.075
33	VP15TF	TSL60	100	0.025	156.59
34	VP15TF	TSL60	100	0.05	172.3
35	VP15TF	TSL60	200	0.025	145.92
36	VP15TF	TSL60	200	0.05	204.06

A 2^3 full factorial design implies that 3 factors are analyzed at two levels each. This amounts to 8 experimental outputs. A full factorial design was drawn up for each type of lubrication tested (flood lubrication, 40 bar high pressure through spindle lubrication, and 80 bar high pressure through spindle lubrication). The first 24 lines of Table 13 contain the data used for these analyses.

The 3 factors that were used were the grade of PCD, the cutting speed and the feed per tooth. For the analysis of the data, it is necessary to choose high and low levels for each factor. Each of these factors had 2 levels (PCD – CMX850 and CTM302, v_c – 100 and 200 m/min, f_z – 0.025 and 0.05 mm/rev per tooth). For the PCD it was decided that CMX850 with the higher hardness would be the high level, while CTM302 with the lower hardness would be the low level. For the cutting speed 200 m/min was chosen as the high level and 100 m/min as the low level. For feed per tooth 0.05 mm/rev was used as the high level and 0.025 mm/rev was used as the low level.

Analyses of these results are expected to yield a better understanding of the relationship between the different factors for each lubrication strategy. Table 14 summarizes the results attained with the full factorial analysis of the PCD inserts. The “H” and “L” values in the row entitled “Relative Effects” indicate the effect of the “High” and “Low” value chosen for each factor, discussed previously, respectively. These results are discussed in more detail in the following sections.

Table 14: Results attained with full factorial design.

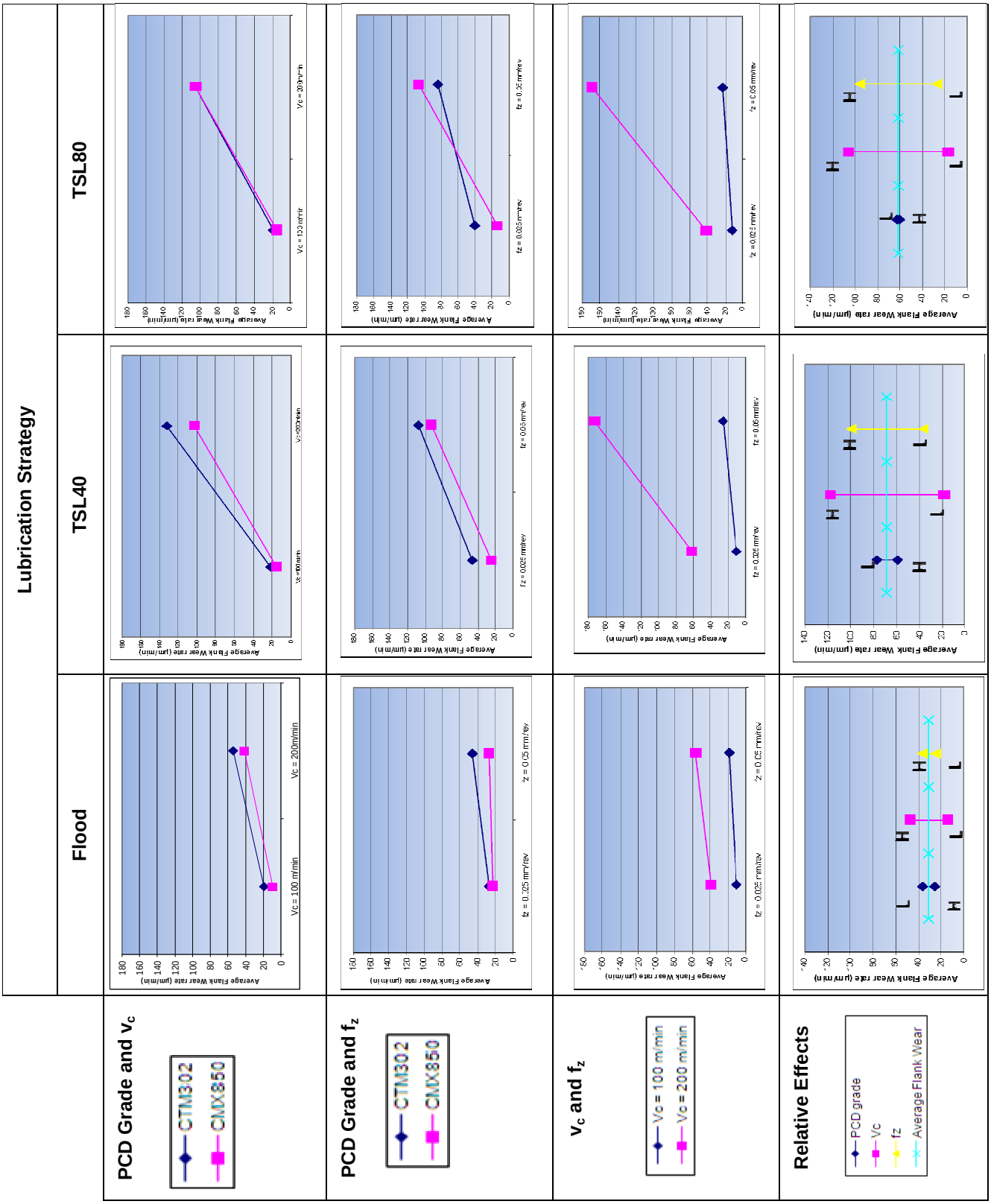

9.2 PCD

9.2.1 Relationship between PCD Grade and v_c

As discussed previously, the flood lubrication is supplied at a pressure of 3 bar and a flow rate of 50 l/min. The lubrication flow rate per insert is 15.5 l/min for TSL40 and 10 l/min for TSL80 (refer Table 9). Figures 47 a), b) and c) is a summary of the first row of Table 13 and illustrate the relationship between the grade of PCD used and the cutting speed for the flood lubrication, TSL40 and TSL80 experiments respectively. The results are interpreted in terms of average flank wear rate. For the purpose of this study, considering the expected exponential reduction in tool life accompanying increased material removal rate, lower values of average flank wear rate will be considered beneficial.

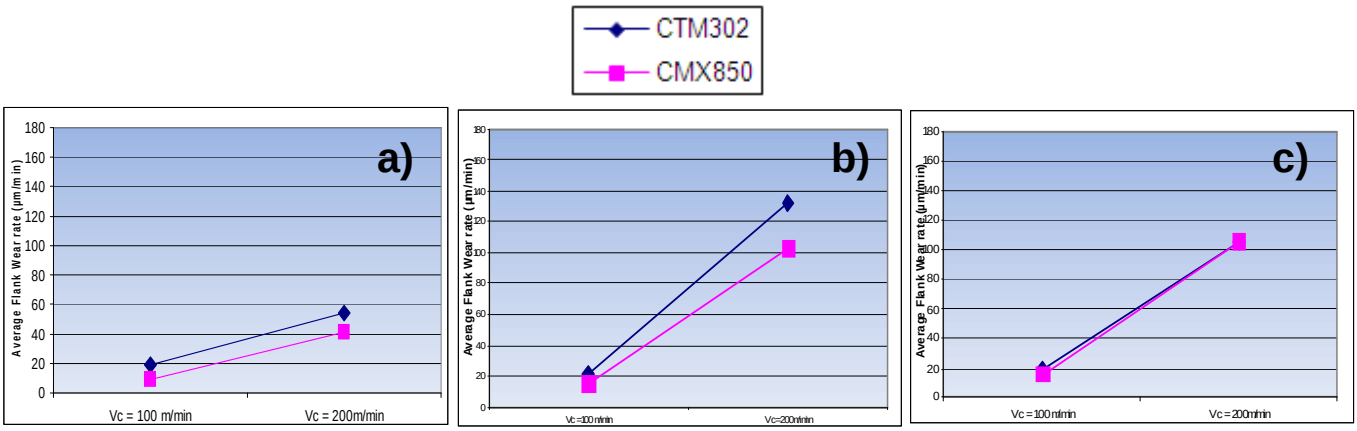

Figure 47: Relationship between PCD grade and v_c for a) Flood, b) TSL40 and c) TSL80.

For Flood, TSL40 and TSL80 an increase in v_c brought forth an increase in flank wear rate for both grades of PCD. An increase in v_c from 100 to 200 m/min will cause the cutting temperature to increase from approximately 1150 to 1350 K [9]. At both the lower and higher cutting speed the CMX850 performed better than the CTM302. The difference between CMX850 and CTM302 that may contribute towards better performance for CMX850, is better TRS and a lower thermal conductivity for CMX850. According to Barnett-Ritcey [16], thermal softening of Ti6Al4V could be considered the reason for an increase in tool life at cutting conditions considered to generate higher cutting temperatures (higher cutting speeds and feed rates). This could explain the lower wear rate of the CMX850 compared to the CTM302. The lower thermal

conductivity of CMX850 could increase the cutting temperatures compared to CTM302. This could lower the cutting forces compared to CTM302, causing a decrease in tool wear rate. Flood lubrication performed significantly better compared to TSL40 and TSL80. This can be attributed to the increased amount of lubricant supplied to the cutting edge. Because titanium machining is done at low cutting speeds compared to other similar machining operations of steel and aluminium, the lubricant can penetrate the interfaces more thoroughly [76]. A reduction in the amount of coolant will therefore not only reduce the cooling capabilities of the lubrication strategy, but will also reduce the lubrication between the workpiece and the flank face of the insert [83]. A lower degree of lubrication will subsequently increase the cutting forces and the coefficient of friction, leading to an increase in cutting temperature [83]. This explains why flood lubrication performance is superior to that of TSL40 and TSL80 in this regard.

Barnett-Ritcey [16] also concluded that thermal softening of Ti6Al4V could assist in increasing tool life at certain cutting conditions where higher temperatures are generated for PCD machining. Relating this theory to this study, it could be argued that a small degree of thermal softening could have occurred in the case of CMX850 machining (with lower thermal conductivity) compared to the CTM302 for the TSL40. A higher load was therefore probably exerted on the CTM302 with the lower TRS. Both of these factors might contribute to a reduction in tool life of CTM302 relative to the CMX850.

In the case of flood cooling, the cutting temperature will be significantly reduced. It could therefore be argued that the thermal softening effect could be considerably less and not large enough to be considered. In this case the TRS of the inserts will play a significant role in determining tool life. This will explain the lower flank wear rate achieved with CMX850.

In the case of the TSL80 the two grades of PCD yielded similar performance. This can be attributed to the increase in lubrication supply pressure resulting in more sufficient rake face lubrication [83]. More sufficient chip removal will reduce the contact length of the chip with the tool, subsequently lowering the cutting forces and the generated cutting temperature [84]. This could explain why TSL80 performance is slightly better than the TSL40. Compared to flood lubrication, the TSL80 provided an insufficient degree of

flank lubrication and cooling capabilities causing higher cutting temperatures and forces to be generated [84].

9.2.2 Relationship between PCD Grade and f_z

The effect of alternating the feed per tooth is an important output. Figures 48 a), b) and c) is a summary of the second row of Table 14 and illustrate the relationship between the grade of PCD used and the feed per tooth for the flood lubrication, TSL40 and TSL80 experiments respectively. The flood lubrication again gave the most satisfactory results. The TSL40 and TSL80 experiments again performed quite similar to each other.

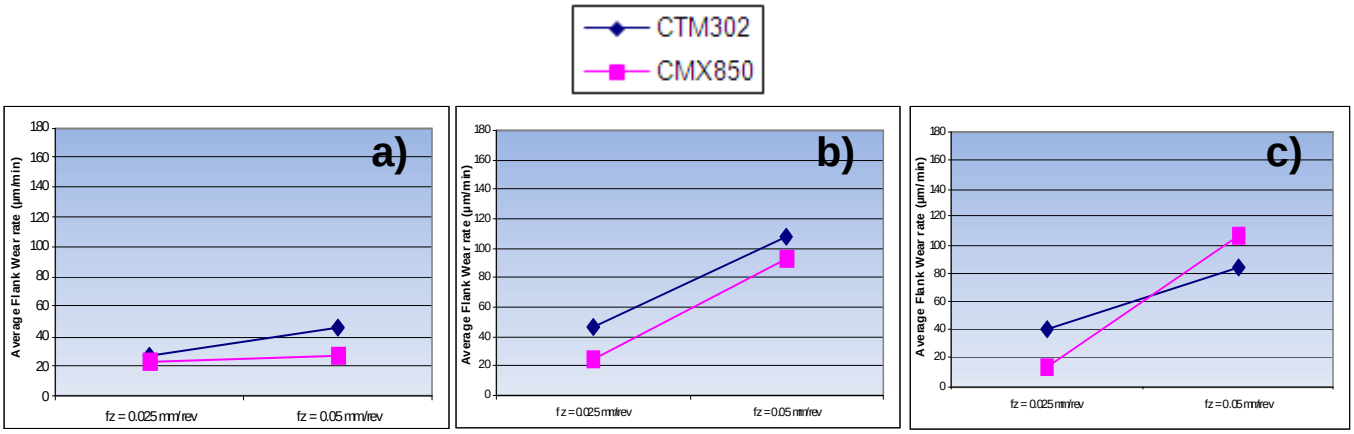

Figure 48: Relationship between PCD grade and f_z for a) Flood, b) TSL40 and c) TSL80.

For both grades of PCD there was an increase in tool wear rate with an increase in f_z from 0.025 to 0.05 mm/rev. This is attributed to an increase in mechanical stresses brought on by an increase in feed [6]. This again illustrates the importance of supplying a sufficient amount of lubricant to the cutting edge for good flank and rake face lubrication. The overall reduction in cutting temperature will also reduce the adhering tendency of the chips to the insert, leading to a reduction in cutting forces [83].

In the case of the flood lubrication, the increased amount of lubricant led to more effective flank face and rake face lubrication than in the case of the TSL40 and TSL80 experiments. This will decrease the forces exerted on the insert compared to the TSL40

and TSL80. The CMX850 performed rather similarly at both feeds per tooth. The reason for this can be attributed to the increased TRS making it more suitable to cope with the increase in load.

The reduced amount of lubricant supplied to the TSL40 and TSL80 experiments compared to the flood lubrication experiments explains why these lubrication strategies performed worse. The reduction in flank face lubrication would cause an increase in cutting forces compared to the flood lubrication. An increase in feed rate would also cause an increase in chip thickness, subsequently increasing cutting forces [6]. This stresses the importance of sufficient chip removal. It could therefore be accepted that the supply of lubricant in the case of the TSL40 and TSL80 strategies were insufficient in penetrating the interface between the chip and the rake face at the higher feed rate. This explains why there is substantial increase in flank wear rate for an increase in feed rate from 0.025 to 0.05 mm.

In the case of TSL80 the CMX850 performed better than the CTM302 at a feed of 0.025 mm, but worse at a feed of 0.05 mm. In a cutting process work is done by deforming the workpiece into a chip and by moving the chip and freshly cut workpiece surface over the insert. Due to the large amount of plastic strain, almost 99% of the work that is done is stored as heat [95]. The rest is stored as elastic energy. This means that an increase in chip thickness (which is brought forth by an increase in feed) will bring forth an increase in plastic strain, causing more heat to be generated. Relating this theory to the lower thermal conductivity of the CMX850 compared to the CTM302, higher temperatures could have been generated in the case of the CMX850. This could lower the TRS of CMX850 to below that of CTM302. Taking into account that the least amount of cooling power is supplied for TSL80, it could perhaps explain why CTM302 performed better than CMX850 at the higher feed.

9.2.3 Relationship between v_c and f_z

The relationships between v_c and f_z for the flood lubrication, TSL40 and TSL80 experiments are illustrated in the third row of Table 14 and summarized in Figures 49 a), b) and c) respectively. From these graphs the sensitivity of increasing feed rate at low and high cutting speeds for each lubrication strategy tested is depicted. Flood lubrication gave the best results. A high degree of similarity in the results attained for the TSL40 and TSL80 is also observed.

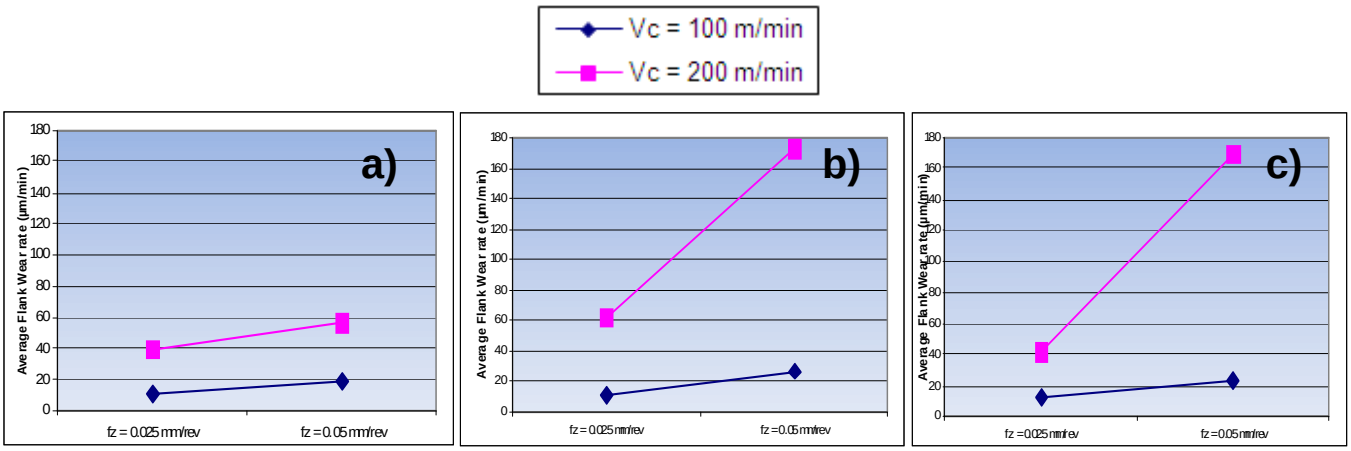

Figure 49: Relationship between v_c and f_z for a) Flood, b) TSL40 and c) TSL80.

In the case of the flood lubrication experiments lower flank wear rates were experienced for at lower feed rates for both cutting speeds used. An increase in cutting speed also increased the tool wear rate at each feed per tooth value. Comparing the tool wear rate curves of the two cutting speeds, it can be seen that the increase in feed per tooth from 0.025 to 0.05 mm/rev had little effect on the flank wear rate at both the low and high cutting speeds. This illustrates that sufficient flank face lubrication and the reduction in chip adhering tendency was brought forth by this lubrication strategy, subsequently lowering cutting forces. Only a slight increase in tool wear rate was observed for an increase in v_c compared to the TSL40 and TSL80. This illustrates that the amount of cooling power was sufficient in coping with the increase in cutting temperature caused by the increase in v_c.

When comparing the graphs of the TSL40 and TSL80 (Figure 49 b) and c)) a high degree of similarity is observed. At the lower cutting speeds the tool wear rate was much lower and the effect of an increase in feed per tooth less pronounced. At the higher cutting speed the increase in feed per tooth had a substantial impact on increasing tool wear. This is accredited to the fact that the reduced cooling power of the TSL40 and TSL80 could not remove heat from the cutting zone at a sufficient rate. Insufficient flank- and rake face lubrication capabilities of these lubrication strategies also caused higher cutting forces to be generated, leading to an increase in cutting forces.

9.2.4 Relative Effects of Each Factor

The relative effects of each factor (PCD grade, v_c and f_z) are illustrated in the last row of Table 14 and summarized in Figures 50 a), b) and c) for flood lubrication, TSL40 and TSL80 respectively. Flood lubrication resulted in the lowest average flank wear rate, while the effects of each factor for TSL40 and TSL80 once again showed similarities.

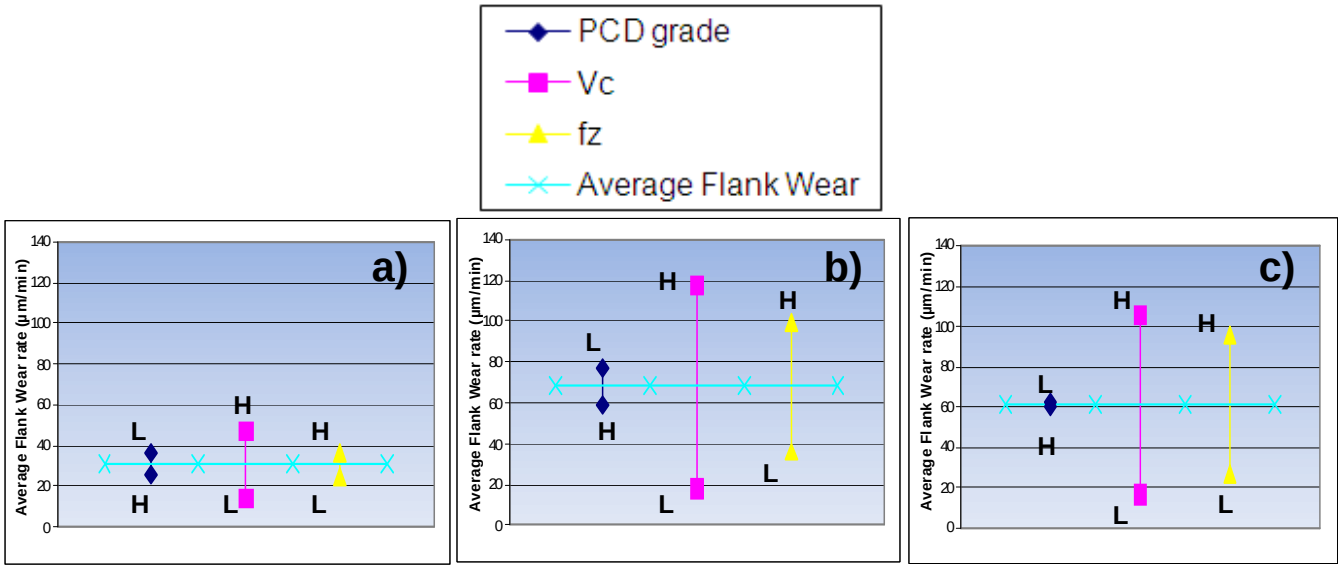

Figure 50: Relative effects of each factor for a) Flood, b) TSL40 and c) TSL80.

In the flood lubrication experiments graph it can be seen that the average flank wear rate is only marginally sensitive to changes in factors from their lower to higher value. Cutting speed had the most pronounced effect on the average flank wear rate when

moved from its lower to higher level. The grade of PCD and feeds per tooth had a less significant effect. This illustrates that sufficient cooling power and lubrication was supplied to the cutting process with this lubrication strategy relative to TSL40 and TSL80. This reduced the cutting forces and temperatures exerted on the insert relative to the TSL40 and TSL80, subsequently lowering the rate of flank wear. The lowest flank wear rate was attained for the CMX850 (H), at a cutting speed of 100 m/min (L) and at a feed per tooth of 0.025 mm/rev (L).

The TSL40 and TSL80 experiments again yielded similar results. The TSL80 had a slightly lower average flank wear rate. Barnett-Ritcey [6] concluded that an increase in supply pressure in directed through spindle lubrication for Ti6Al4V machining with PCD inserts provided more sufficient penetration between the tool and the chip, resulting in an increased tool life. This explains the lower rate of flank wear observed with the TSL80 compared to the TSL40. The higher supply pressure provided a higher degree of chip removal, subsequently reducing cutting forces and increasing tool life.

The TSL40 and TSL80 were also much more sensitive to a change in the factors from their lower to higher values. Cutting speed had the biggest effect on the flank wear rate in both cases. This confirms the theory that the reduction in lubricant resulted in insufficient cooling power to the cutting process in the TSL40 and TSL80 experiments. The increased sensitivity of the feed per tooth also confirms the theory that insufficient flank – and rake face lubrication and chip removal capabilities were supplied by these lubrication strategies. The lowest flank wear rates for both the TSL40 and TSL80 were achieved when using CMX850 (H), v_c = 100 m/min (L) and f_z = 0.025 mm/rev.

9.2.5 Conclusions from Factorial Design

From the results attained in this section it becomes clear that flood lubrication was the superior cooling technique used for the PCD grades. This can most likely be attributed to the low susceptibility of the PCD inserts to thermal shock and high susceptibility to mechanical impact discussed in section 8.1.2. The increased cooling power and lubrication provided by the flood lubrication therefore contributed to a reduction in cutting

forces, subsequently lowering the rate of flank wear. In the 40 bar and 80 bar through spindle lubrication experiments the reduced amount of lubricant supplied to the cutting process provided insufficient cooling and lubrication power. This caused higher temperatures and cutting forces to be generated, leading to an increase in tool wear rate. The higher pressure 80 bar through spindle lubrication performed marginally better than 40 bar through spindle lubrication in most of the experiments. This is considered due to the fact that while both processes supplies insufficient cooling power to the cutting edge, the 80 bar through spindle lubrication assisted in more sufficient swarf removal. This can subsequently lead to a slight decrease in cutting temperatures and forces.

9.3 Tungsten Carbide

It was decided to compare the results attained for the VP15TF experiments to the results attained for the best performing PCD grade (CMX850). Due to the difference in cutting edge geometry, amount of lubricant supplied to the cutting edges, the fact that a maximum pressure of only 60 bar could be attained opposed to the 80 bar for the PCD experiments and the fact that the angle at which the through spindle lubricant was supplied to the cutting edges differed, it was decided that a full factorial design could not be used and that the performance of the two grades should rather be compared graphically.

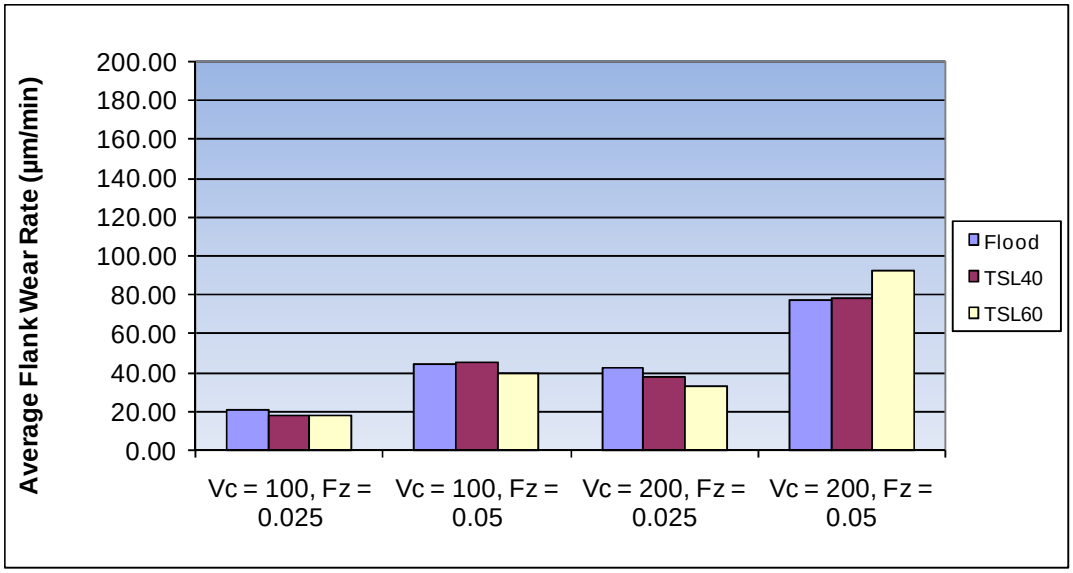

Figure 51: VP15TF – Performance of different lubrication strategies.

Figure 51 illustrates the performance as measured by the average flank wear rate of the different lubrication strategies used in combination with different cutting parameters. When compared to the best performer for the PCD grades (CMX850) the results show promise (refer figure 52).

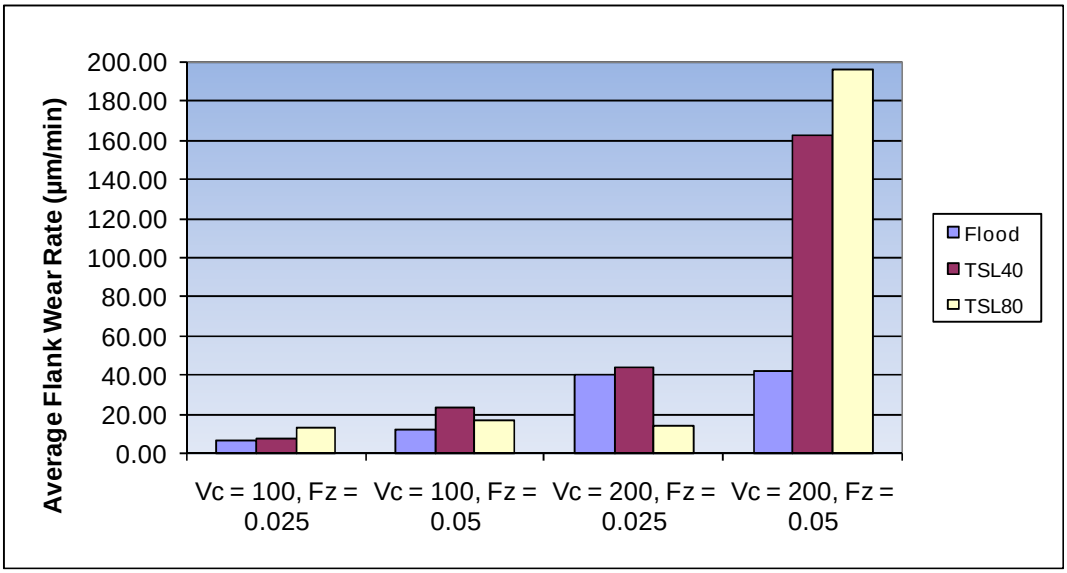

Figure 52: CMX850 – Performance of different lubrication strategies.

The CMX850 performed better than the VP15TF at all cutting conditions, except for the high cutting speed and feed per tooth cutting configuration. Variation of the flank wear rate between different cutting parameters seemed less for VP15TF over the different cooling strategies. What is interesting for the VP15TF is that the through spindle lubrication strategies performed better than the flood lubrication strategy in most of the experiments. This can be attributed to the fact that the tungsten carbide is more susceptible to thermal shock and less susceptible to mechanical impact than in the case of PCD inserts [6]. As in the experiments of Viera et al. [38] and Lui et al [39], an abundance of coolant will therefore amplify the thermal shock experienced by the insert during machining operations leading to a decrease in tool life. It therefore seems to suggest that a softer cool is needed for tungsten carbide milling of Ti6Al4V. The effect of increasing the pressure for the through spindle lubrication strategies lowered the average flank wear rate in most cases. This can be attributed to more sufficient chip removal associated with an increase in supply pressure [6]. An increase in supply pressure also caused a decrease in coolant supplied to the cutting edge. This would lower the thermal shock experienced by the insert and would also explain the decrease in wear rate observed for an increase in pressure.

The highest cutting temperature will be generated at the cutting configuration with the highest feed per tooth and the cutting speed. At this condition 40 bar through spindle

lubrication outperformed 60 bar through spindle lubrication. The flood lubrication also performed better than the two through spindle lubrications used. This is quite different than the results attained at the high cutting speed and lower feed per tooth. This is considered to be due to the fact that the flood lubrication provided better lubrication between the flank face of the insert and the workpiece at the higher feed per tooth, subsequently lowering the cutting forces [83]. At the lower feed per tooth and high cutting speed, the smaller effective chip thickness implies that the insert is more susceptible to thermal shock than mechanical load, therefore explaining the reason why the through spindle lubrication strategies performed better than the flood lubrication strategy.

From Figure 51 it becomes clear that an increase in feed per tooth for the lower cutting speed experiments has a less significant impact than at the high cutting speed. The increase in feed per tooth had the most significant effect on increasing flank wear rate for the 60 bar through spindle. This is due to the lack of lubrication discussed previously. The increase in cutting speed had its biggest effect on increasing tool wear rate at the higher feed per tooth experiments. The 60 bar through spindle lubrication experiments were most affected by the increase in cutting speeds.

9.4 Tool Life Determination

All of the preliminary tests that were conducted were done for 560 mm^3 material removed. When considering the tool life of PCD and tungsten carbide (WC) inserts recorded in the studies of Nurul Amin et al. [89], this is already a substantial amount of material removed (refer Figure 53). At cutting speeds of 100 and 200 m/min used in the final experimentation of this thesis, it can be seen that 560 mm^3 of material removed is already a huge improvement over the performance of the inserts in the studies of Nurul Amin et al. [89]. It was therefore decided to determine the tool life of the tungsten carbide and PCD inserts at the different lubrication strategies examined in this thesis. These experiments were conducted for the same cutting configurations (cutting speed and feed per tooth). The outputs of these experiments show the effect of each lubrication strategy on tool life and the amount of material that can be removed for the different lubrication strategies before tool failure.

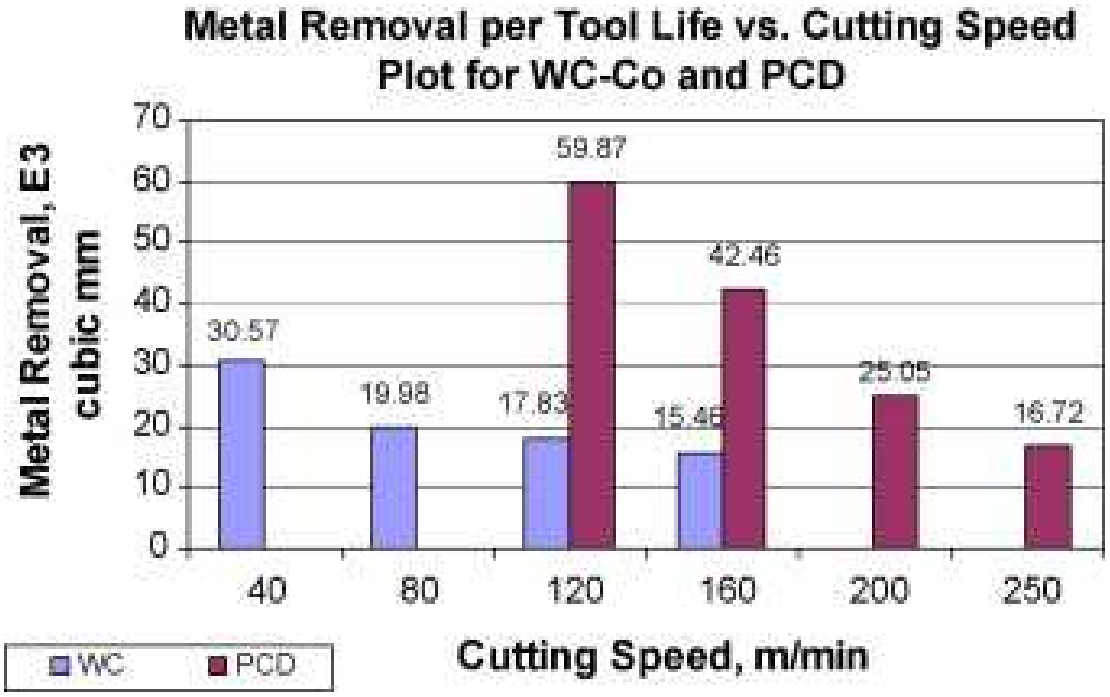

Figure 53: Material removed per tool life [89].

9.4.1 PCD

From the preliminary experiments it became clear that the CMX850 with the higher TRS and lower thermal conductivity outperformed the CTM302 in most experiments. It was therefore decided to determine the tool life of the CMX850 at different lubrication strategies. Although the best results for the CMX850 were attained at cutting configurations of 100 m/min cutting speed and 0.025 mm/rev feed per tooth and flood lubrication, it was concluded that an increase in the feed per tooth at a cutting speed of 100 m/min had little effect on increasing flank wear across all the lubrication strategies tested (refer Figures 49 a), b) and c)). This implies that an increase in feed per tooth from its lower level to its higher level will increase the material removal rate from 32 mm^3/min to 64 mm^3/min, without sacrificing tool life (in terms of cutting time) to a great extent. This is also confirmed for the VP15TF in Figure 51, where there is little difference in tool wear rate for all three lubrication strategies for an increase in feed per tooth at a cutting speed of 100 m/min. The higher material removal rate was measured against the lower tool wear rate, and it was decided that more useful data would be attained at cutting speeds of 100 m/min and a feed per tooth of 0.05 mm/rev. Failure criteria were chosen to be either a maximum flank wear of more than 300 µm, or an average surface roughness value (Ra) of more than 1.6 µm. These values are similar to those chosen by Barnett-Ritcey et al [6] and through conversation with Element Six (Pty) Ltd. researchers [87]. Chips were also collected during the machining operations.

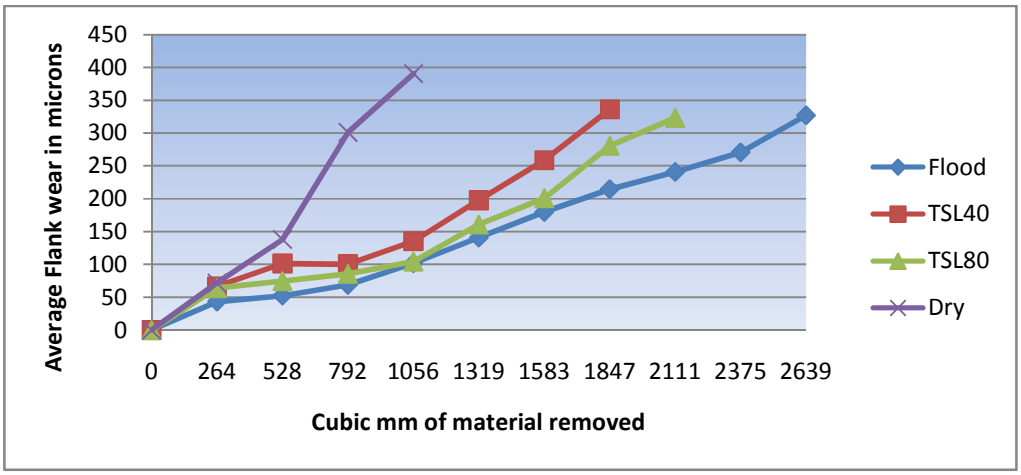

Figure 54: CMX850 – Tool life determination.

Figure 54 illustrates the progression of flank wear as a function of mm^3 material removed for the different lubrication strategies for the CMX850. From this it can be clearly seen that flood lubrication was superior to all the other lubrication techniques. The preliminary tests showed that the increased rate of failure for the through spindle experiments were probably attributed to the reduced cooling power of supplying less lubricant to the cutting edge. For this reason it was decided to also determine the tool life for dry machining operations. This will enable the illustration of the difference brought on by adding the relatively small amount of lubricant to the cutting edge, as in the case of the through spindle lubrication strategies. The trends of the lines are very similar to the results found in the preliminary experiments. Flood lubrication had the slowest flank wear rate, enabling the inserts to reach more material removal before a flank wear of 300 µm was reached. 80 bar through spindle lubrication also performed slightly better than 40 bar through spindle lubrication. The shapes of the flood lubrication, 40 bar and 80 bar through spindle lubrication graphs are quite similar. The line illustrating the flank wear progression for dry machining illustrates the accelerated wear pattern. When this pattern is compared with the flood lubrication and the two through spindle graphs, the importance of supplying a sufficient amount of coolant is stressed. The cooling power supplied with the 40 bar and 80 bar through spindle lubrication strategies enabled the insert to reach more than twice the tool life compared to dry machining, while flood lubrication reached more than 3 times the tool life compared to dry machining.

It can be concluded from this graph that dry machining of Ti6Al4V with PCD inserts are not recommended and that using flood lubrication with an abundance of coolant is the superior cooling technique for the milling of Ti6Al4V. The amount of material that was removed for each lubrication strategy up to the point of failure is summarized in Figure 55.

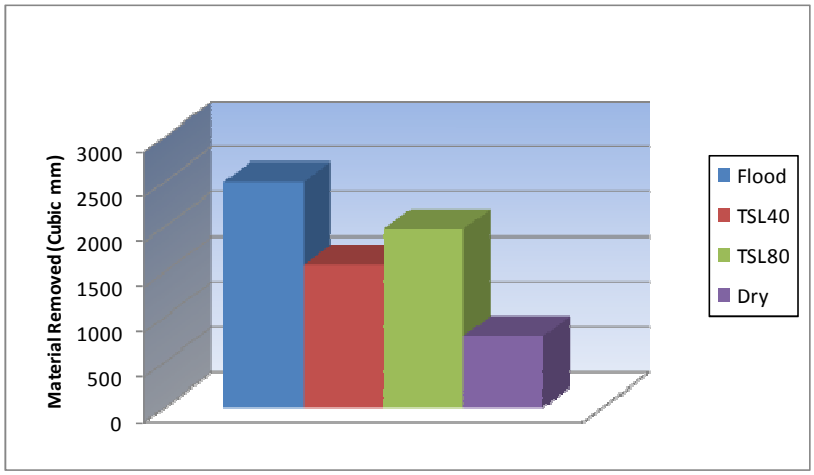

Figure 55: CMX850 - Material removed before tool failure.

Another important output for machining purposes is to determine the average surface roughness of each cutting process. The reason for this is that surface roughness is a good indication of the surface integrity of the finished part. A profilometer was used to determine average surface roughness values for the different lubrication strategies. According to researchers at Element Six (Pty) Ltd. [87], a surface roughness exceeding 1.6 µm is an unacceptable quality characteristic in the aerospace industry. In this study, therefore a surface roughness of more than 1.6 µm was used as an indicator that the tool has failed. The primary wear criterion was however still wear scar dimensions. Wear scar analysis therefore identified tool failure before the 1.6 µm surface roughness value was measured in most cases. Figure 56 indicates the average surface roughness values attained after 1056 mm^3 of Ti6Al4V had been removed.

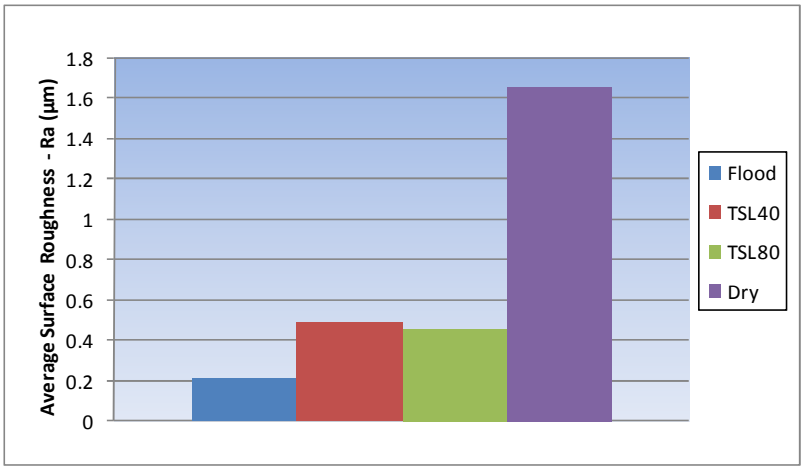

Figure 56: CMX850 – Average surface roughness values.

All the values, except for the dry machining, were below the required quality boundary of 1.6 µm. The flood lubrication produced the lowest average surface roughness with Ra = 0.21 µm, while the 40 bar through spindle lubrication and 80 bar through spindle lubrication experiments produced surface roughness's of 0.49 and 0.46 µm respectively. When this is compared to the average size of the flank wear after 1056 mm^3 of material had been removed, it can be seen that there exists a similarity between the average surface roughness and the size of the flank wear (refer Figure 57). This similarity between surface roughness and the size of the flank wear stresses the importance of keeping the flank wear rate to a minimum.

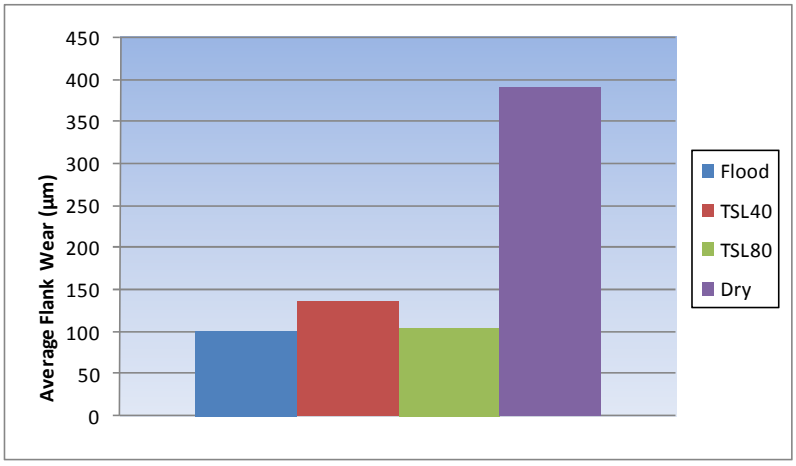

Figure 57: CMX850 - Average flank wear of the different lubrication strategies.

From the tool life experiments conducted with the CMX850 it was once again proven that flood lubrication was the superior lubrication strategy. This can be attributed to the lower cutting temperatures and cutting forces associated with using an abundance of coolant. Lower cutting temperatures will slow the rate of chemical diffusivity. Better lubrication between the tool and the insert will also reduce friction and subsequently also lead to a reduction in cutting temperatures. Better lubrication will also reduce the mechanical load exerted on the insert during cutting operations.

The fact that PCD is less susceptible to thermal shock can be said to be the main reason for the increase in tool life associated with flood lubrication strategies. The failure mechanism for PCD can therefore still be attributed to mechanical impact rather than thermo-chemical wear. This tends to suggest that the best lubrication strategy would be to reduce temperature as much as possible and to lubricate the interface between the tool and the workpiece in order to minimize cutting forces.

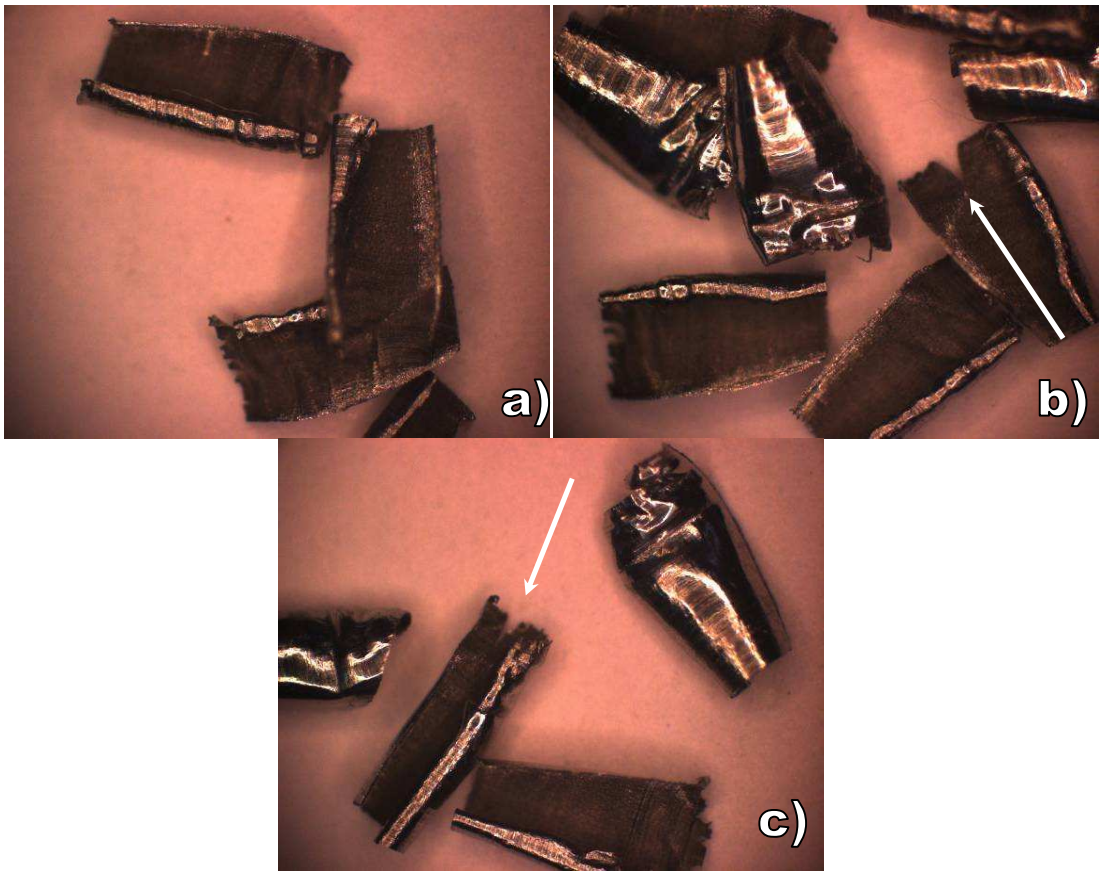

Figure 58: The chips collected for the a) flood lubrication, b) 40 bar through spindle lubrication and c) 80 bar through spindle lubrication (x50).

Figures 58 a), b) and c) illustrates the chips collected for the flood lubrication, 40 bar through spindle lubrication and 80 bar through spindle lubrication experiments respectively. The chips that were produced during these experiments were rather small. There is little difference between the forms of the chips. In the experiments conducted with the 40 bar and 80 bar through spindle lubrication the chips appeared rather similar. No real primary serration could be witnessed in any of the chips. This could probably be due to the lack of magnification achieved with the optical microscope. The magnification was only x50. Although this may seem to be a too small magnification, segmentation for the chips produced with tungsten carbide could already be seen at this magnification. The micrograph for the tungsten carbide was also taken at a magnification of x70 (refer Figure 60). It can be mentioned though that the chips formed during the two through spindle experiments exhibited much more secondary serration (see arrows in Figures 58 b) and c)). This could lead to the conclusion that the frequency of serration is much

higher for the PCD inserts. This could probably be due to the smaller rake angle of the PCD pushing the material rather than cutting it. This causes higher deformation in the primary shear zone, which will lead to higher temperatures and eventually catastrophic shear, leading to the segmentation of the chips.

9.4.2 Tungsten Carbide

The results attained from the first tests showed little difference between the results attained for the 40 bar and 60 bar through spindle lubrication strategies. The 60 bar through spindle lubrication showed a slight improvement over the 40 bar through spindle lubrication. This was attributed to the higher coolant supply pressure resulting in more sufficient swarf removal and a reduction in the amount of coolant reducing the degree of thermal shock experienced by the insert. For this reason it was deemed necessary to only test the VP15TF at flood and 60 bar through spindle lubrication. Dry machining was not tested for these inserts due to the results found in the pilot testing (refer section 7.1.1). Failure criteria were the same as in the case of the CMX850. The cutting speed and feed per tooth were also kept the same at 100 m/min and 0.05 mm/rev respectively.

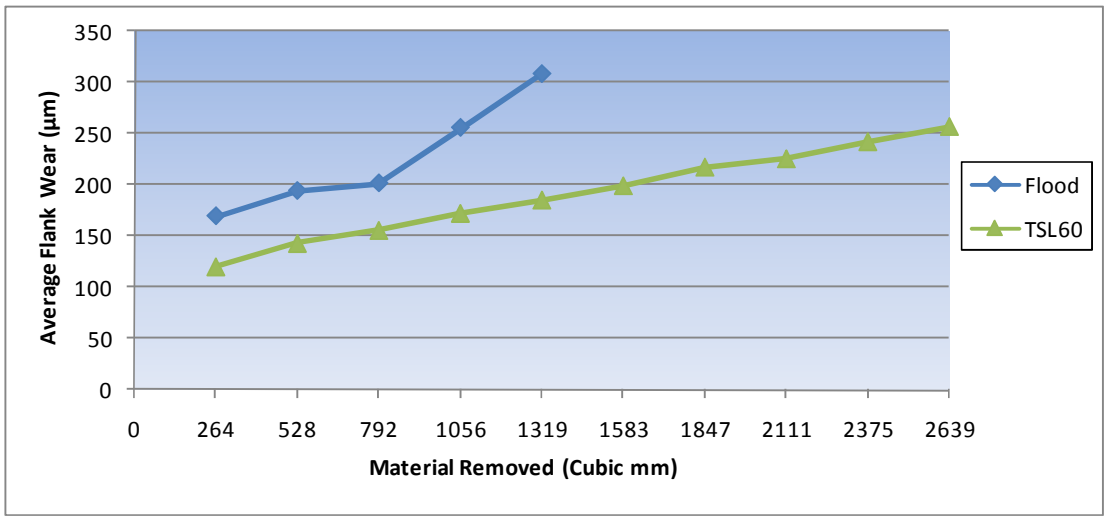

Figure 59: VP15TF – Tool life determination.

Figure 59 illustrates the results found for the VP15TF. The results found here differ from the results found for the CMX850. Not only did the flood lubrication perform much worse than in the case of the CMX850, but the through spindle lubrication also performed a lot better than the CMX850. Even after 2639 mm^3 of material had been removed, the inserts used at 60 bar through spindle lubrication had not yet reached the end of its tool life.

It has to be taken into account that Mitsubishi's VP15TF inserts and tool holder used for the experiments are specialized tools for titanium machining and have been developed over many years of experimentation. The CMX850 inserts that were used is a new material that is still in its developmental stages. The customized toolholder also had internal coolant channels that could be deemed less sufficient than the optimized and advanced developed internal coolant channels of the Mitsubishi toolholder.

The shortened tool life of the inserts used in the flood lubrication strategies illustrates the impact that thermal shock has on the reduction in tool life. The abundance of coolant supplied to the insert will cause an increase in thermal shock as the hot insert exits the workpiece and enters the coolant stream. This will cause thermal cracks to develop, leading to an increase in tool wear.

In the case of the 60 bar through spindle lubrication excellent tool performance was achieved. This confirmed the theory of thermal shock leading to a reduction in tool life. In the case of the 60 bar through spindle lubrication the amount of lubricant supplies sufficient cooling to the cutting edge to reduce thermally activated chemical wear, but supplies a small enough amount of coolant to reduce the thermal shock exerted on the tool. The directed streams of the through spindle lubricant also penetrated the tool-chip interface more sufficiently than in the case of the CMX850. This contributed to much more sufficient chip removal. The shorter contact time between the chip and the tool will reduce the amount of heat that is generated. This will subsequently reduce the thermal shock experienced by the insert even more.

Figure 60: A segmented chip collected for the VP15TF experiments (x70).

Figure 60 indicates a typical chip that was formed during the flood lubrication experiments. Due to the nature of the through spindle experiments, it was not possible to collect any of the chips for these experiments. It is clear that much longer chips are formed than in the case of the CMX850 experiments. This can be attributed to the chip forming geometry of the of the VP15TF inserts. This chip clearly indicates the segmentation mentioned in the literature. The frequency of segmentation is much lower than the case of the PCD inserts. This can be attributed to the tungsten carbide insert's chip forming geometry and higher rake angle. This will cause the rate at which material deformation occurs in front of the tool to be much lower than in the case of the PCD. The lower rate of deformation implies that more time passes before catastrophic shear will occur. This explains the why the frequency of serration is lower for the tungsten carbide inserts.

10. Conclusions and Recommendations

10.1 Chip Formation

The chip formation for the tungsten carbide and PCD inserts differed substantially. This can mainly be attributed to the insert geometry differences between the tungsten carbide and the PCD inserts, with the PCD inserts having a much smaller rake angle. The tungsten carbide inserts also has chip forming geometry and chip breaking assistance. Serrated chips were formed for both insert types, with the main difference between the grades being the frequency of serration. The larger rake angle of the tungsten carbide inserts assisted in producing longer chips. The chip forming geometry also reduced the rate of material deformation, causing serrations to be further apart. In the case of the PCD inserts the smaller rake angle increases the rate of material deformation, causing a decrease in the distance between serrations.

10.2 Tool Wear Mechanisms

Before analysis of the flank wear results could be done, the mechanisms behind the flank wear firstly had to be determined. SEM and EDS analyses were conducted in order to determine the reason for tool failure. The first run of SEM and EDS analyses proved the presence of a Ti6Al4V buildup edge on the wear scars of the PCD inserts. It was decided to remove the Ti6Al4V in order to determine mechanisms for tool wear.

After the Ti6Al4V buildup was successfully removed with HCl leaching, the wear scar was once again analysed with SEM and EDS analyses. The formation and propagation of cracks were observed. The wear mechanism was therefore concluded to be the formation of subsurface lateral cracks that developed due to the repeated impact and flow of workpiece material with the flank face. These lateral cracks propagate through the bulk of the material and will eventually propagate to the free surfaces of the flank face, leading to the delamination of insert material.

From the analysis of the PCD inserts it became clear that mechanical impact causes the initiation of tool failure. Once the initial abrasively activated chipping occurs, higher tool

temperatures will be generated and subsequently increase the rate of tool wear. It can therefore be accepted that in order to reduce the rate of tool wear, it is necessary to suppress the generated cutting temperatures and forces as much as possible. Tool failure is primarily brought on by mechanical impact and secondarily by high cutting temperatures. This explains why the CMX850 with the better mechanical properties performed better than the CTM302. It can therefore be accepted that the mechanical properties of PCD inserts are more important to increasing tool life than its thermal properties for the machining of Ti6Al4V.

All the cutting configurations and lubrication strategies were tested for a material removal of 560 mm^3. These initial tests were used to determine the sensitivity of the cutting speed, feed per tooth and insert material used. The results proved that the longest tool life (as a function of material removed) could be attained for cutting configurations of 100 m/min cutting speed and a feed per tooth of 0.05 mm/rev (a material removal rate of 64 mm^3/min). The following conclusions and recommendations could be made from these experiments:

10.3 Lubrication Strategies – PCD

10.3.1 Flood Lubrication

The flood lubrication performed the best of all the lubrication strategies used for the PCD experiments. As mentioned previously in the tool wear mechanisms section, the best cutting strategies for PCD inserts would involve strategies where cutting forces and cutting temperatures are kept to a minimum.

Flood lubrication solves both of these problems. The abundance of lubricant supplied to the cutting edge will not only assist in lowering the generated cutting temperature, but it will also assist in more sufficient lubrication between the flank face of the insert and the workpiece material, subsequently lowering cutting forces.

The sensitivity analysis of cutting parameters indicates that an increase cutting speed will have the biggest impact on reducing tool life. The effect of increasing feed per tooth and the choice between PCD grades had less of an impact on the reduction in tool life

over the distance machined. From the experiments it became clear that the best tool life (in terms of cutting time) could be reached by using CMX850 at a cutting speed of 100 m/min and a feed per tooth of 0.025 mm/rev. It is probably not the best configuration when considering tool life in terms of material removed though. The small increase in tool wear rate brought on when moving from the lower feed per tooth to the higher feed per tooth for the lower cutting speeds led to the conclusion that more material could be removed at a cutting speed of 100 m/min and a feed per tooth of 0.05 mm/rev. At these conditions the flood lubrication performed the best. A total amount of 2507 mm^3 material could be removed before a tool wear of 300 µm per cutting edge was reached. The surface finish was also good with an average roughness (Ra) value of 0.21 µm after 1056 mm^3 of material had been removed.

10.3.2 40 Bar Through Spindle Lubrication

The inferior performance of TSL40 cooling can be attributed to the reduced amount of lubricant supplied to the cutting edge when compared to the flood lubrication.

A reduction in the amount of lubricant implies that there is a reduced amount of cooling power and a lower degree of lubrication between the flank face of the insert and the workpiece. This implies that higher cutting forces and temperatures are generated when compared to the flood lubrication experiments.

The sensitivity analysis of the 40 bar through spindle lubrication showed that cutting speed was again the factor that had the biggest impact on an increase in flank wear rate. The effect of increasing cutting speed was much more prominent than in the case of the flood lubrication. This can be attributed to the reduced cooling power supplied by this lubrication strategy. Another difference when compared to flood lubrication is the impact of the increase in feed per tooth on the tool wear rate. This lubrication is much more sensitive to a change in feed per tooth than the flood lubrication. The reason for this can again be attributed to the reduced amount of coolant supplied to the cutting edge. This implies that less lubrication occurs, leading to higher cutting forces. This is why an increase in feed will cause an increase in tool wear rate. The CMX850 performed better

than the CTM302. This can be attributed to the improved mechanical properties associated with the CMX850 helping it to cope better with the increased cutting force demand. The longest tool life (in terms of cutting time) for this lubrication strategy could once again be achieved at a cutting speed of 100 m/min and a feed per tooth of 0.025 mm/rev with CMX850 inserts. For conformity it was decided to do tool life determination at the same cutting parameters as in the case of the flood lubrication.

When the tool life determination was conducted it was found that the 40 bar through spindle lubrication performed superior only to dry machining experiments. A total amount of 1583 mm^3 material was removed before failure occurred. This is almost 1000 mm^3 of material removed less than in the case of the flood lubrication. The surface roughness, Ra = 0.49 µm, was a bit more than for the flood lubrication, but it is still within the quality criteria range of below 1.6 µm.

10.3.3 80 Bar Through Spindle Lubrication

This lubrication strategy performed worse than the flood lubrication strategy but better than the 40 bar through spindle lubrication. The reason for this is that it can be accepted that the reduced amount of lubricant supplied to the cutting edge will increase the cutting forces and temperatures relative to the flood lubrication. The increase in pressure will however assist in more sufficient chip removal compared to the 40 bar through spindle lubrication. This will reduce the contact length of the chips with the insert subsequently reducing the cutting forces and temperatures relative to the 40 bar through spindle lubrication.

The sensitivity analysis showed a large degree of similarity to the 40 bar through spindle lubrication. This confirmed the theory that the amount of lubricant supplied to the cutting edge is directly related to the tool life of the insert. As in the case of 40 bar through spindle lubrication, too little lubrication could be supplied to the cutting edge to sufficiently reduce the cutting forces and temperatures at the cutting edge. Cutting speed again had the most prominent influence on increasing the tool wear rate, while the feed per tooth also had a substantial effect. The two grades of PCD performed very

similar for this lubrication strategy. The lowest tool wear rate was again attained at cutting configurations of 100 m/min cutting speed and 0.025 mm/rev feed per tooth with CMX850 inserts. As in the case of flood lubrication and 40 bar through spindle lubrication, a cutting speed of 100 m/min and a feed per tooth of 0.05 mm/rev was used for the tool life determination experiments.

This lubrication strategy performed better than the 40 bar through spindle lubrication strategy concerning both tool life and surface finish. A total amount of 1979 mm^3 material was removed before tool failure. This is almost 400 mm^3 of material removed more than in the case of the 40 bar through spindle lubrication. This can be attributed to the higher supply pressure assisting in more sufficient chip removal. An average surface roughness of Ra = 0.46 µm was also achieved which is still very much in the quality criteria range.

10.3.4 Dry Machining

Dry machining with PCD inserts were used in order to determine whether this strategy will work similar to the through spindle lubrication strategies. It was found that this strategy led to an accelerated tool wear compared to the other lubrication strategies. The high thermal conductivity of the inserts could not dissipate the heat from the cutting edge at a fast enough rate. The lack of coolant also meant that there was no lubrication between the flank face of the tool and the workpiece. This will further increase the cutting temperature and forces compared to the other lubrication strategies.

When this strategy was tested with CMX850 inserts at a cutting speed of 100 m/min and a feed per tooth of 0.05 mm/rev, it performed the worst of all the lubrication strategies. The tool only lasted for a material removal of 792 mm^3 before failure and produced an average surface roughness of Ra = 1.65 µm. This is the only strategy that produced surface roughness values of more than the quality boundary of 1.6 µm.

10.3.5 Recommendations for PCD Insert Lubrication Strategies

From the experiments it became clear PCD inserts are more susceptible to mechanical impact than thermal shock in milling operations of Ti6Al4V. This explains why CMX850, with better mechanical properties, performed better than the CTM302. It is therefore necessary to reduce the mechanical load on the insert in order to reduce the tool wear rate. Flood lubrication performed the best in this regard. The abundance of coolant helped to not only reduce the temperatures of the entire cutting process, but also assisted in reducing the forces exerted on the tool. The results that were achieved with flood lubrication were very satisfactory at cutting parameters of 100 m/min cutting speed and a feed per tooth of 0.05 mm/rev (a material removal rate of 64 mm^3/min). It can therefore be recommended that in order to maximize tool life, an abundance of lubrication needs to be supplied in order to supply sufficient cooling power and lubrication to the cutting process. Dry machining is not recommended for the milling of Ti6Al4V with PCD inserts. High pressure through spindle lubrication is not recommended for PCD inserts at cutting speeds above 100 m/min, due to a reduction in cooling power, but could possibly be used at lower cutting speeds where lower temperatures are generated.

10.4 Lubrication Strategies – Tungsten Carbide

The biggest difference between PCD inserts and tungsten carbide inserts is that tungsten carbide inserts are more susceptible to thermal shock than mechanical impact, opposed to the PCD inserts for which the opposite is true. These characteristics will play an important part in determining the correct lubrication strategy to use.

The results that were attained from the experiments differed a lot form the PCD results. It was found that the through spindle lubrication strategies performed better than the flood lubrication for most of the experiments. This confirmed the theory surrounding the effect of thermal shock on the tungsten carbide inserts. The through spindle lubrication strategies worked best due to the fact that they supply a 'softer' cool as opposed to flood lubrication that supplies a 'harder' cool. This implies that for the through spindle lubrication strategies the temperature differential is less as the tool exits the workpiece and enters the coolant stream than for the flood lubrication. The thermal shock experienced by the tool is thus less for through spindle lubrication strategies than for the flood lubrication strategies.

When considering the effect of different cutting parameters on the tool wear rate of the inserts, it was found that an increase in cutting speed and feed per tooth led to an increase in tool wear rate. As is expected, the increase in cutting speed had a much higher influence on the tool wear rate than the feed per tooth. This can be credited to the fact that cutting temperature is more dependent on cutting speed than on feed per tooth. An increase in cutting speed will therefore amplify the thermal shock experienced by the insert, causing an increase in the tool wear rate.

The analyses of the 40 bar and 60 bar through spindle lubrication strategies showed that the 60 bar through spindle lubrication strategy performed slightly better than the 40 bar through spindle lubrication. This can be attributed to the increased pressure supply contributing to more sufficient chip removal.

The tool life determination for the tungsten carbide inserts were tested at the same cutting conditions of 100 m/min cutting speed and 0.05 mm/rev feed per tooth as in the

case of the PCD inserts. The only lubrication strategies that were tested were flood lubrication and 60 bar through spindle lubrication. It was deemed unnecessary to test 40 bar through spindle lubrication, due to the similarity in results compared to the 60 bar through spindle lubrication for the initial tests. Dry machining was also not tested due to the conclusions made in the pilot testing.

The results that were found showed that 60 bar through spindle lubrication was superior to flood lubrication. This is due to the increased thermal shock associated with flood lubrication. Although PCD inserts performed better in most of the experiments, the 60 bar through spindle lubrication performed a lot better than the PCD in the tool life determination. Even after 2639 mm^3 of material had been removed, the tool still did not reach the end of its life. The flood lubrication performed a lot worse as it only removed 1319 mm^3 material before tool failure. This is a shorter tool life than both the 40 bar and 80 bar through spindle lubrication experiments for the PCD inserts. The geometry of the inserts allow for very good surface finish. The flood lubrication experiments produced an average surface roughness of Ra = 0.23 µm, while the 60 bar through spindle lubrication produced an average surface roughness of Ra = 0.21 µm.

10.4.1 Recommendations for Tungsten Carbide Insert Lubrication Strategies

The difference in results for tungsten carbide inserts compared to PCD inserts can be related to the lower thermal conductivity of tungsten carbide compared to the PCD inserts. This makes the inserts more susceptible to thermal shock than in the case of PCD inserts. The results of the experiments also confirm this theory. It was found that for experiments where an abundance of lubricant is supplied the thermal shock exerted on the inserts are increased to such an extent that tool life is decreased substantially. It is therefore recommended that a high pressure ‘soft’ cool is needed for sufficient machining of Ti6Al4V with tungsten carbide inserts. This will minimize the thermal shock exerted on the insert. A higher through spindle pressure also performs better as it assists in more sufficient chip removal.

References

[1] Website visited November 2008, Boeing Current Market Outlook for 2008 – 2027, http://www.boeing.com/commercial/cmo/index.html.

[2] RMI Titanium Company (subsidiary of RTI International Metals), JSF Supplier Conference, 14 April 2005.

[3] Website visited November 2008, Timet, Annual Report for 2007, http://www.timet.com/pdfs/07annual.pdf

[4] China's Impact on Metals Prices in Defence Aerospace, December 2005.

[5] U.S. Geological Survey, Mineral Information, Titanium Statistics and Information, December 2005.

[6] D.D. Barnett-Ritcey, R. Hachmoller, M.A. Elbestawi, 2001, Milling of Titanium Alloy Using Directed Through Spindle Coolant, Transactions of the North American Manufacturing Research Institution of the Society of Manufacturing Engineers, Vol. 26, pp. 167-174.

[7] F. Nabhani, 2001, Wear Mechanisms of Ultra-Hard Cutting Tools Materials, Journal of Materials Processing Technology, Vol. 115 (3), pp. 402-412.

[8] E. Kuljanic, M. Fioretti, L. Beltrame, F. Miani, 1998, Milling Titanium Compressor Blades with PCD Cutter, CIRP Annals, Vol. 47 (1), University of Udine, pp. 61-64.

[9] N. Narutaki, A. Murakoshi, 1985, Study on Machining of Titanium Alloys, CIRP Annals, Vol. 32 (1), pp. 65-69.

[10] W.D. Callister, Jr., 2003, Material Science and Engineering – An Introduction, Sixth Edition, John Wiley and Sons. Inc., pp. 264-382.

[11] M.J. Donachie, S.J. Donachie, 2002, Superalloys – A Technical Guide, Second Edition, ASM International, pp. 8-201.

[12] D.C. Kirk, 1976, Cutting Aerospace Materials (Nickel-, Cobalt-, and Titanium-Based Alloys), Rolls Royce (1971) Ltd, pp. 77-98.

[13] M.V. Ribeiro, M.R.V. Moreira, J.R. Ferreira, 2003, Optimization of Titanium Alloy (6Al-4V) Machining, Journal of Materials Processing Technology, Vol. 143-144 (1), pp. 458-463.

[14] S.K. Bhaumik, C. Divakar, A.K. Singh, 1995, Machining Ti-6Al-4V Alloy with a wBN-cBN Composite Tool, Materials & Design, Vol. 16 (4), pp. 221-226.

[15] D.D. Barnett-Ritcey, M.A. Elbestawi, 2002, Tool Performance in High Speed Finish Milling of Ti6Al4V, Proceedings of International Mechanical Engineering Congress and Exposition, pp. 1-9.

[16] D.D. Barnett-Ritcey, 2004, High-Speed Milling of Titanium and Gamma-Titanium Aluminide: An Experimental Investigation, Ph.D. thesis, Mc Master University, Canada.

[17] D.G. Pettifor, 1995, Bonding and Structures of Molecules and Solids, Oxford University Press, pp. 12-13.

[18] J. Wilks, E. Wilks, 1991, Properties and Applications of Diamond, Butterworth Heinemann, pp. 17-20.

[19] A. Bakon, A. Szymanski, 1993, Practical Uses of Diamonds, Ellis Horwood Ltd. and Polish Scientific Publishers PWN Ltd., pp. 57-60.

[20] S. Webzell, 2007, Exotic Substrates, www.machinary.co.uk, pp. 39-40.

[21] D. Fowler, 1988, Milling with Polycrystalline Diamond, Carbide Tool Journal Vol. 20 (5), pp. 23-25.

[22] G. Spur, U. Lachmund, 1993, Type-Specific applicability of polycrystalline Diamond, Production Engineer Vol. 1 (1), pp. 77-80.

[23] B.M. Kramer, D. Viens, S. Chin, 1993, Theoretical Considerations of Rare Earth Compounds as Tool Materials for Titanium Machining, Annals of the CIRP, Vol. 42, pp. 111-114.

[24] H. Schulz, A. Sahm, 2002, Influence of Heat Treatment and Cutting Parameters on Chip Formation and Cutting Forces, Metal Cutting and High Speed Machining, Kluwer Academic/Plenum Publishers, pp. 69-78.

[25] J. Barry, G. Byrne, D. Lennon, 2001, Observations on Chip Formation and Acoustic Emission in Machining Ti-6Al-4V Alloy, International Journal of Machine Tools and Manufacture, Vol. 41 (7), pp. 1055-1070.

[26] R. Komanduri, 1982, Some Clarifications on the Mechanisms of Chip Formation when Machining Titanium Alloys, Wear, Vol. 76, pp. 15-34.

[27] R. Komanduri, T. Schroeder, J. Hazra, B.F. von Turkovich, D.G. Flom, 1982, On the catastrophic Shear Insability in High-Speed Machining of an AISI 4340 Steel, Journal of Engineering for Industry, Vol. 104, pp. 121-131.

[28] Z. Bing Hou, R. Komanduri, 1997, Modelling of Thermomechanical Shear Instability in Machining, International Journal of Mechanical Sciences, Vol. 39 (11), pp. 1273-1314.

[29] P. Li, C. Ma, Z. Lai, 1996, Strain evaluation of adiabatic shear band produced by orthogonal cutting in high strength low alloy steel, Materials Science and Technology, Vol. 12, pp. 351-354.

[30] B.E. Klamecki, 1982, Catastrophe Theory Models of Chip Formation, Journal of Engineering for Industry, Transactions of the ASME, Vol. 104 (4), pp. 369-374.

[31] A.L. Wingrove, 1973, The Influence of Projectile Geometry on Adiabatic Shear and Target Failure, Metallurgical Transactions, Vol. 4 (8), pp. 1829-1833.

[32] R. Komanduri, R.H. Brown, 1981, On the Mechanics of Chip Segmentation in Machining, Journal of Engineering for Industry, Transactions of the ASME, Vol 103 (1), pp. 33-51.

[33] K. Nakayama, 1974, Formation of “Saw-Toothed Chip” in metal cutting, IEE conference publication, pp. 572-577.

[34] M.C. Shaw, A. Vyas, 1998, The Mechanism of Chip Formation with Hard Turning Steel, CIRP Annals, Vol. 47 (1), pp. 77-82.

[35] M.C. Shaw, A. Vyas, 1999, Mechanics of Saw-Tooth Chip Formation in Metal Cutting, Journal of Manufacturing Science and Engineering, Transactions of the ASME, Vol. 121 (2), pp. 163-172.

[36] Z.Y. Wang, C. Sahay, K.P. Rajurkar, 1996, Tool Temperatures and Crack Development in Milling Cutters, International Journal of Machine Tools and Manufacture, Vol. 36 (1), pp. 129-140.

[37] Y. Su, N. He, L. Li, X.L. Li, 2006, An Experimental Investigation of Effects of Cooling/Lubrication Conditions on Tool Wear in High-Speed End Milling of Ti-6Al-4V, Wear, Vol. 261 (7-8), pp. 760-766.

[38] J.M. Viera, A.R. Machado, E.O. Ezugwu, 2001, Performance of Cutting Fluids During Face Milling of Steels, Journal of Materials Processing Technology, Vol. 116 (2-3), pp. 244-251.

[39] N. Lui, G.Y. Xu, Y.D. Xu, 1997, Thermal Shock Fatigue Behaviours of Cemented Carbide YG20, Transactions of Nonferrous Metals Society of China, Vol. 7 (2), pp. 149-154.

[40] M. Wang, 1985, Studies on Tool Wear in Milling of Titanium Alloys, Ph.D. thesis, Nanjing University of Aeronautics and Astronautics, China.

[41] T. Numora, H. Moriguchi, K. Tsuda et al., 1999, Material Design Method for the Functionality Graded Cemented Carbide Tool, International Journal of Refractory Metals and Hard Materials, Vol. 17 (6), pp. 397-404.

[42] K. Uehara, 1981, Fundamental Approach to the Thermal Crack of Cermet Cutting Tools, CIRP Annals, Vol. 30 (1), pp. 47-51.

[43] M. Mori, M. Furuta, T. Nakai, T. Fukaya, J. Lui, K. Yamazaki, 1999, High-Speed Machining of Titanium by New PCD Tools, SAE Technical Paper Series, pp. 1-6.

[44] R. Komanduri, W.R. Reed Jr., 1983, Evaluation of Carbide Grades and a New Cutting Geometry for Machining Titanium Alloys, Wear, Vol. 92, pp. 13-123.

[45] W. Koening, 1979, Applied Research on the Machinability of Titanium and its Alloys, Proceedings of the 47th Meeting of AGARD Structural and Materials Panel, pp. 1.1-1.10.

[46] M. Fritzsimmons, T. El-Wardany, P. FitzPatrick, 2000, Efficient Machining of Titanium Rotorcraft Components, American Helicopter Society, 56th Annual Forum.

[47] C.R. Lui, X. Yang, 1999, Machining Titanium and its Alloys, Machining Science and Technology, Vol. 3 (1), pp. 107-139.

[48] Titanium Machining Application Guide, 2004, Sandvik Coromant, Sweden.

[49] J.F. Kelley, M.G. Cotterell, 2002, Minimal lubrication machining of aluminium alloys, Journal of Materials Processing Technology, Vol. 120, pp. 327-334.

[50] J.A. Arsecularatne, L.C. Zhang, C.Montross, 2005, Wear and Tool Life of Tungsten Carbide, PcBN and PCD Cutting Tools, International Journal of Machine Tools and Manufacturing Vol. 46, pp. 482-491.

[51] M.P. Groover, 2002, Fundamentals of Modern Manufacturing. Second Edition. John Wiley & sons, inc.

[52] N.P. Hung, N.L. Loh, V.C. Venketesh, 1999, Machining of Metal Matrix Composites in Machining of Ceramics and Composites, S. Jahanmir, M. Ramulu, P. Koshy (Eds.), pp. 295-356.

[53] J.T. Lin, D. Bhattacharyya, C. Lane, 1995, Machinability of a Silicon Carbide Reinforced Aluminium Metal Matrix Composite, Wear, Vol. 181-183 (2), pp. 883-888.

[54] C.A.C. Antonio, J.P. Davim, 2001, Optimum Cutting Conditions in Turning of Particle Metal Matrix Composites Based on Experimental and a Generic Search Model, Composites Part A: Applied Science and Manufacturing, Vol. 33 (2), pp. 213-219.

[55] M. El-Gallab, M. Sklad, 1998, Machining of Al/SiC Particulate Metal Matrix Composites Part I: Tool Performance, Journal of Materials Processing Technology, Vol. 83, pp. 151-158.

[56] C.J.E. Andrews, H.Y. Feng, W.M. Lau, 2002, Machining of an Aluminium/SiC Composite Using Diamond Inserts, Journal of Materials Processing Technology, Vol. 102, pp. 25-29.

[57] J.P. Davim, A.M. Baptista, 2000, Relationship Between Cutting Force and PCD Tool Wear in Machining Silicon Carbide Reinforced Aluminium, Journal of Materials Processing Technology, Vol. 103, pp. 417-423.

[58] G. Lane, 1992, The Effect of Different Reinforcement on PCD Tool Life for Aluminium Composites, Proceedings of the Machining of Composites Materials Symposium, ASM Materials Week, Chicargo, IL, pp. 3-15.

[59] M. Nouari, G. List, F. Girot, D. Géhin, 2005, Effect of machining parameters and coating on wear mechanisms in dry drilling of Al alloys, International Journal of Machine Tools and Manufacture, Vol. 45 (12-13), pp. 1436-1442.

[60] M.S. Carrilero, M. Marcos, 1996,Surface Roughness of AA7050 Alloy Turned Bars Analysis of the Influence of the Length of Machining, Journal of the Mechanical Behavior of Materials, Vol. 7**,** pp. 179–191.

[61] T.N. Loladze, 1962, Adhesion and Diffusion Wear in Metal Cutting, Proceedings of the 42nd Annual Convention, Calcutta, Jl. Inst. of Engineers Vol. 43, India, pp. 108-141.

[62] B. Bhushan, 2002, Introduction to Tribology, John Wiley & Sons, New York, pp. 332-379.

[63] B.J. Ranganath, 1989, On the Wear Mechanism in Sintered Titanium carbide Cutting Tools, Key Engineering Materials Vol. 29-31, pp. 555-564.

[64] A. Moufki, A. Molinari, D. Dudzinski, 1998, Modelling of Orthogonal Cutting with a Temperature Dependent Friction Law, Journal of the Mechanics and Physics of Solids, Vol. 46, pp. 2103–2138.

[65] B.R. Lawn, Fracture of Brittle Materials 2nd Edition, 1993, Cambridge University Press, Cambridge, UK.

[66] D. Wang, Y. Xue, Q. Jiao, P. Liu, 1990, A Study on the Oxidation Resistance of Sintered Polycrystalline Diamond with Dopants, Science and Technology of New Diamond, pp. 437-439.

[67] Website visited November 2008, http://members.tm.net/lapointe/Carbon_Phase_Diagram.gif

[68] L.A. Kendall, 1992, Friction and wear of cutting tools and cutting tool material, ASM Metal Handbook, Friction, Lubrication and Wear Technology, Vol. 18, p. 613.

[69] E.M. Trent, 1989, Metal Cutting, Butterworths, London, UK.

[70] S.A. Klimanko, Y.A. Mukovoz, L.G. Polonsky, 1996, Advanced Ceramic Tools for Machining Applications – II, Key Engineering Materials, Vol. 114, pp. 1-63.

[71] L. De Chiffre, 1988, Function of Cutting Fluids in Machining, Lubrication Engineering, Vol. 44 (6), pp. 514-518.

[72] W.J. van der Bijl, 2006, Drilling of Aluminium Wheels with Minimal Quantity Lubrication: A Test Setup to Simulate an Industrial Production Environment, South Africa.

[73] J.F. Kelly, M.G. Cotterell, 2002, Minimal lubrication machining of aluminium alloys, Journal of Materials Processing Technology, Vol. 120 (1-3), pp. 327-334.

[74] A.R. Machado, J. Wallbank, 1996, The Effect of Extremely Low Lubricant Volumes in Machining, Wear, Vol. 210, pp. 76-82.

[75] H. Limper, K. Cavanaugh, 2008, What do you want your Coolant to do?, American Machinist, Vol. 152 (2), pp. 8-13.

[76] M.B. Da Silvia, J. Wallbank, 1998, Lubrication and Application Method in Machining, Industrial Lubrication and Tribology, Vol. 50 (4), pp. 149-152.

[77] A. Attanasio, M. Gelfi, C. Giardini, C. Remino, 2006, Minimal Quantity Lubrication in Turning : Effect on Tool Wear, Wear, Vol. 260 (3), pp.333-338.

[78] S.Y. Hong, I. Markus, W.-C. Jeong, 2001, New Cooling Approach and Tool Life Improvement in Cryogenic Machining of Titanium Alloy Ti-6Al-4V, International Journal of Machine Tools Manufacture, Vol. 41 (15), pp. 2245-2260.

[79] Z.Y. Wang, K.P. Rajurkar, J. Fan, 1996, Turning Ti-6Al-4V with Cryogenic Cooling, Transactions of the North American Manufacturing Research Institution of the Society of Manufacturing Engineers, Vol. 24, pp. 3-8.

[80] R. Kovacevic, C. Cherukuthota, M. Mazurkiewiez, 1995, High Pressure Waterjet Cooling/Lubrication to Improve Machining Efficiency in Milling, International Journal of Machine Tools Manufacture, Vol. 35 (10), pp. 1459-1473.

[81] Z.L. Man, 2003, Study on the High Speed Milling of Ti-Alloy Based on Green Manufacturing, Ph.D. thesis, Nanjing University of Aeronautics and Astronautics, China.

[82] T. Yamakazi, K. Miki, U. Sato, 2003, Cooling Air Cutting of Ti-6Al-4V Alloy, Journal of Japan Institute of Light Metals, Vol. 53 (10), pp. 416-420.

[83] L. De Chiffre, 1981, Lubrication in Cutting-Critical Review and Experiments with Restricted Contact Tools, Tribology Transactions, Vol. 24 (3), p.340-344.

[84] L. De Chiffre, 1977, Mechanics of Metal Cutting and Cutting Fluid Action, International Journal of Machine Tool Design and Research, Vol. 17 (4), p.225-234.

[85] M.Y. Friedman, E. Lenz, 1973, The Effect of Thermal Conductivity of Tool Material on Cutting Forces and Crater Wear Rate, Wear, Vol. 25, p.39.

[86] H.K. Tönschoff, F. Kroos, W. Sprintig, D. Brandt, 1994, Reducing Use of Coolants in Cutting Processes, Production Engineering, Vol. 1 (2), pp. 5–8.

[87] Discussion with Element Six Pty (Ltd) employees, January – April 2008, Springs.

[88] Website visited November 2008, Quadrant, http://www.quadrantepp.com/assets/base/Climb_milling.jpg

[89] A.K.M. Nurul Amin, A.F. Ismail, M.K. Nor Khairusshima, 2007, Effectiveness of Uncoated WC–Co and PCD Inserts in End Milling of Titanium Alloy—Ti–6Al–4V, Journal of Materials Processing Technology, Vol. 192-193, pp. 147-158.

[90] Elmagrabi N.H., Che Hassan C.H., Jaharah A.G., Shuaeib F.M., 2008, High Speed Milling of Ti-6Al-4V Using Coated Carbide Tools, European Journal of Scientific Research, Vol. 22 (2), pp. 153-162.

[91] Website visited February 2009 http://www.azom.com/details.asp?ArticleID=1547

[92] Website visited February 2009 http://www.dynamettechnology.com/titanium_alloys_files/image003.jpg

[93] Sandvik Metal Cutting Technical Guide, 2005, Elanders, Publication number C-2900:3 ENG/04, pp. D177.

[94] Hartung P.D., Kramer B.M., 1982, Tool Wear in Titanium Machining, Annals of the CIRP, Vol. 33 (1), pp. 75-80.

[95] Trent E.M., Wright P.K., 2000, Metal Cutting, Butterworth-Heinemann, pp. 97-131.

[96] Kitagawa T., Kubo A., Maekawa K., 1997, Temperature and Wear of Cutting Tools in High-Speed Machining of Inconel 718 and Ti6Al6V2Sn, Wear, Vol. 202 (2), pp. 142-148.

Appendices

Appendix A: Hermle C40 Machine Specifications

Maximum power output	43 kVA
Maximum spindle speed	18 000 rpm
Maximum feed (Rapid Transverse)	45 m/min
Transverse Range:	
X – axis	850 mm
Y – axis	700 mm
Z – axis	500 mm

Appendix B: CNC Program for PCD Experiments

```
0  BEGIN PGM PCD MM
1  BLK FORM 0.1 Z  X+0  Y+0  Z-26
2  BLK FORM 0.2  X+310  Y+12  Z+0
3  TOOL CALL 6 Z S2547 F1000
4  L  X+0  Y-41.5 F5000 M3
5  L  Z+0 F5000
6  APPR LCT  X+0  Y+0  Z+0 R14.5 RR F96
7  L  X+280 F96
8  DEP LCT  X+280  Y-41.5  Z+0 R14.5 F96 M5
9  L  Z+200 FMAX
10 L  X+0  Y-41 F5000 M3
11 L  Z+0 F5000
12 APPR LCT  X+0  Y+0.5  Z+0 R14.5 RR F96
13 L  X+280 F96
14 DEP LCT  X+280  Y-41  Z+0 R14.5 F96
15 L  Z+200 FMAX
16 TOOL CALL 0
17 END PGM PCD MM
```

Appendix C: CNC Program for VP15TF Experiments

```
0  BEGIN PGM VP15TF MM
1  BLK FORM 0.1 Z  X+0  Y+0  Z-26
2  BLK FORM 0.2  X+310  Y+12  Z+0
3  TOOL CALL 6 Z S2547 F1000
4  L  X+0  Y-41.5 F5000 M3
5  L  Z+0 F5000 M8
6  APPR LCT  X+0  Y+0  Z+0 R14.5 RL F64
7  L  X-280 F64
8  DEP LCT  X-280  Y-41.5  Z+0 R14.5 F64
9  L  Z+200 F5000
10 L  X+0  Y-41 F5000
11 L  Z+0 F5000 M8
12 APPR LCT  X+0  Y+0.5  Z+0 R14.5 RL F64
13 L  X-280 F64
14 DEP LCT  X-280  Y-41  Z+0 R14.5 F64
15 L  Z+200 FMAX M5
16 END PGM VP15TF MM
```